TP 76-10

The Statistical Anatomy of Ocean Wave Spectra

by

Leon E. Borgman

TECHNICAL PAPER NO. 76-10

JULY 1976

Prepared for

U.S. ARMY, CORPS OF ENGINEERS

COASTAL ENGINEERING RESEARCH CENTER

Kingman Building

Fort Belvoir, Va. 22060

REPORT DOCUMENTATION PAGE

READ INSTRUCTIONS BEFORE COMPLETING FORM

1. REPORT NUMBER TP 76-10	2. GOVT ACCESSION NO.	3. RECIPIENT'S CATALOG NUMBER
4. TITLE (and Subtitle) THE STATISTICAL ANATOMY OF OCEAN WAVE SPECTRA		5. TYPE OF REPORT & PERIOD COVERED Technical Paper 6. PERFORMING ORG. REPORT NUMBER Research Report 73-1
7. AUTHOR(s) Leon E. Borgman		8. CONTRACT OR GRANT NUMBER(s) DACW72-72-C-0001
9. PERFORMING ORGANIZATION NAME AND ADDRESS University of Wyoming Laramie, Wyoming 82071		10. PROGRAM ELEMENT, PROJECT, TASK AREA & WORK UNIT NUMBERS A31463
11. CONTROLLING OFFICE NAME AND ADDRESS Department of the Army Coastal Engineering Research Center (CERRE-OC) Kingman Building, Fort Belvoir, Virginia 22060		12. REPORT DATE July 1976 13. NUMBER OF PAGES 102
14. MONITORING AGENCY NAME & ADDRESS(if different from Controlling Office)		15. SECURITY CLASS. (of this report) UNCLASSIFIED 15a. DECLASSIFICATION/DOWNGRADING SCHEDULE

16. DISTRIBUTION STATEMENT (of this Report)

Approved for public release; distribution unlimited.

17. DISTRIBUTION STATEMENT (of the abstract entered in Block 20, if different from Report)

18. SUPPLEMENTARY NOTES

19. KEY WORDS (Continue on reverse side if necessary and identify by block number)

Gulf of Mexico
Hurricane Carla
Hurricane waves
Ocean wave spectra
Spectral analysis

20. ABSTRACT (Continue on reverse side if necessary and identify by block number)

The statistical variations in wave energy spectral estimates for hurricane waves are examined empirically for 12 separate intervals of wave records measured during Hurricane Carla in September 1961. Measurements were made on a Chevron Oil Company platform in South Timbalier Block 63, Gulf of Mexico, at a water depth of 100 feet. Hurricane waves were chosen for the analysis because these waves show, in exaggerated form, the effects of departures from linearity on the statistical variability in spectral estimates.

(continued)

This report gives the analysis for Hurricane Carla and develops certain implications and consequences of the empirical results.

PREFACE

This report is published to provide coastal engineers with the empirical results of statistical variations in wave energy spectral estimates for 12 intervals of wave data measured during Hurricane Carla in September 1961. The measurements were made on a Chevron Oil Company platform in the Gulf of Mexico at a water depth of 100 feet. The work was carried out under the wave mechanics program of the U.S. Army Coastal Engineering Research Center (CERC).

This report is published, with only minor editing, as received from the contractor; results and conclusions are those of the author and do not necessarily represent those of CERC or the Corps of Engineers.

The report was prepared by Leon E. Borgman, University of Wyoming, Laramie, Wyoming, under CERC Contract No. DACW72-72-C-0001. Dr. D. Lee Harris, Chief, Oceanography Branch, was the CERC contract monitor for the report, under the general supervision of Mr. R.P. Savage, Chief, Research Division.

Comments on this publication are invited.

Approved for publication in accordance with Public Law 166, 79th Congress, approved 31 July 1945, as supplemented by Public Law 172, 88th Congress, approved 7 November 1963.

JOHN H. COUSINS
Colonel, Corps of Engineers
Commander and Director

CONTENTS

CONTENTS

TABLES

FIGURES

CONTENTS

FIGURES — Continued

CONTENTS

FIGURES — Continued

CONTENTS

FIGURES — Continued

THE STATISTICAL ANATOMY OF OCEAN WAVE SPECTRA

by

Leon E. Borgman

I. INTRODUCTION

In the future, more and more ocean engineering design considerations will involve the wave energy spectrum. Typically, various secondary calculations will be made from the spectral and cross-spectral estimates at and between various space locations. The statistical reliability of the values obtained from the secondary calculations depend critically on the inherent statistical variability of the spectral estimates.

The estimation of directional wave spectra is obtained by just such secondary calculations on the auto- and cross-spectral densities or corresponding finite Fourier transform coefficients for various wave properties measured at one or more space locations. The reliability of the directional spectrum depends both on the method of computation and on the intrinsic statistical variability of the Fourier coefficients or spectral estimates. Such characterizing quantities as the main direction of wave travel for a given wave frequency or some measure of the arc of directions from which waves of a given frequency are coming each have their own confidence intervals which ultimately relate back, through the method of calculation, to the spectral and Fourier coefficient variability.

Over the years various theoretical probability relations have been derived which apply to linear waves (Pierson, 1955; Goodman, 1957; Blackman and Tukey, 1958). However, engineers are usually concerned with wave heights large enough to make linear assumptions questionable. Waves in hurricanes and other severe storms are prime examples of this situation. Yet it is just in such situations where probability confidence statements for the wave spectra or for derived secondary quantities are needed.

In the following report, the statistical variations in wave energy spectral estimates for hurricane waves are examined empirically for 12 separate intervals of wave record measured during Hurricane Carla (September 1961). The measurements were made on a Chevron Oil Company platform in South Timbalier Block 63, Gulf of Mexico, in a 100-foot water depth. Hurricane waves were chosen for the analysis because they would illustrate, in exaggerated form, the effects of departures from linearity on the statistical variability in spectral estimates.

Various aspects of the study were reported at the 13th International Conference on Coastal Engineering in Vancouver, B.C., 10 to 14 July 1972, for one 20-minute record (Borgman, 1972). This study gives the analysis for the whole storm and develops certain implications and consequences of the empirical results.

II. THE SPECTRAL COMPUTATION

Two basic methods have been used in the past for computing the wave spectrum. The earlier one was based on the covariance function which was then numerically Fourier transformed and smoothed. That is, if η_n ($n = 0,1,2..., N-1$) is the water level elevation above mean water level, then the covariance function is:

$$\hat{\hat{C}}_k = \frac{1}{N-k} \sum_{n=0}^{N-k-1} \eta_n \eta_{n+k} \quad . \tag{1}$$

(The quantity, N, is 4,096 for the analysis of Hurricane Carla.) Usually $\hat{\hat{C}}_k$ would be negligible for k larger than some value, say k_m. Thus, the N numbers would be adequately summarized in the k_m+1 values of $\hat{\hat{C}}_k$. Ordinarily, k_m is selected to be around one-tenth of N for most analysis of this type. The spectral density would be obtained from the numerical transform of the $\hat{\hat{C}}_k$:

$$\tilde{\tilde{p}}(f_r) = \Delta t \left[\hat{\hat{C}}_o + 2 \sum_{q=1}^{k_m-1} \hat{\hat{C}}_q \cos \frac{q\pi r}{m} + \hat{\hat{C}}_m \cos \ r\pi \right] , \tag{2}$$

where

$$f_r = \frac{r}{2k_m \Delta t} \tag{3}$$

for $r=0,1,3,..., k_m$ (Blackman and Tukey, 1958). The quantity, Δt, is the timelag between successive measurements of η_n ($\Delta t = 0.2$ second for the Hurricane Carla data).

The computation of equation (1) entails a loss of information (N values replaced by k_m values). This causes $\tilde{\tilde{p}}(f_r)$ in equation (2) to be a smoothed version of the true spectral density and distorts or eliminates features of the spectrum. The method of computation prevents the user from seeing aspects of the spectrum which may be important.

The second method for computing the spectral density, which has come into wide favor during the last few years, is based on the application of the fast Fourier transform computing algorithm to the water level elevations (Borgman, 1973). Complex-valued Fourier coefficients, A_m, are obtained (for $m=0,1,2,..., N-1$) by:

$$A_m = \Delta t \sum_{n=0}^{N-1} \eta_n \cos \frac{2\pi mn}{N} - i\Delta t \sum_{n=0}^{N-1} \eta_n \sin \frac{2\pi mn}{N} = U_m - iV_m \ . \tag{4}$$

Thus, U_m is the cosine transform while V_m is the sine transform of the water level elevations. The spectral lines are then computed by the formula,

$$\hat{p}(f_m) = (U_m^2 + V_m^2)/(N\Delta t) \quad , \tag{5}$$

where

$$f_m = \frac{m}{N\Delta t} \tag{6}$$

for m=0,1,2,3,..., N-1. These N spectral lines can be computed with great rapidity on a digital computer with the fast Fourier transform (FFT) procedure (Cooley and Tukey, 1965; Robinson, 1967).

The frequency

$$f_{Ny} = 1/2\Delta t \tag{7}$$

is called the Nyquist frequency. A symmetry relation

$$\hat{p}(f_m) = \hat{p}(f_{N-m}) \tag{8}$$

holds because of intrinsic mathematical properties of equations (4), (5), and (6). Hence, it is only necessary to specify $\hat{p}(f_m)$ for $0 \le m \le N/2$ (i.e., for frequencies between zero and the Nyquist frequency). The spectral density defined in equation (5) is defined by analogy to the conventions used by Blackman and Tukey (1958) to be a two-sided spectral density in which only the right-hand side is reported. That is, the total variance of the water level elevations would be equal to $2\sum_{m=0}^{N-1} \hat{p}(f_m)\Delta f$.

The second procedure, involving the fast Fourier transform, was selected for the spectral computations for Hurrican Carla because it incurred less loss of information than the covariance procedure. The FFT method permits the inspection of all 2,048 spectral lines for frequencies up to the Nyquist frequency before the lines are averaged to yield a smooth estimate, $\hat{\hat{p}}(f)$, of the spectral density. The covariance method gives only the smoothed spectral density.

However, conclusions concerning statistical confidence for spectral estimates based on data computed with the FFT method are valid also for spectral estimates based on the covariance method. The two procedures for computing the spectral density give essentially the same result.

III. ESSENTIAL EQUIVALENCE OF THE FFT AND COVARIANCE METHODS

The covariance procedure gives spectral estimates which approximate a smoothing of the population or "true" spectral density. The effective width of the smoothing is approximately $1/(2k_m\Delta t)$, where $k_m\Delta t$ is the maximum lag used in the covariance estimate (i.e., k_m is the maximum value of k used in computing equation (1)) and Δt is the time increment between water level measurements (Blackman and Tukey, 1958). (See App. A for the definition of effective width.) If "hamming" smoothing,

$$\tilde{\tilde{p}}_s(f_r) = (1/4)\tilde{p}(f_{r-1}) + (1/2)\tilde{p}(f_r) + (1/4)\tilde{p}(f_{r+1}) \quad , \tag{9}$$

is then made, the effective smoothing width for the estimates, $\tilde{\tilde{p}}_s(f_r)$, is changed to $1/(k_m\Delta t)$ (Blackman and Tukey, 1958).

The FFT method also yields estimates which are smoothed versions of the true underlying population spectral density. This can be seen from the following derivation.

The true or population spectral density is defined as the integral Fourier transform of the theoretical covariance function. That is,

$$C(\tau) = E[\eta(t)\ \eta(t + \tau)] \quad , \tag{10}$$

where $E[\cdot]$ denotes the expectation operator and

$$p(f) = \int_{-\infty}^{\infty} C(\tau)\ e^{-i2\pi f\tau}\ d\tau \tag{11}$$

(Blackman and Tukey, 1958). Since $C(\tau)$ is symmetric about $\tau = 0$ for stationary stochastic processes, it follows that equation (11) reduces to:

$$p(f) = \int_{-\infty}^{\infty} C(\tau)\ \cos\ (2\pi f\tau)\ \ d\tau \quad . \tag{12}$$

Equations (1) and (2) are obvious analogues to equations (10) and (12). It is not immediately obvious that the same thing can be said for equations (4) and (5), although it is true there also. To see this, let

$$\hat{C}_k = \frac{1}{N} \sum_{n=0}^{N-1} \eta_n \eta_{n+k} \quad , \tag{13}$$

where $N = 4{,}096$ in the context of the Hurricane Carla records and the η_n for $n \geq N$ and $n<0$ required for the computation of equation (13) are defined by periodicity as:

$$\eta_n = \eta_{n-N} \quad . \tag{14}$$

Equation (13) will give almost the same estimate of the covariance function as equation (1) for $0 \leq k \leq N/2$. There is, of course, a little distortion related to the effects of equation (14). However, this will be overwhelmed by the averaging against the other "within sequence" lag products provided water level observations separated by more than k_m time increments are essentially independent of each other and k_m is small.

The periodicity introduced in equation (14) causes a corresponding periodicity in $\hat{C}_k$.

$$\hat{C}_k = \hat{C}_{-k} = \hat{C}_{N-k} \quad \text{for} \quad N/2 \leq k \leq N \quad . \tag{15}$$

An approximation to equation (12) would be

$$\hat{p}(f_m) = \sum_{k=\frac{N}{2}+1}^{N/2} \hat{C}_k \cos\,(2\pi f_m k \Delta t)\,\Delta t \quad . \tag{16}$$

With the introduction of equation (15) and the definition of f_m (equation 6), this becomes:

$$\hat{p}(f_m) = \Delta t \sum_{k=0}^{N-1} \hat{C}_k \cos\left(2\pi \frac{m}{N\Delta t}\, k\, \Delta t\right) = \Delta t \sum_{k=0}^{N-1} \hat{C}_k \cos\,(2\pi mk/N) \quad . \tag{17}$$

The last equation is algebraically equivalent to equation (5) although it appears somewhat different. The equivalence can be seen after equation (13) is substituted for $\hat{C}_k$ and the transform is shifted to exponential form. Thus,

$$\hat{p}(f_m) = \Delta t \sum_{k=0}^{N-1} \left(\frac{1}{N} \sum_{n=0}^{N-1} \eta_n \eta_{n+k} \right) \exp\,(-i2\pi mk/N)$$

$$= \frac{\Delta t}{N} \sum_{k=0}^{N-1} \sum_{n=0}^{N-1} \left[\eta_n \exp\,(+i2\pi mn/N)\right] \left[\eta_{n+k} \exp(-i2\pi m(n+k)/N\right]$$

$$= \frac{\Delta t}{N} \sum_{n=0}^{N-1} \left[\eta_n \exp\,(i2\pi mn/N)\right] \sum_{k=0}^{N-1} \left[\eta_k \exp\,(-i2\pi mk/n)\right] \tag{18}$$

after the introduction of the periodicity assumed in equation (14). It follows that

$$\hat{p}(f_m) = (\overline{A_m}\ A_m)/N\Delta t = (U_m^2 + V_m^2)/N\Delta t \quad , \tag{19}$$

where $\overline{A_m}$ denotes the complex conjugate of A_m. This is the desired conclusion and equations (5) and (17) have been shown to be equivalent.

Returning to the question of the amount of spectral smoothing involved in the estimate, $\hat{p}(f_m)$, define the finite Dirac comb (Blackman and Tukey, 1958) as:

$$\nabla_c\ (\tau;\Delta t) = \frac{\Delta t}{2}\ \delta\ (\tau + c\ \Delta t) + \Delta t \sum_{k=-c+1}^{c-1} \delta(\tau - k\Delta t) + \frac{\Delta t}{2}\ \delta(\tau - c\ \Delta t) \quad , \tag{20}$$

where $\delta(x)$ is the Dirac function which has the properties:

$$\int_{-\infty}^{\infty} \delta(x)dx = 1 \tag{21}$$

$$\delta(x) = 0 \quad , \quad \text{if } x \neq 0 \tag{22}$$

and for any bounded function $g(x)$:

$$\int_{-\infty}^{\infty} \delta(c - x)g(x)dx = g(c) \quad . \tag{23}$$

Now suppose the sampling questions involved $\hat{C}_k$ are ignored and $C(k\Delta t)$ is inserted in place of $\hat{C}_k$ in equation (16). Then,

$$\hat{p}(f_m) \approx \int_{-\infty}^{\infty} C(\tau)\ \nabla_{N/2}\ (\tau;\Delta t)\ e^{-i2\pi f_m \tau}\ d\tau \quad . \tag{24}$$

The right-hand side of this equation is the Fourier transform of $C(\tau)\ \nabla_{N/2}\ (\tau;\Delta t)$. Thus, by Fourier transform theory $\hat{p}(f_m)$ is the convolution of the transforms of the separate functions or

$$\hat{p}(f_m) \approx p(f_m) * \sum_{k=-\infty}^{\infty} Q_0\left(f_m - \frac{k}{\Delta t}\right) \quad . \tag{25}$$

In the above $p(f_m)$ is the transform of $C(\tau)$ by equation (11) and $\sum_{k=-\infty}^{\infty} Q_0\left(f - \frac{k}{\Delta t}\right)$ is the transform of $\nabla_{N/2}$ $(\tau;\Delta t)$ (Blackman and Tukey, 1958). The function $Q_0(f)$ is (Blackman and Tukey, with $T_m = N\Delta t/2$):

$$Q_0(f) = \frac{\sin(\pi f N \Delta t)}{\pi f} \quad . \tag{26}$$

Hence,

$$\hat{p}(f_m) \approx \sum_{k=-\infty}^{\infty} \int_{-\infty}^{\infty} Q_0\left(f_m - \frac{k}{\Delta t} - y\right) p(y)\,dy \quad . \tag{27}$$

This shows that $\hat{p}(f_m)$, to the extent that $\hat{C}_k$ behaves like $C(k\Delta t)$, is the result of smoothing with the $Q_0(f)$ function and then summing or aliasing as indicated by the summation.

The function $Q_0(f)$ has an effective width of $(1/N\Delta t)$. Hence, $\hat{p}(f_m)$ represents a smoothing approximately over a frequency interval of $(1/N\Delta t)$. This is the spacing between the f_m in equation (6). It follows that each FFT spectral estimate represents approximately a smoothing of $p(f)$ over the interval $f_m \pm (1/2N\Delta t)$.

It should be noted that problems related to the side lobes of $Q_0(f)$, the aliasing, and the sampling variability have been ignored in the above discussion. These effects will now be discussed briefly. The distortion due to aliasing can be mitigated by choosing the Nyquist frequency sufficiently large. The sampling variability shows up in the statistical fluctuations of the estimates and can be examined from that perspective. If the true spectra are relatively smooth and linearly changing, the side lobes of $Q_0(f)$ will compensate for each other somewhat. However, if the true spectra are not smooth, there will be unavoidable leakage of large spectral departures or spikes into neighboring spectral estimates.

IV. FFT AVERAGING NEEDED TO GIVE SPECTRA EQUIVALENT TO THOSE FROM THE COVARIANCE METHOD

From the previous section, the covariance spectral estimates (after hamming) represent a smoothing over the frequency interval of width, $(1/k_m \Delta t)$, while the FFT spectral estimates involve a smoothing over a frequency interval of width, $(1/N \Delta t)$. Hence, the number of FFT spectral lines that should be averaged together to yield an estimate with approximately the same smoothing as the covariance spectral estimates is:

$$\text{number} = \frac{(1/k_m \Delta t)}{(1/N \Delta t)} = N/k_m \quad . \tag{28}$$

V. SUMMARY OF COMPUTATIONAL FORMULAS USED FOR THE HURRICANE CARLA WAVE SPECTRA

Twelve pieces of record at various times in the storm (Table 1) were chosen for analysis. Each piece consisted of $N = 4,096$ values of water level elevations taken at a time increment of $\Delta t = 0.2$. Thus, each of these records was $N\Delta t = 13.65$ minutes long. The frequency scale increment would be $\Delta f = 1/N\Delta t = 0.00122$ sec.$^{-1}$. The Nyquist frequency for this choice is $f_{Ny} = 1/2\Delta t = 1/0.4 = 2.5$ sec.$^{-1}$ which corresponds to a period of 0.4 second. Energy in waves with periods smaller than 0.4 second would thus be aliased into lower frequencies. An examination of the final spectra produced little evidence of much energy past this selected Nyquist frequency.

Table 1. Hurricane Carla data analyzed.

Date	Time	Data code
8 Sept. 1961	0600	6877
	1200	6878
	1800	6879
9 Sept. 1961	0000	6880
	0600	6881-1
	0620	6881-2
	1200	6882
	1500	6883
	1800	6884
	2100	6885
10 Sept. 1961	0000	6886-1
	0020	6886-2

The 4,096 water level elevations were transformed by the fast Fourier transform algorithm to yield Fourier coefficients, for $0 \leq m < N$:

$$A_m = \Delta t \sum_{n=0}^{4,095} \eta_n \, e^{-i2\pi mn/N} \tag{29}$$

The spectral lines were then computed from

$$\hat{p}(f_m) = |A_m|^2/(819.2) \quad , \tag{30}$$

when $|A_m|$ denotes the complex modulus of A_m . The spectral density was estimated by a moving average of the spectral lines:

$$\hat{\hat{p}}(f_m) = \sum_j w_j \, \hat{p}(f_{m-j}) / \sum_j w_j \quad , \tag{31}$$

where

$$w_j = \exp(-j^2/18) \quad . \tag{32}$$

These weights are, thus, Gaussian smoothers with a standard deviation of $\sigma = 3\Delta f = 0.00366 \text{ sec.}^{-1}$. The numerical values of the w_j are given in Table 2. In the vicinity of zero frequency, the subscript j in equation (31) was summed over the possible values and the divisor normed the weights appropriately. At $m = 6$, for example, j was summed over $-6 \leq j \leq 13$ (the left tail of the moving average was truncated off).

Table 2. Weights used in the moving average of the spectral lines to produce the estimates of the spectral density.

j	w_j
0	1.0000
1	0.9460
2	0.8007
3	0.6065
4	0.4111
5	0.2494
6	0.1353
7	0.0657
8	0.0286
9	0.0111
10	0.0039
11	0.0012
12	0.0003
13	0.0001

Note: $w_{-j} = w_j$.

The effective width of the Gaussian smoother in equation (32) is $\sqrt{2\pi}\,\sigma$ where $\sigma = 3\Delta f$, if lags are measured on the frequency scale and $\sigma = 3$, if lags are measured relative to the number of spectral lines. The effective width in terms of number of spectral lines encompassed is thus $3\sqrt{2\pi} = 7.52$, or rounding to the nearest integer, 8 spectral lines. By equation (28), the FFT spectral density estimates so produced would be comparable to covariance spectral density estimates with maximum covariance lag derived from:

$$\frac{N}{k_m} = 8 \tag{33}$$

or

$$k_m = \frac{4{,}096}{8} = 512 \quad . \tag{34}$$

VI. DISCUSSION OF HURRICANE CARLA WAVE SPECTRA

The spectral lines (shown as dots) and the spectral density estimates averaged from the lines (shown as a line or a string of pluses) are given in Figures 1 through 12.

Close examination yields two very interesting facts. First, the peak values of the spectral densities are related closely to one or two spectral lines. Only in record 6883 is the peak related to four exceptionally large lines. In the other cases it is always one or two. Second, these exceptionally large spectral lines do not seem to persist. The two members of record pairs (6881-1 and 6881-2; 6886-1 and 6886-2) are separated from each other by only 20 minutes. Yet in both cases, exceptionally large spectral lines are present in one member of the pair but not in the other.

A general examination of the spectral lines versus the spectral density estimates cannot help but develop a sense of healthy skepticism concerning the general reality of the fine structure in the spectral density. Also, it is felt that the exceptionally large spectral lines, often twice as large as the nearest other line value, must belong to another population from the rest of the lines. Perhaps some sort of resonant phenomenon is creating a main wave train with the rest of the lines functioning as superimposed noise.

VII. STATISTICAL VARIABILITY OF THE SPECTRAL LINES

The spectral density was subtracted from each spectral line for $6 \leq m \leq 305$ to provide 300 residual values, R_m ,

$$R_m = \hat{p}(f_m) - \hat{\hat{p}}(f_m) \quad . \tag{35}$$

A positive and negative standard deviation for the residuals were computed with the weights introduced in Table 2. Let J_+ be the values of the index m for which the residuals are positive while J_- are the values of m for which the residuals are negative. The positive and negative variance of the residuals are defined as:

$$\sigma^2_{+,m} = \sum_{j\varepsilon J_+} w_j R^2_{m-j} \Big/ \sum_{j\varepsilon J_+} w_j \tag{36}$$

$$\sigma^2_{-,m} = \sum_{j\varepsilon J_-} w_j R^2_{m-j} \Big/ \sum_{j\varepsilon J_-} w_j \tag{37}$$

where "ε" means "belongs to the set of." Thus, $\sigma_{+,m}$ will be a moving average estimate of the root-mean-square (rms) of the positive residuals in the vicinity of the frequency f_m. A similar statement relative to $\sigma_{-,m}$ and the negative residuals will also hold.

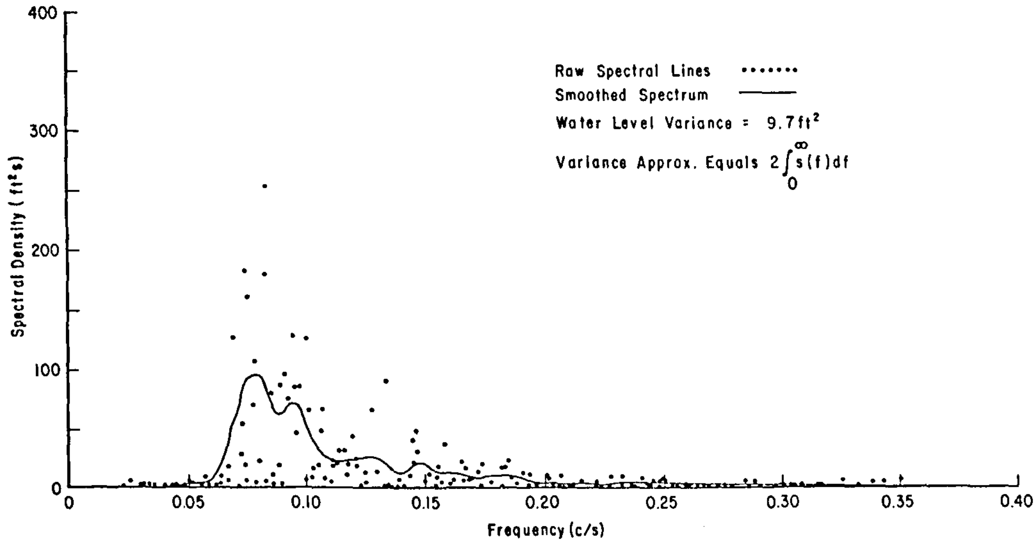

Figure 1. Hurricane Carla spectrum record number 6877, 0600 hours, 8 September 1961.

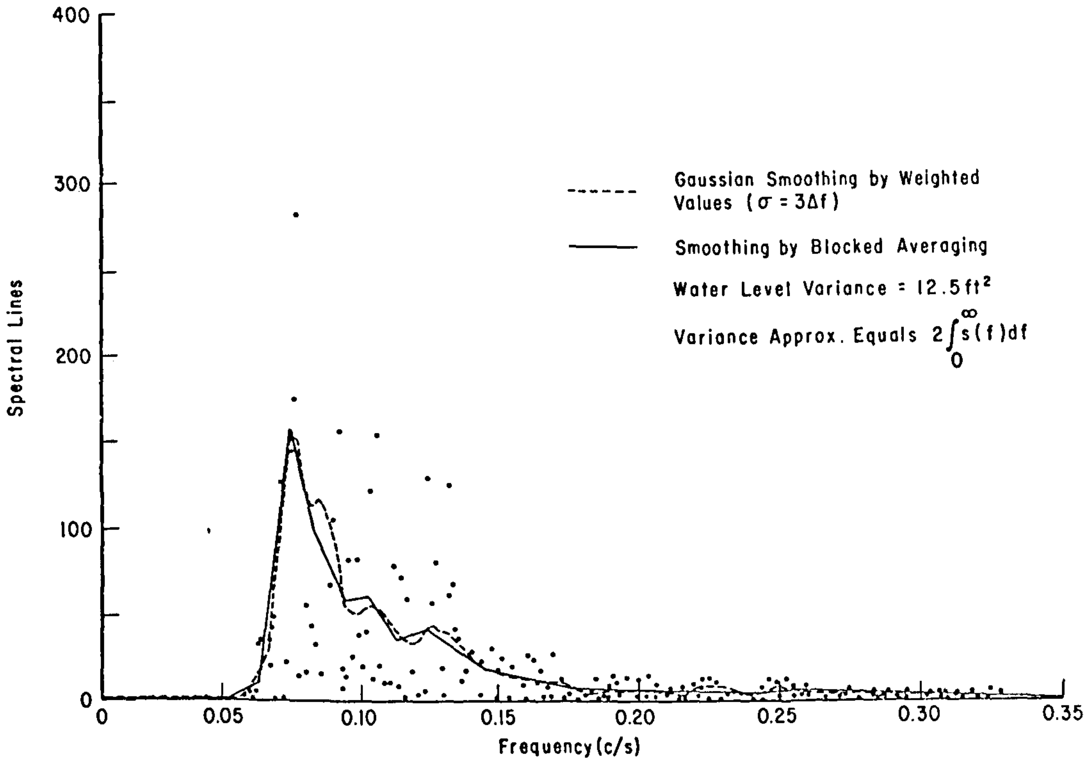

Figure 2. Hurricane Carla data number 6878, 1200 hours, 8 September 1961. Various smoothings of spectral data.

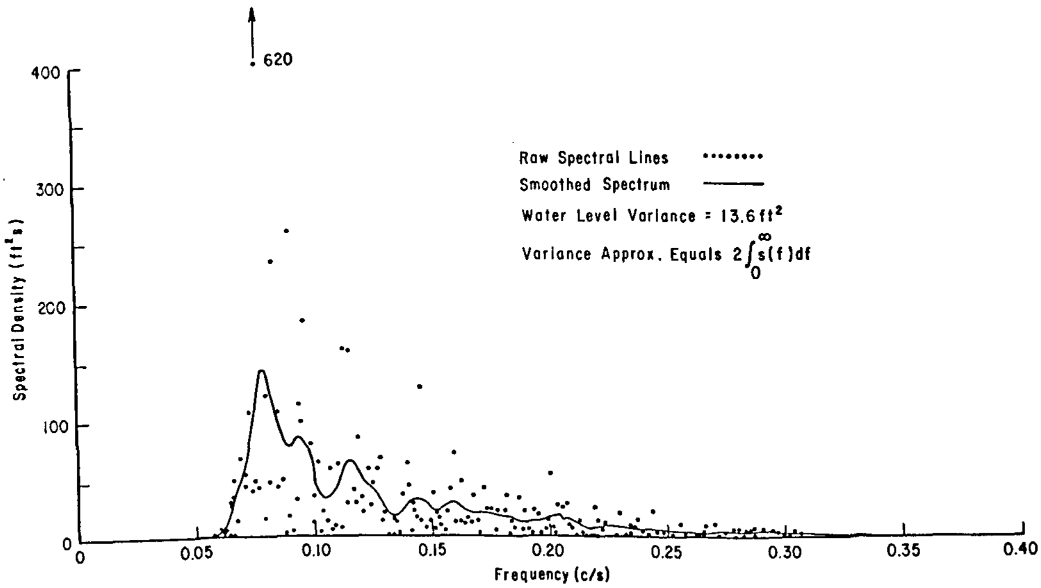

Figure 3. Hurricane Carla spectrum record number 6879, 1800 hours, 8 September 1961.

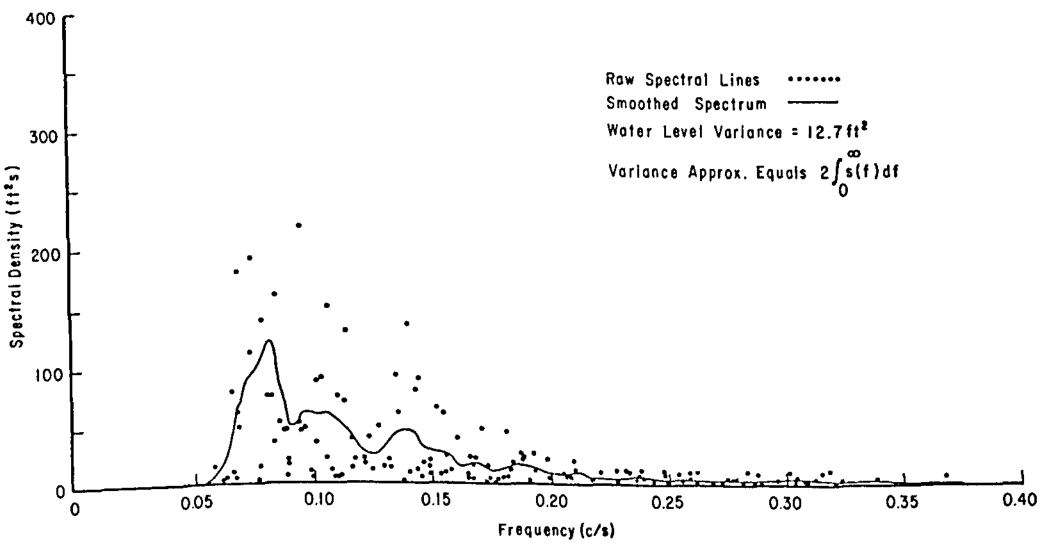

Figure 4. Hurricane Carla spectrum record number 6880, 0000 hours, 9 September 1961.

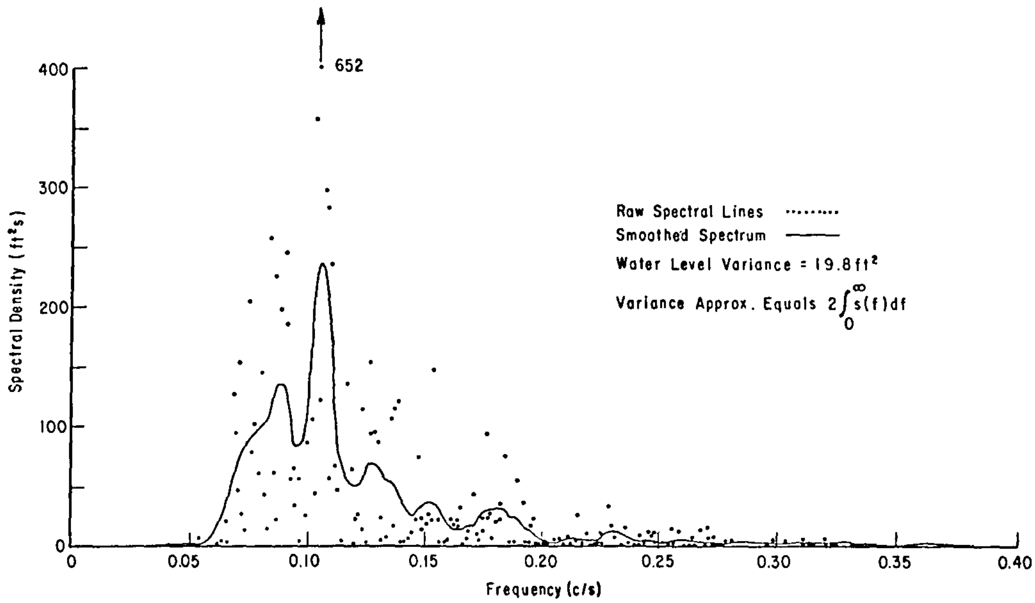

Figure 5. Hurricane Carla spectrum record number 6881-1, 0600 hours, 9 September 1961.

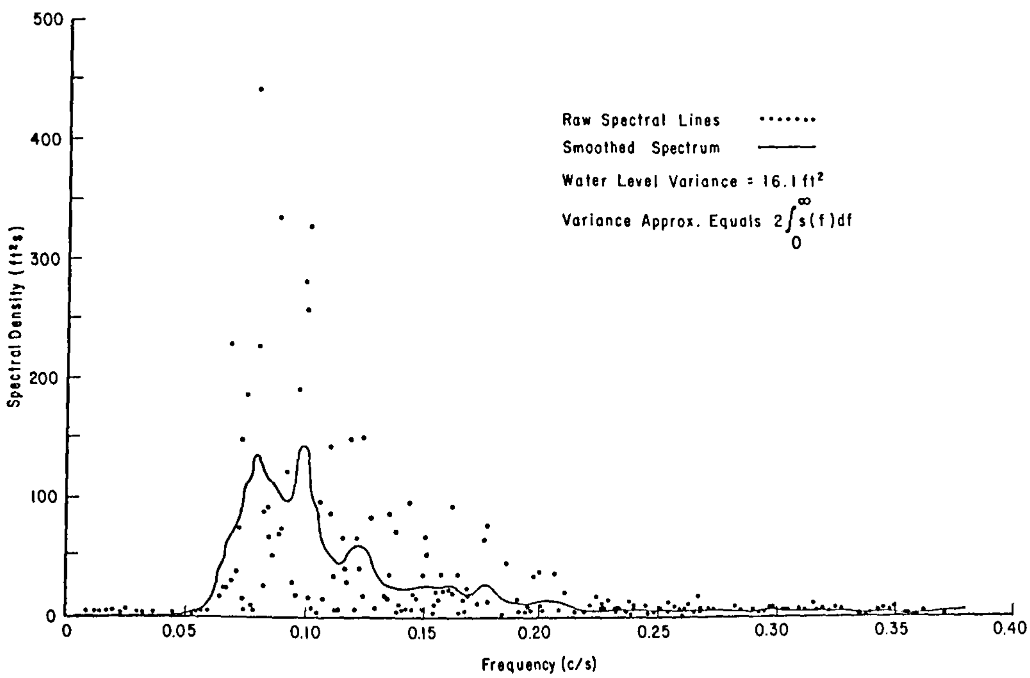

Figure 6. Hurricane Carla spectrum record number 6881-2, 0620 hours, 9 September 1961.

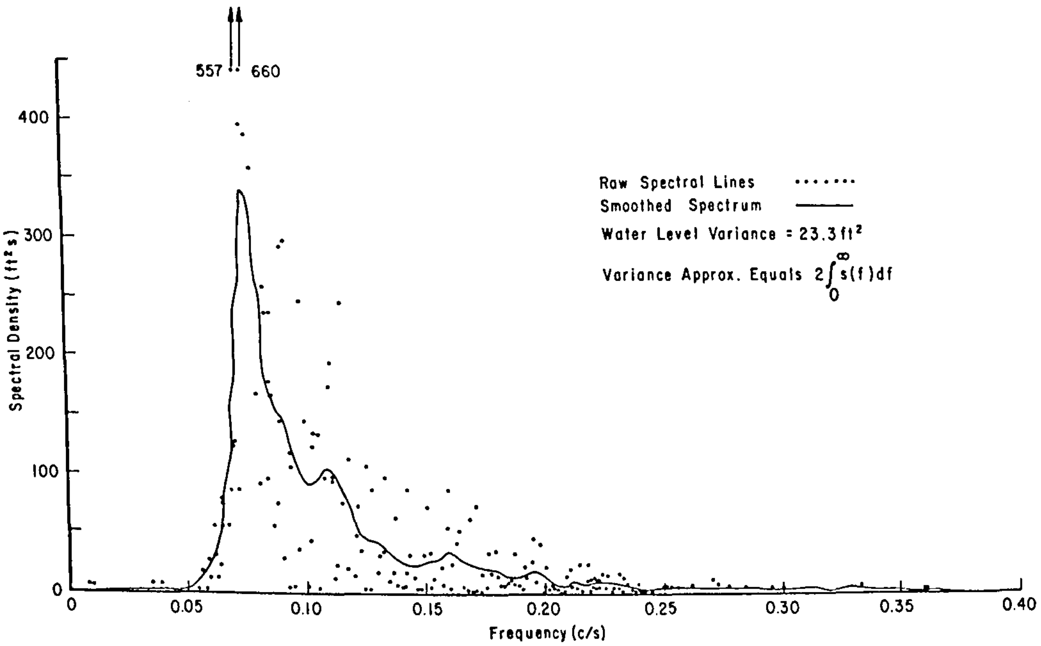

Figure 7. Hurricane Carla spectrum record number 6882, 1200 hours, 9 September 1961.

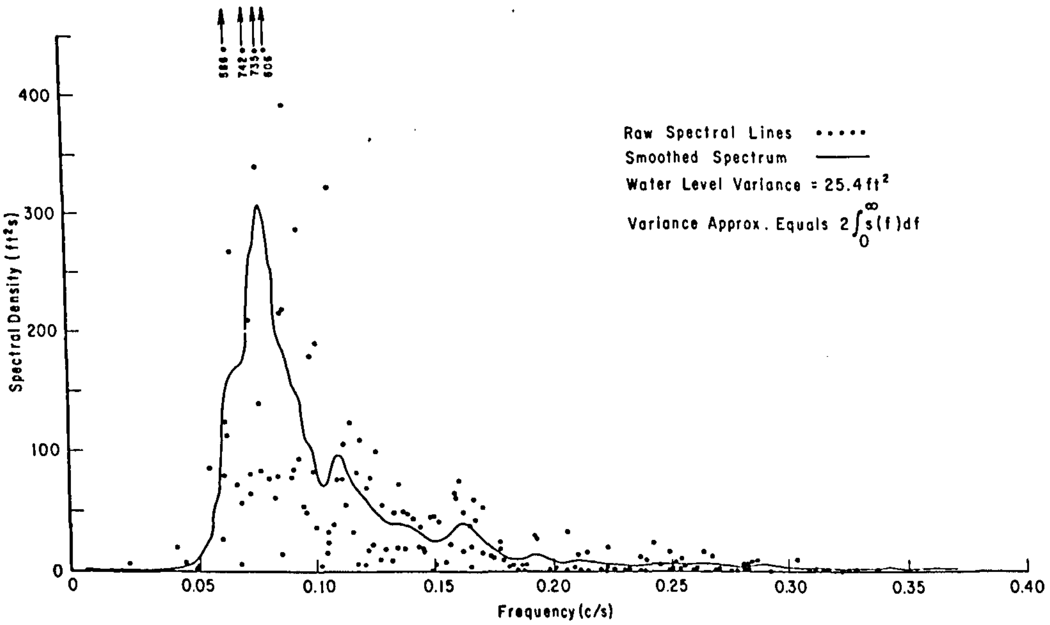

Figure 8. Hurricane Carla spectrum record number 6883, 1500 hours, 9 September 1961.

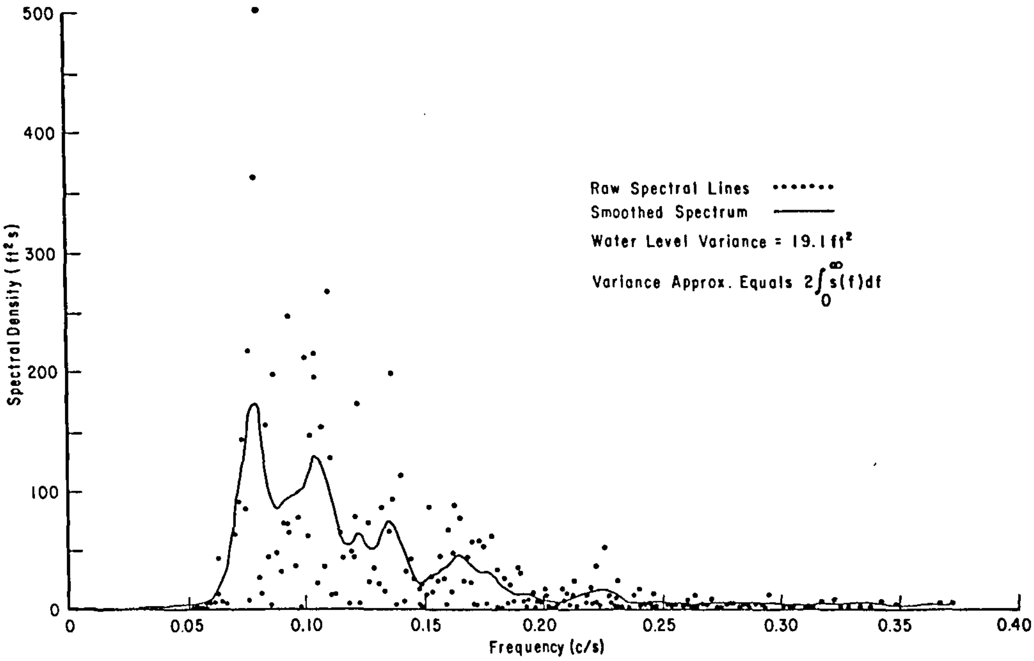

Figure 9. Hurricane Carla spectrum record number 6884, 1800 hours, 9 September 1961.

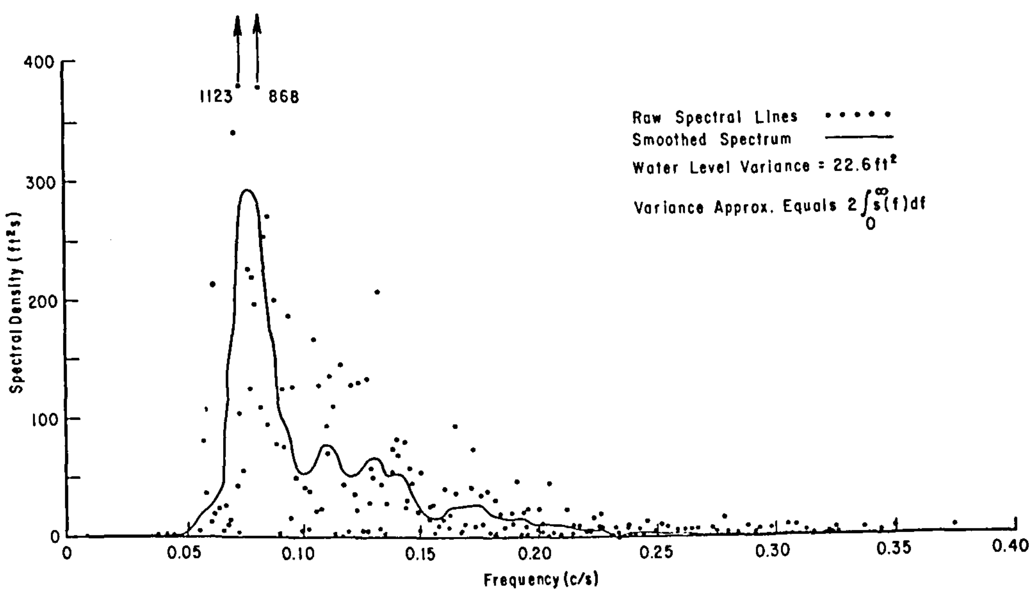

Figure 10. Hurricane Carla spectrum record number 6885, 2100 hours, 9 September 1961.

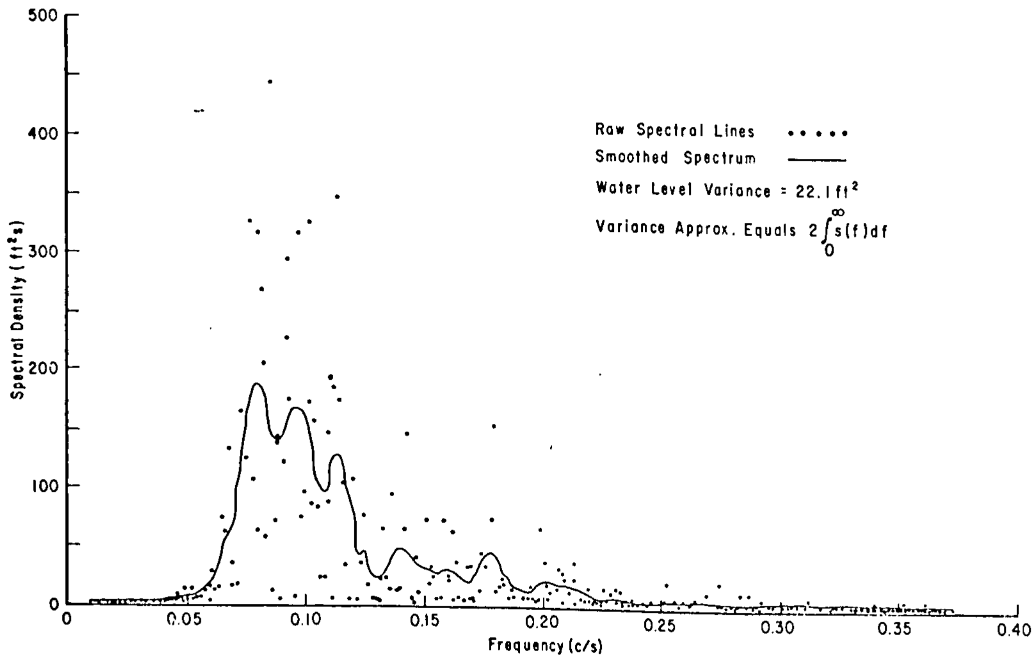

Figure 11. Hurricane Carla spectrum record number 6886-1, 0000 hours, 10 September 1961.

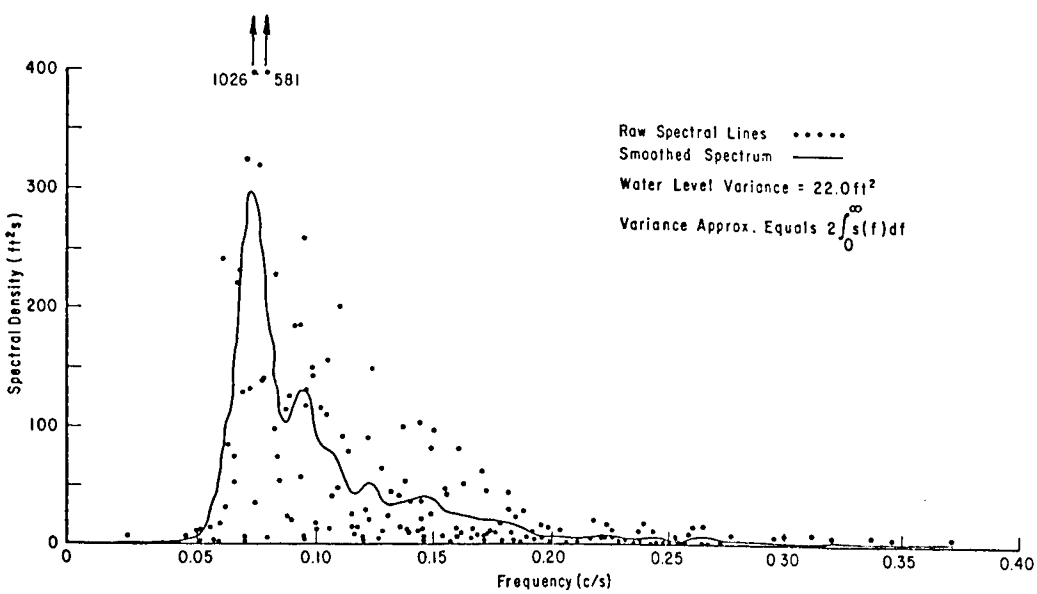

Figure 12. Hurricane Carla spectrum record number 6886-2, 0020 hours, 10 September 1961.

Symmetrically normed residuals (SNR) are then defined as:

$$\text{SNR} = \begin{cases} R_m / \sigma_{+,m} & , \text{ if } R_m \geq 0 \\ \\ R_m / \sigma_{-,m} & , \text{ if } R_m < 0 \end{cases} \quad . \tag{38}$$

Thus, the symmetrically normed residuals are ratios of the residuals to the rms positive or negative residuals, as the case may be.

Originally, the analysis was made with rms residual, disregarding whether the residuals were positive or negative. This, however, led to ridiculous results particularly in the subsequent use in simulation. The use of different norming divisors for negative and positive residuals avoided these peculiarities completely.

The residuals and the corresponding SNR's are plotted in Figures 13 through 24. The symmetrical normalization seems to very adequately produce a uniform cloud of points. There does not seem to be any tendency for the SNR's to be systematically large or small at any particular frequency. Generally about 60 percent of the SNR's fall below zero.

As a check against sequential dependence among the SNR's, neighboring pairs of SNR's were plotted on a scatter diagram in two-dimensional space. The first member of the pair of SNR's was the x-coordinate while the second member was the y-coordinate for the plotted point. Any tendency fo big values to follow big values (or the reverse) would show up as a clustering tendency on such a plot. Complete independence, on the other hand, would show up as a uniform cloud of points.

The plots of this type for the 12 Hurricane Carla data sets are given in Figures 25 through 36. The point scatter is really quite uniform for all of the records with no obvious dependencies showing up. However, it should be emphasized that this type of examination only reveals overall average dependencies. There may be dependencies between neighboring SNR's at certain frequencies which are counteracted by opposing dependencies at other frequencies. However, the earlier graphs (Figs. 13 through 24) would show any strong dependencies tied to frequencies if they were present.

Everything considered, the analyses strongly support the conclusion that the spectral fluctuations have been successfully decomposed into a smoothed spectrum plus a constant (either σ_+ or σ_-) times independent random noise. The smoothed spectrum and the constants are frequency dependent. The noise apparently does not depend on frequency. In symbols, this decomposition can be written:

$$\hat{p}(f_m) = \hat{\hat{p}}(f_m) + c \cdot (\text{SNR}) \quad , \tag{39}$$

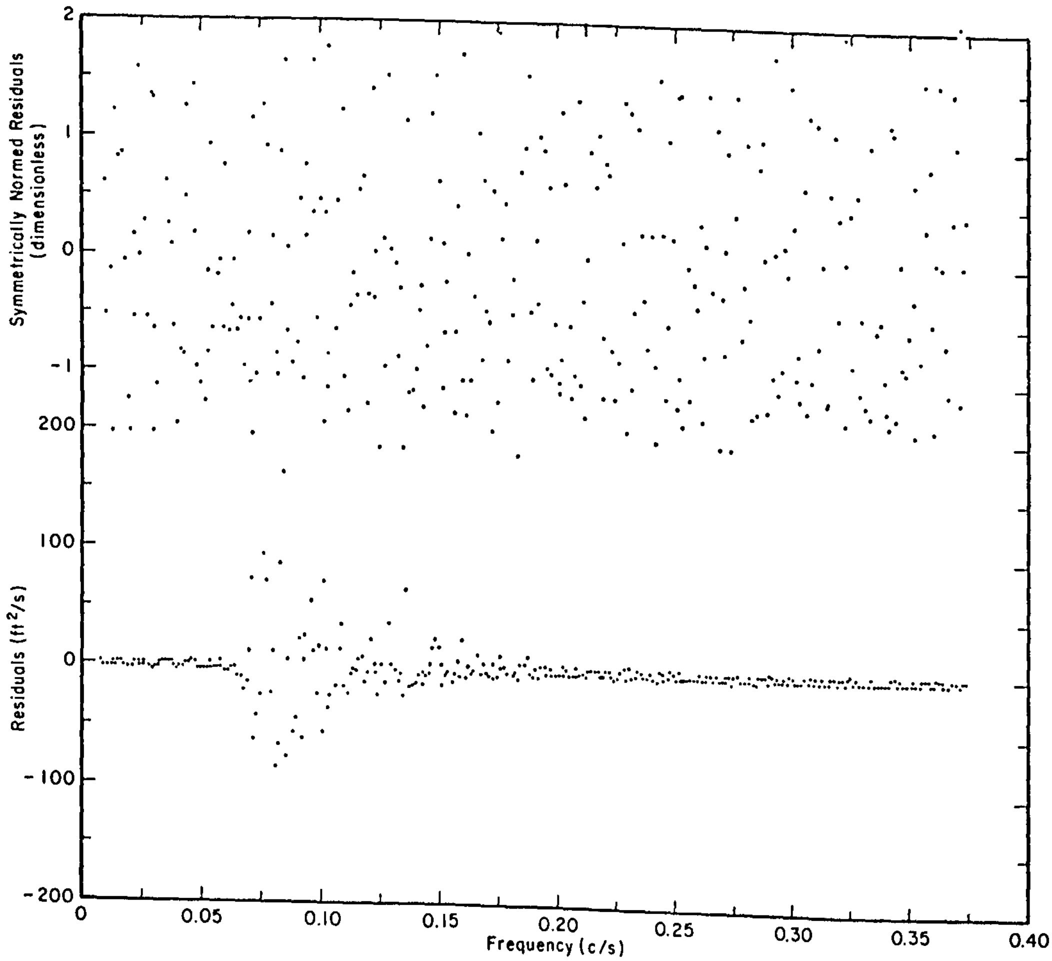

Figure 13. Residual analysis, Hurricane Carla data number 6877.

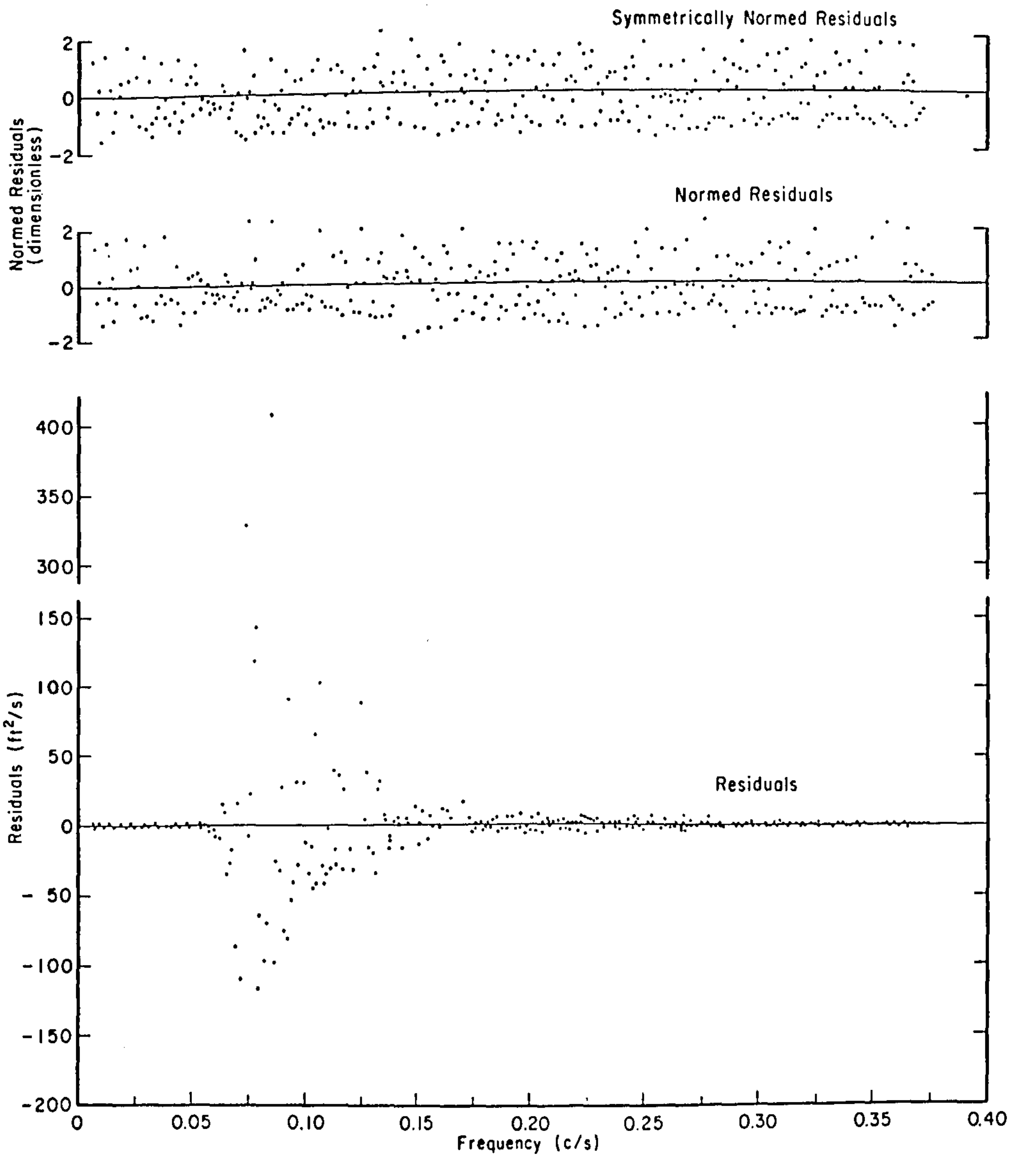

Figure 14. Hurricane Carla data number 6878, 1200 hours, 8 September 1961. Residual analysis, Gaussian smoothing on spectral lines.

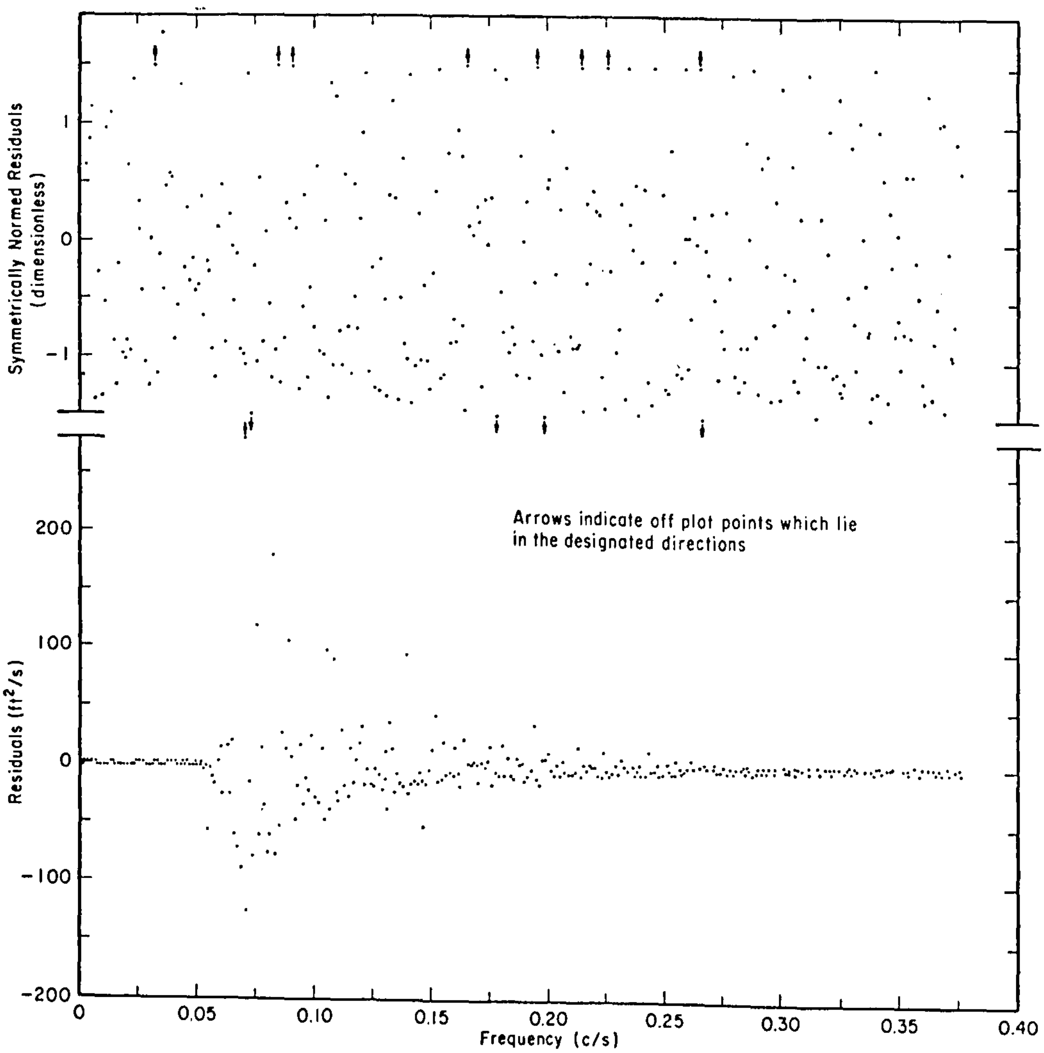

Figure 15. Residual analysis, Hurricane Carla data number 6879.

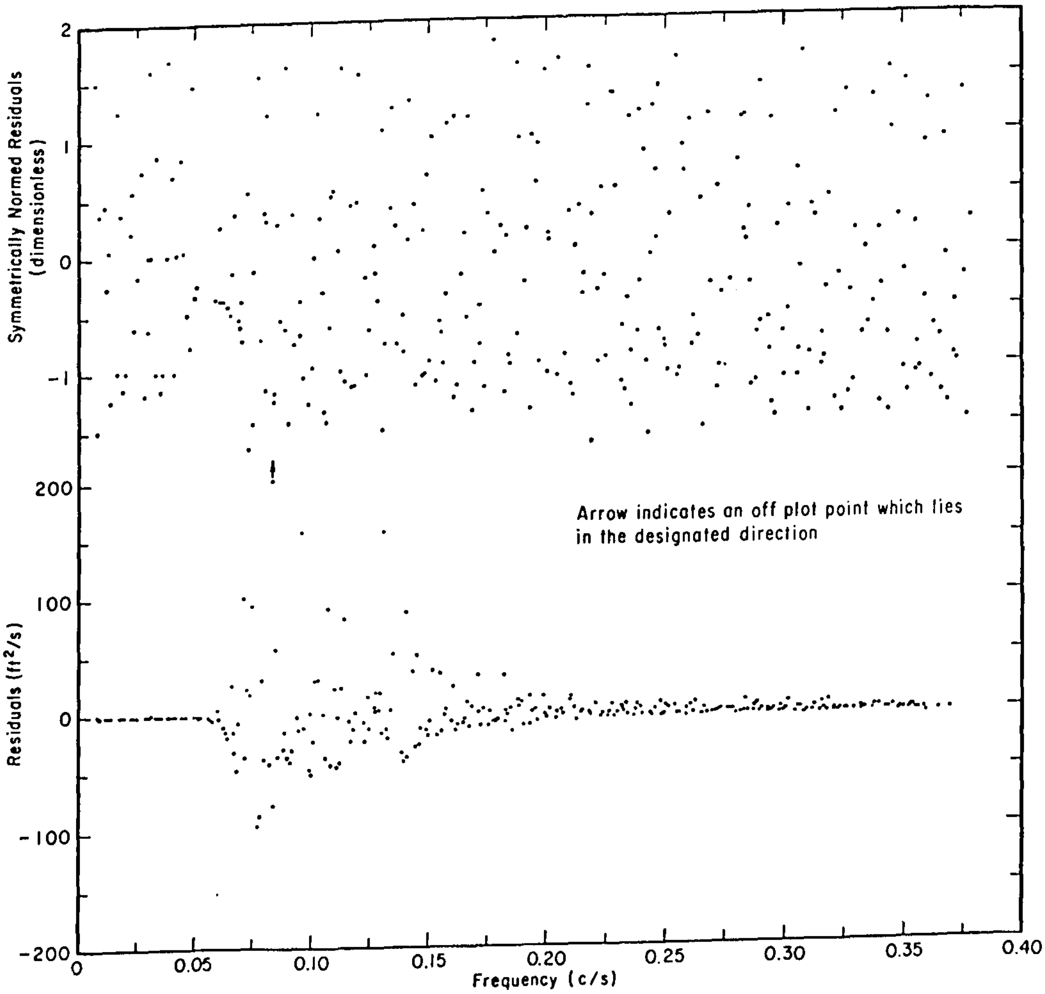

Figure 16. Residual analysis, Hurricane Carla data number 6880.

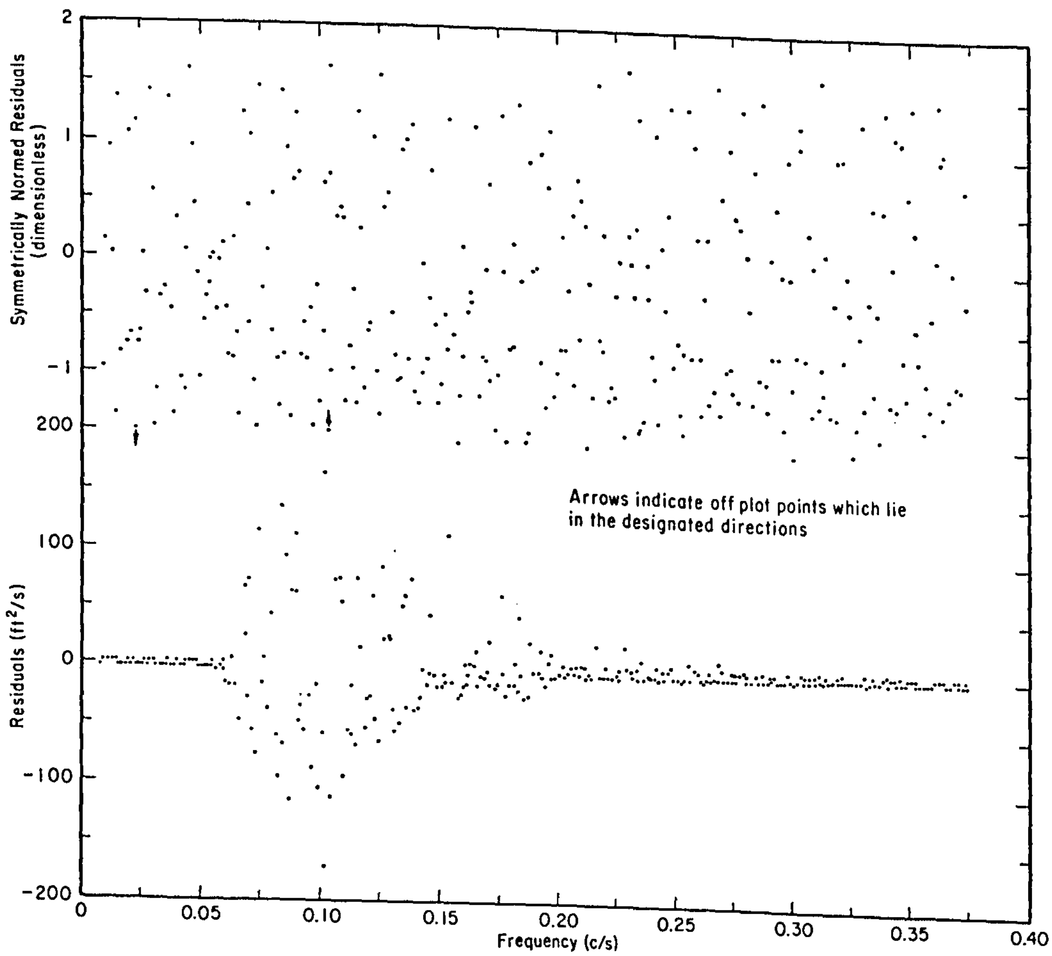

Figure 17. Residual analysis, Hurricane Carla data number 6881-1.

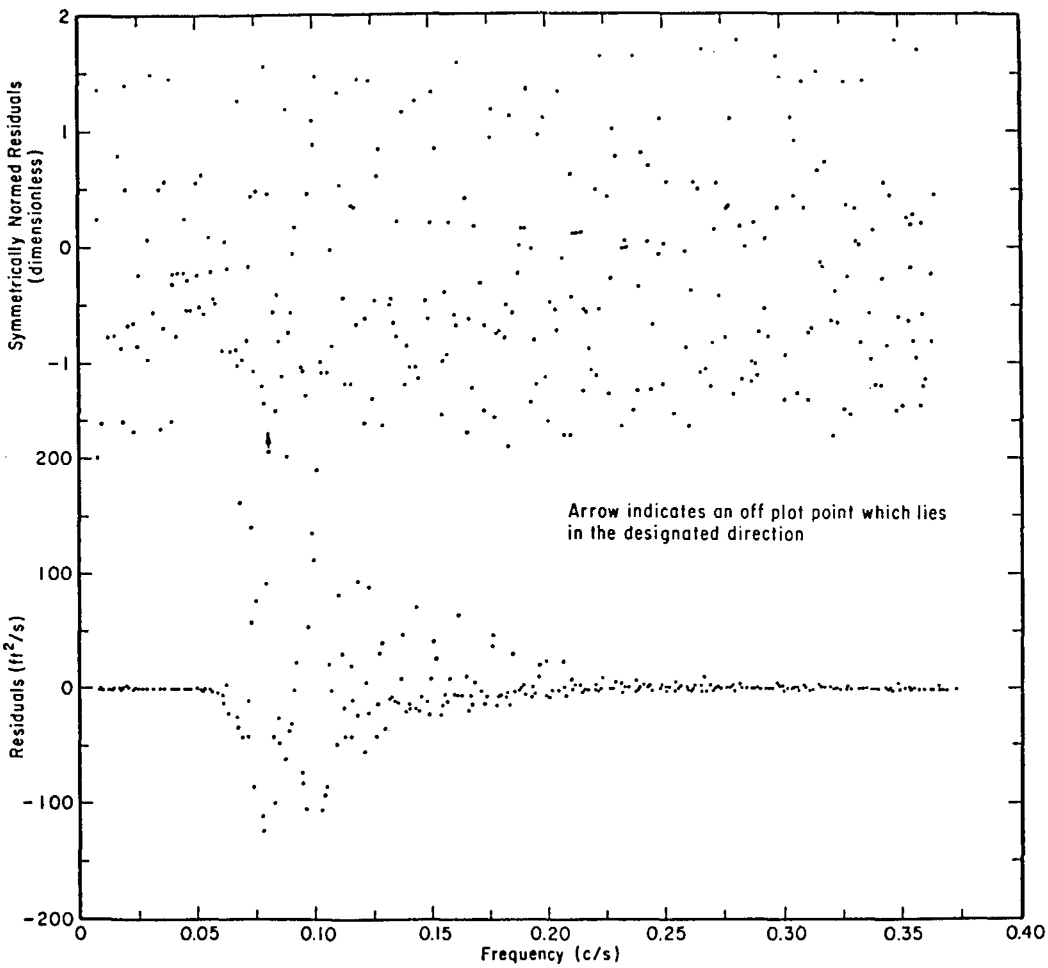

Figure 18. Residual analysis, Hurricane Carla data number 6881-2.

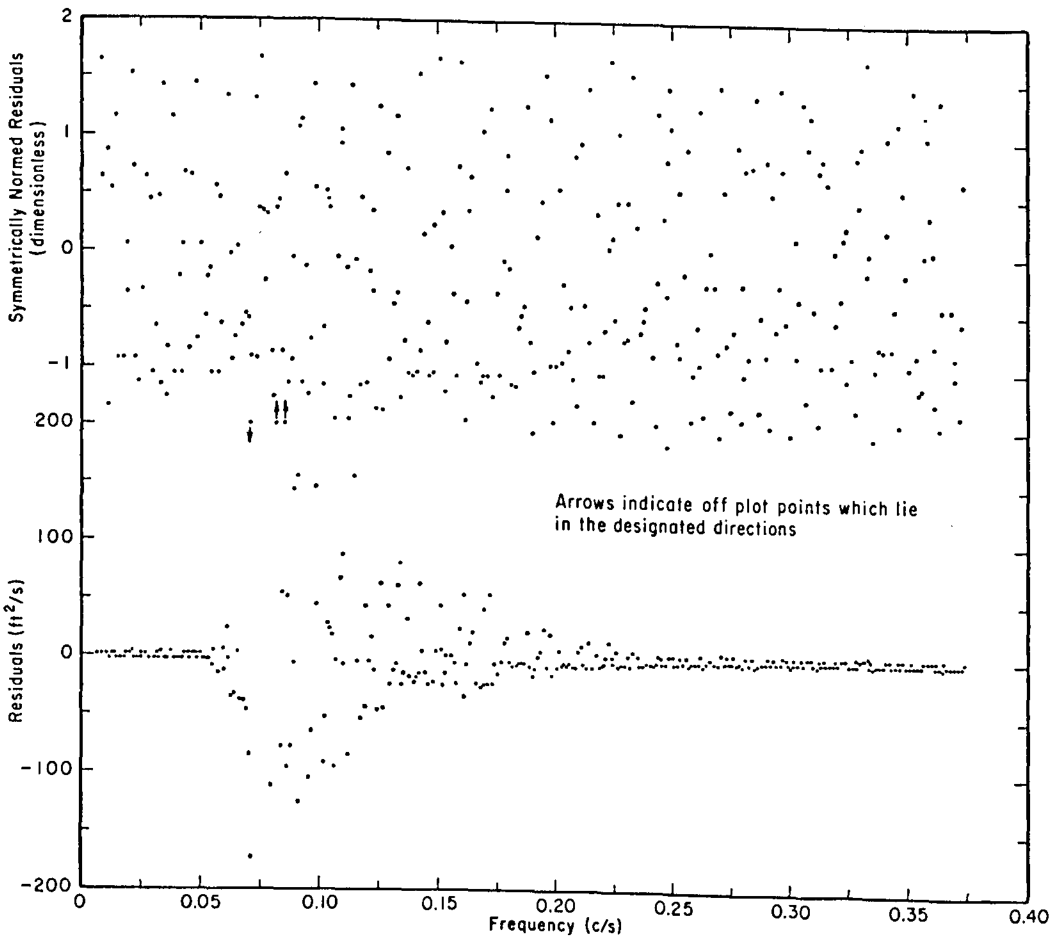

Figure 19. Residual analysis, Hurricane Carla data number 6882.

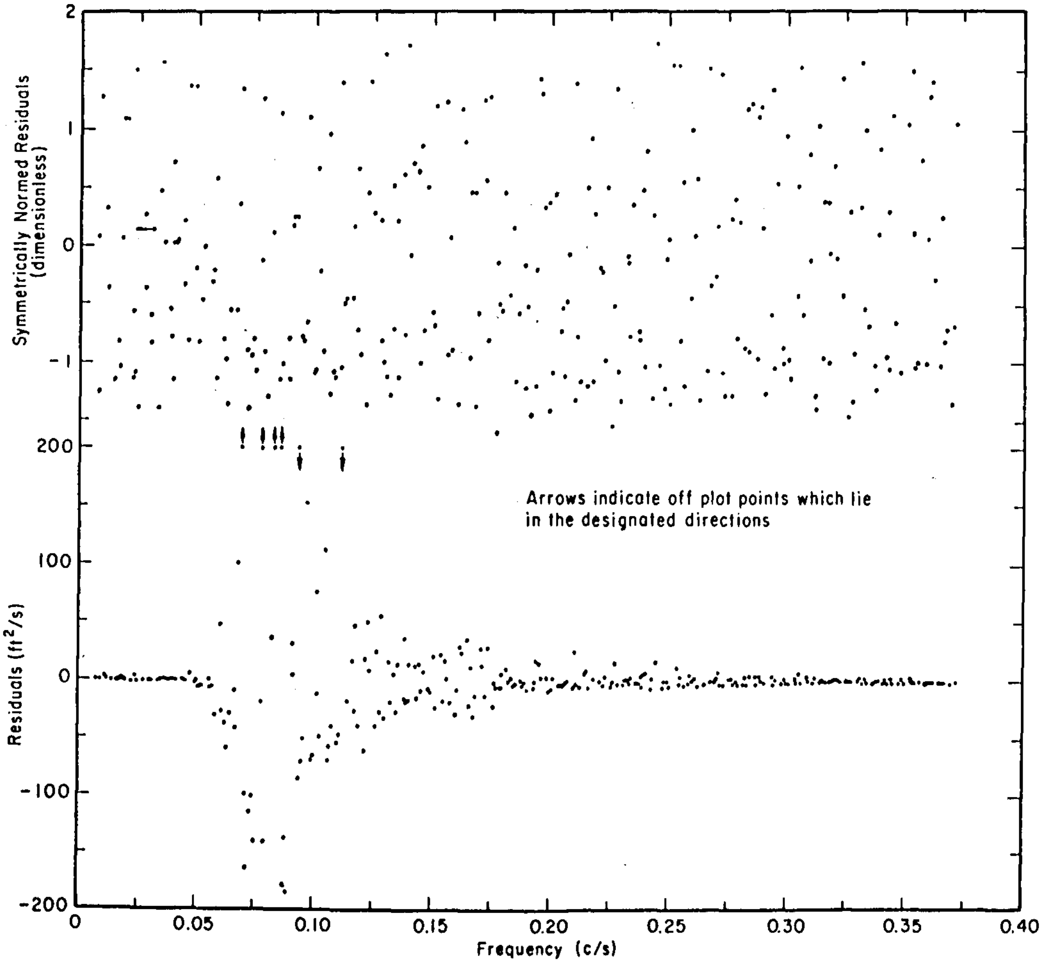

Figure 20. Residual analysis, Hurricane Carla data number 6883.

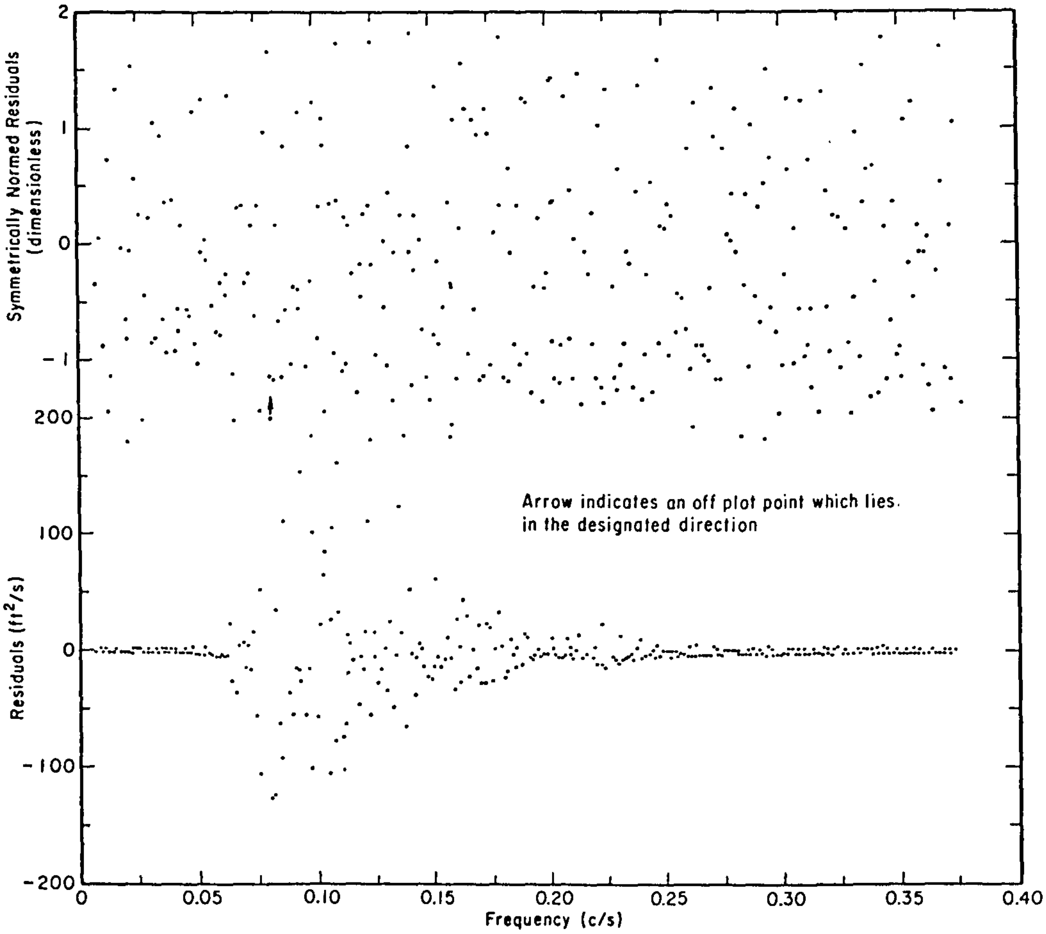

Figure 21. Residual analysis, Hurricane Carla data number 6884.

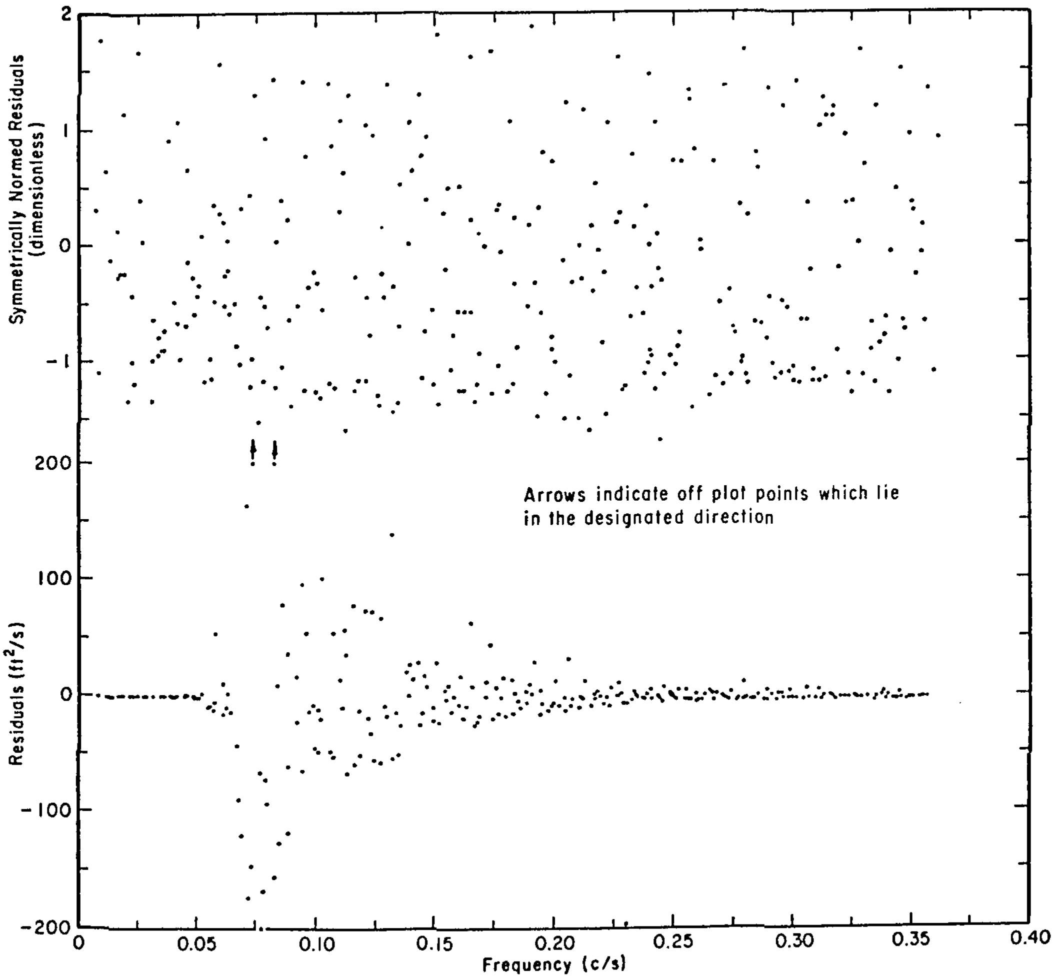

Figure 22. Residual analysis, Hurricane Carla data number 6885.

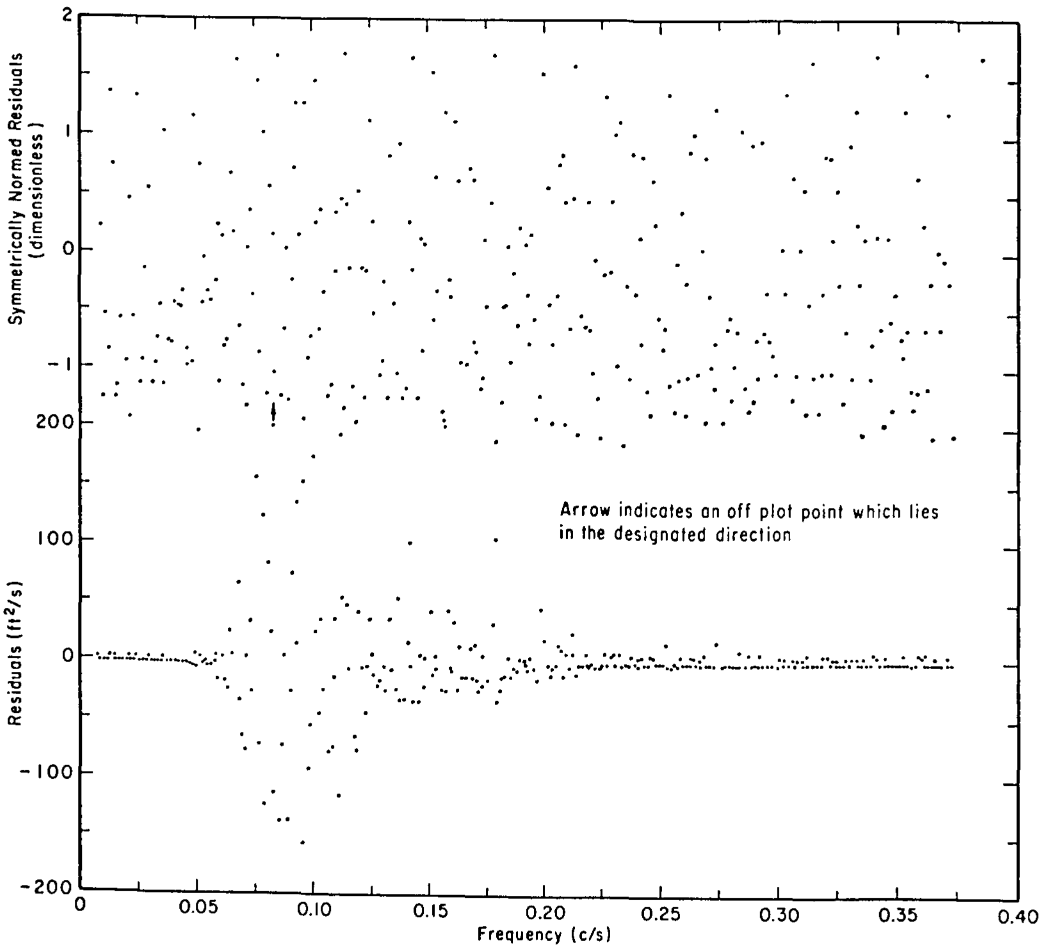

Figure 23. Residual analysis, Hurricane Carla data number 6886-1.

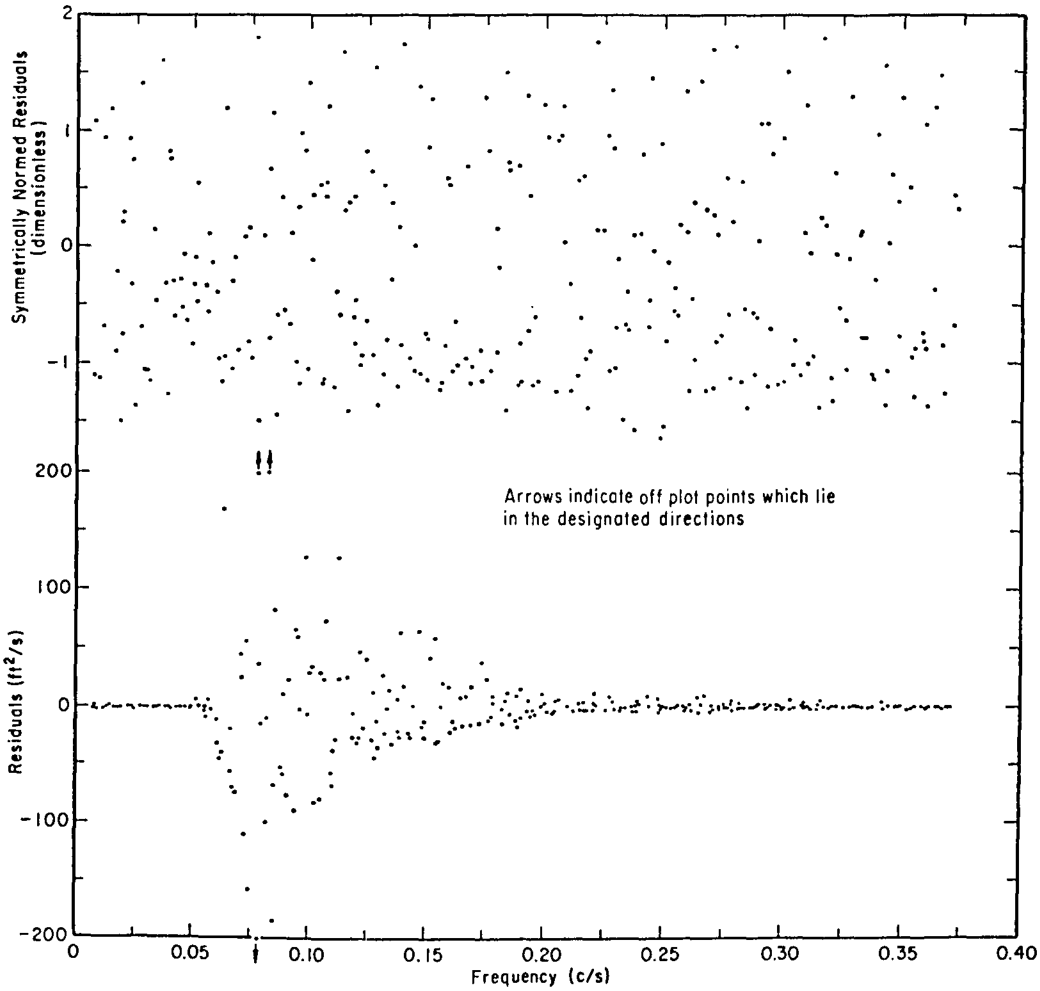

Figure 24. Residual analysis, Hurricane Carla data number 6886-2.

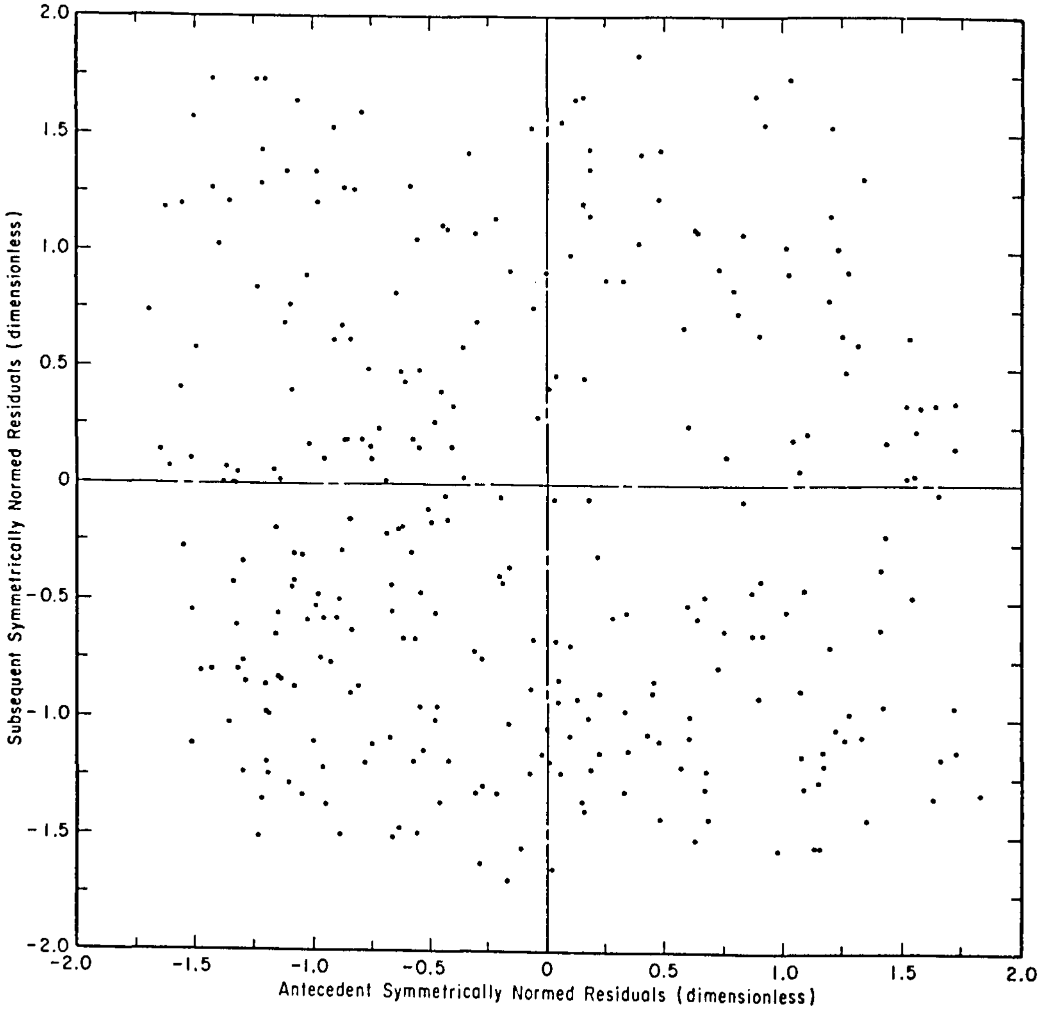

Figure 25. Scatter diagram: Sequential pairs of symmetrically normed residuals, data number 6877.

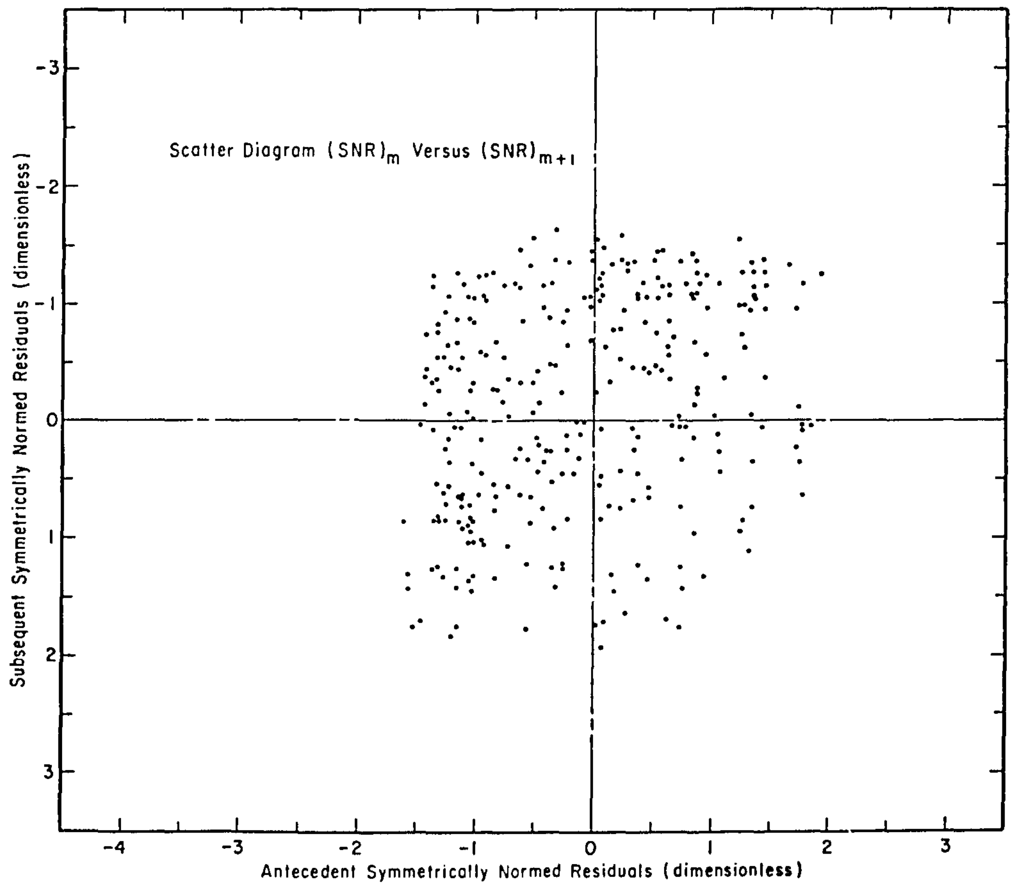

Figure 26. Scatter diagram: Sequential pairs of symmetrically normed residuals, data number 6878.

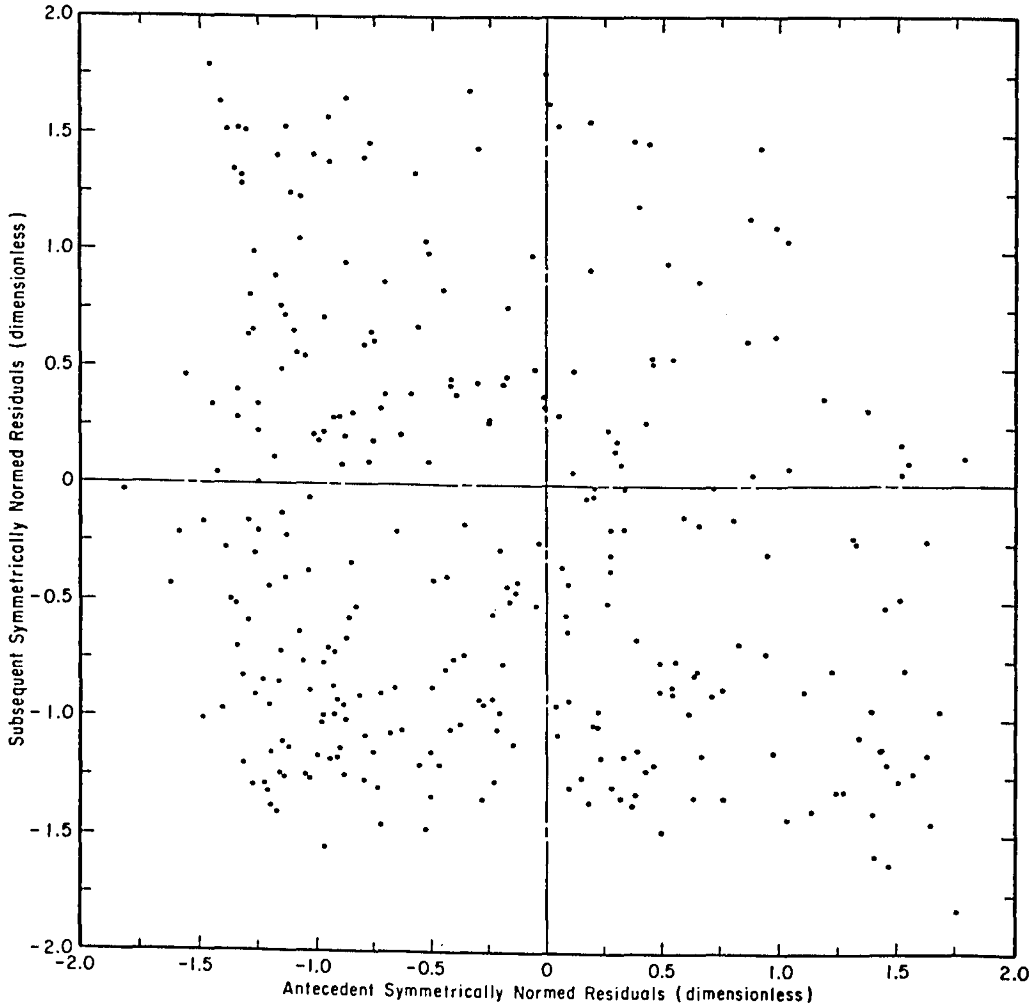

Figure 27. Scatter diagram: Sequential pairs of symmetrically normed residuals, data number 6879.

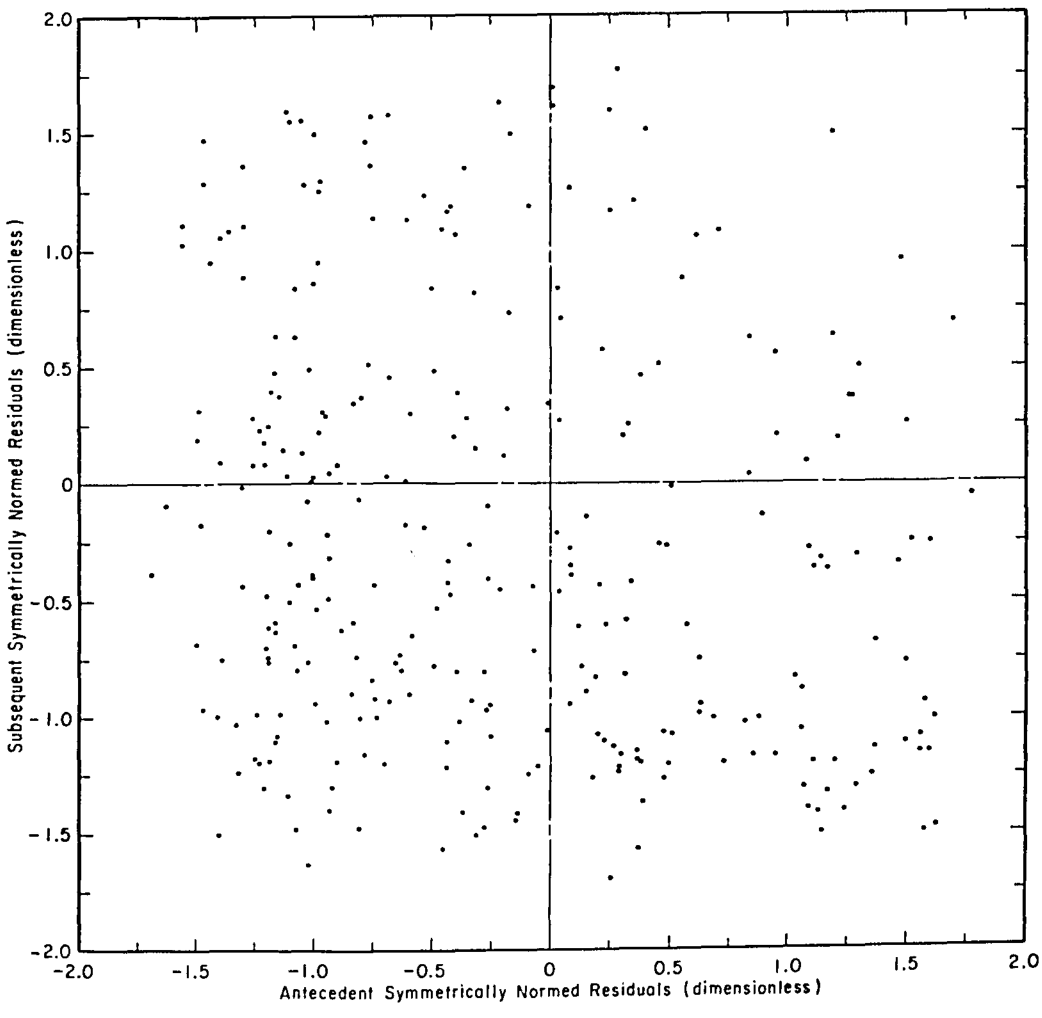

Figure 28. Scatter diagram: Sequential pairs of symmetrically normed residuals, data number 6880.

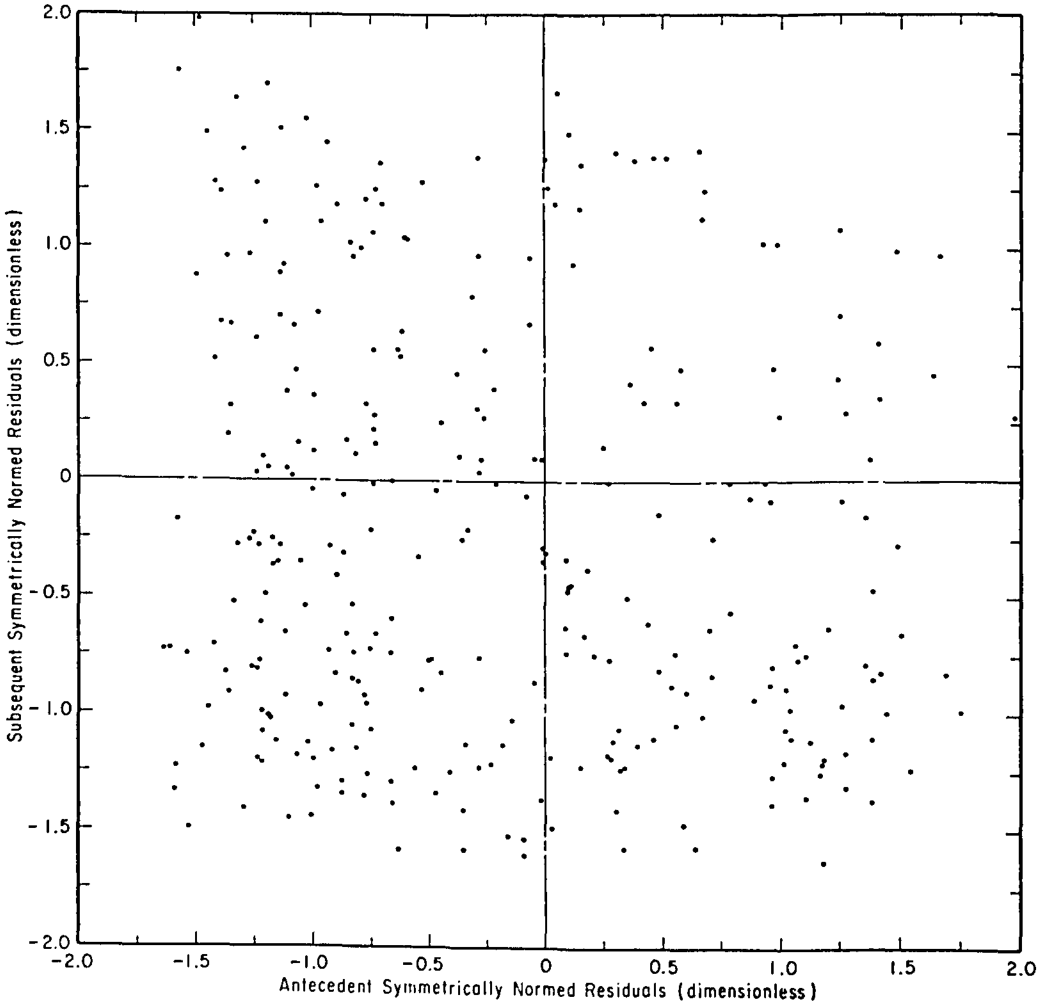

Figure 29. Scatter diagram: Sequential pairs of symmetrically normed residuals, data number 6881-1.

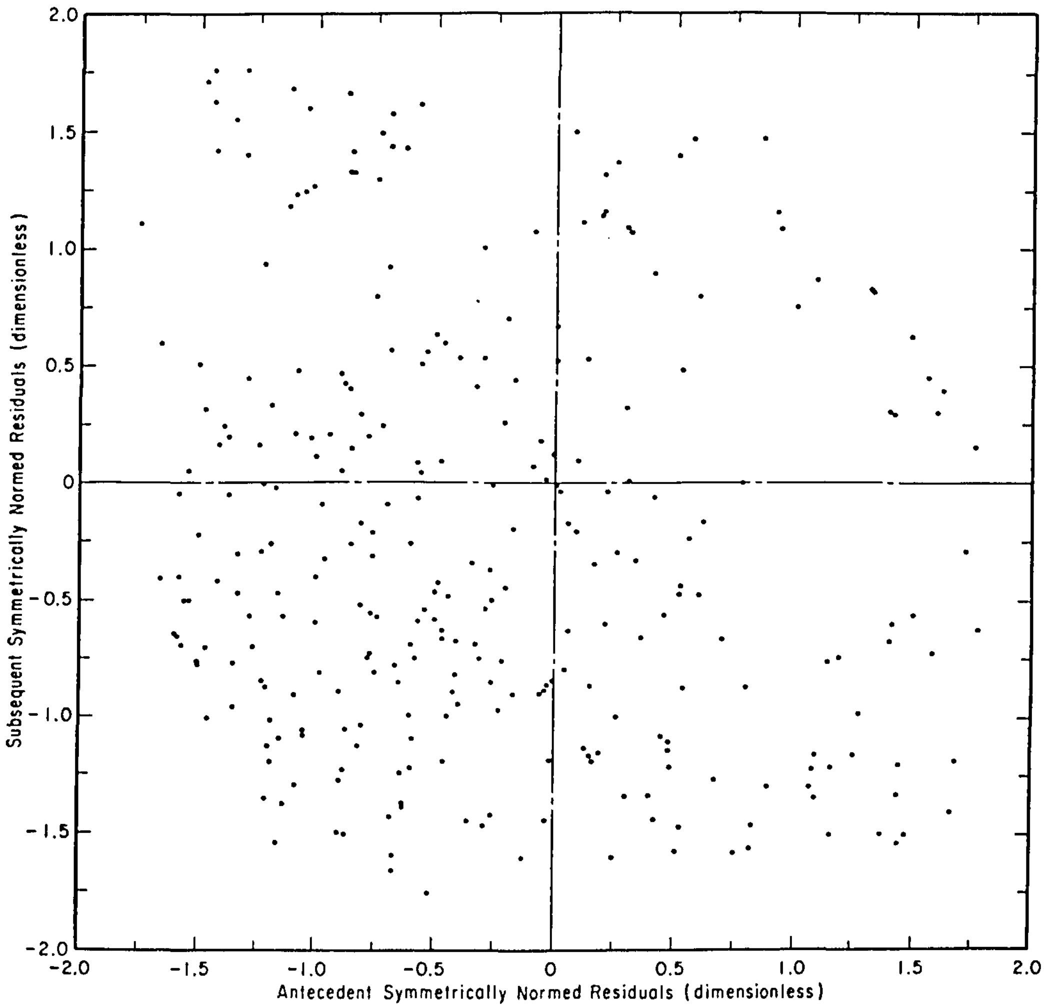

Figure 30. Scatter diagram: Sequential pairs of symmetrically normed residuals, data number 6881-2.

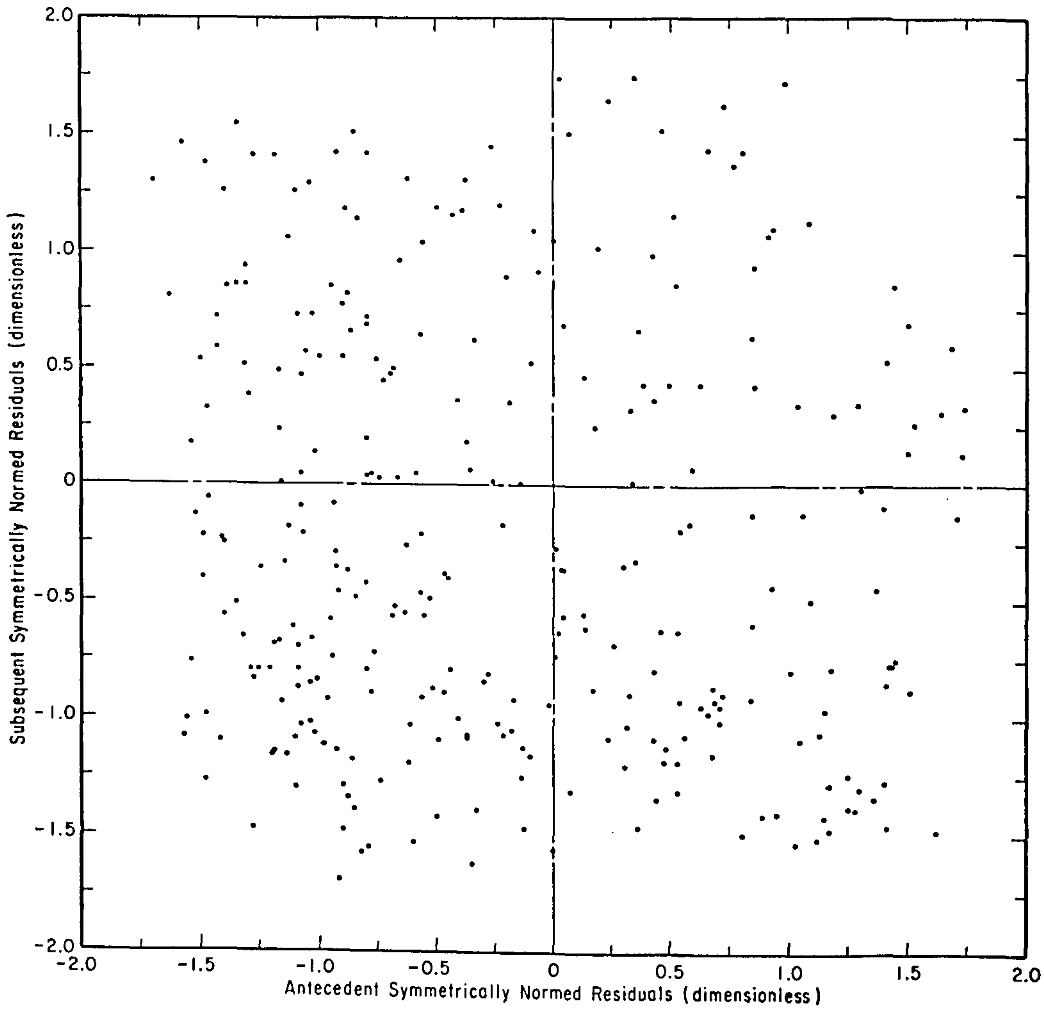

Figure 31. Scatter diagram: Sequential pairs of symmetrically normed residuals, data number 6882.

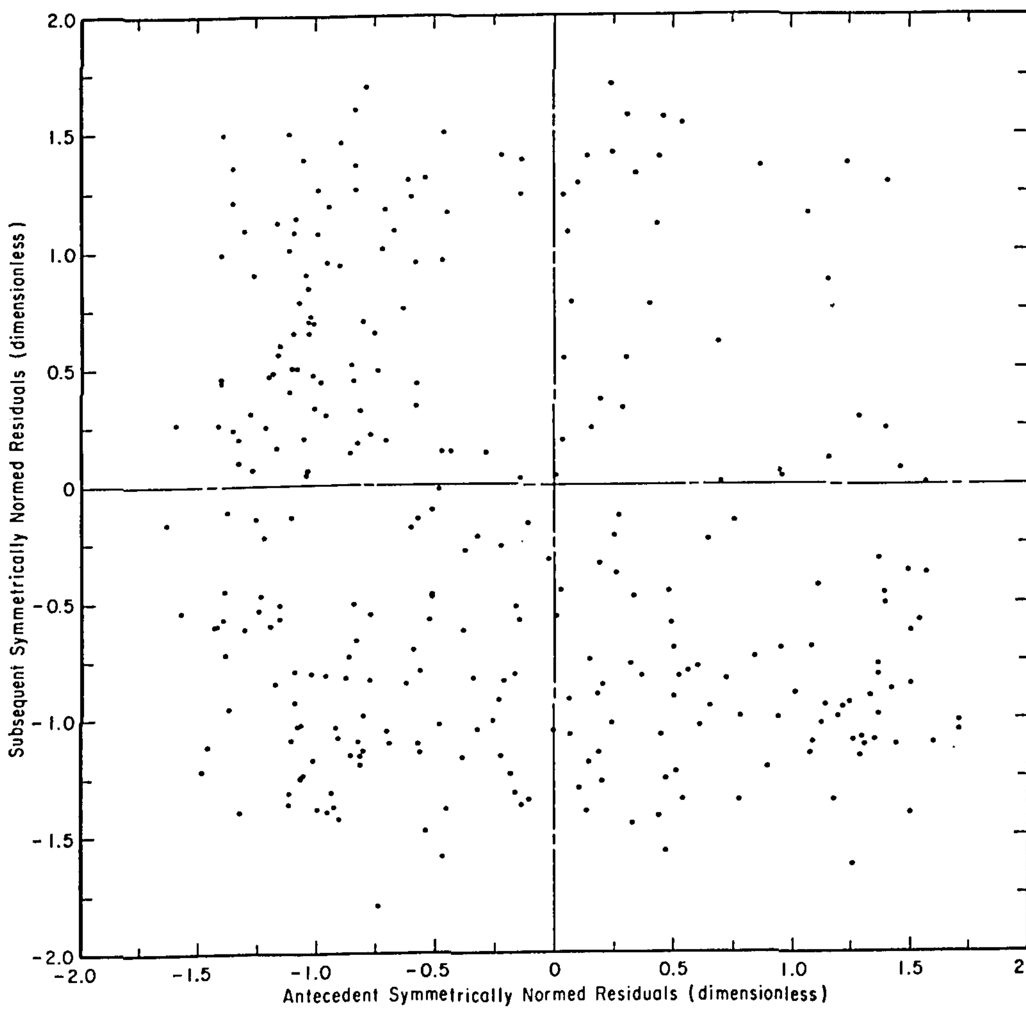

Figure 32. Scatter diagram: Sequential pairs of symmetrically normed residuals, data number 6883.

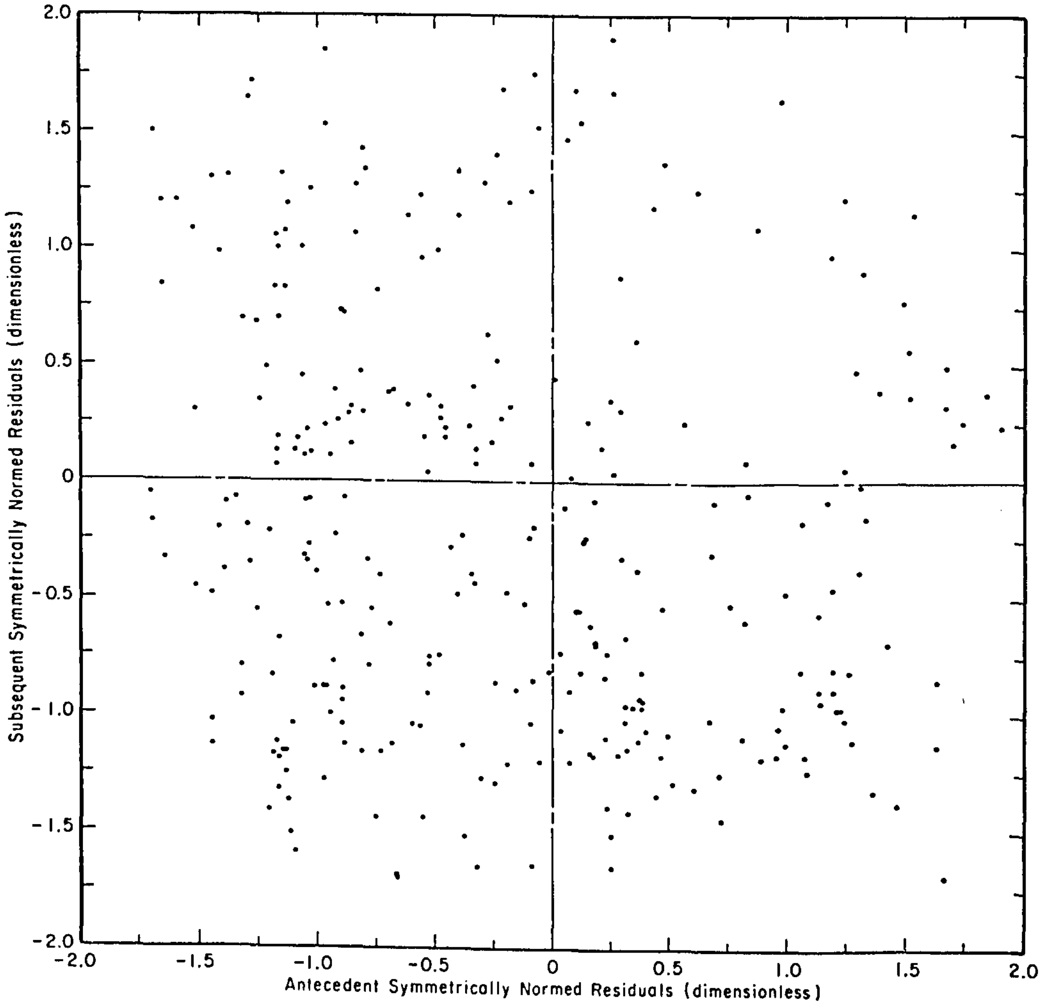

Figure 33. Scatter diagram: Sequential pairs of symmetrically normed residuals, data number 6884.

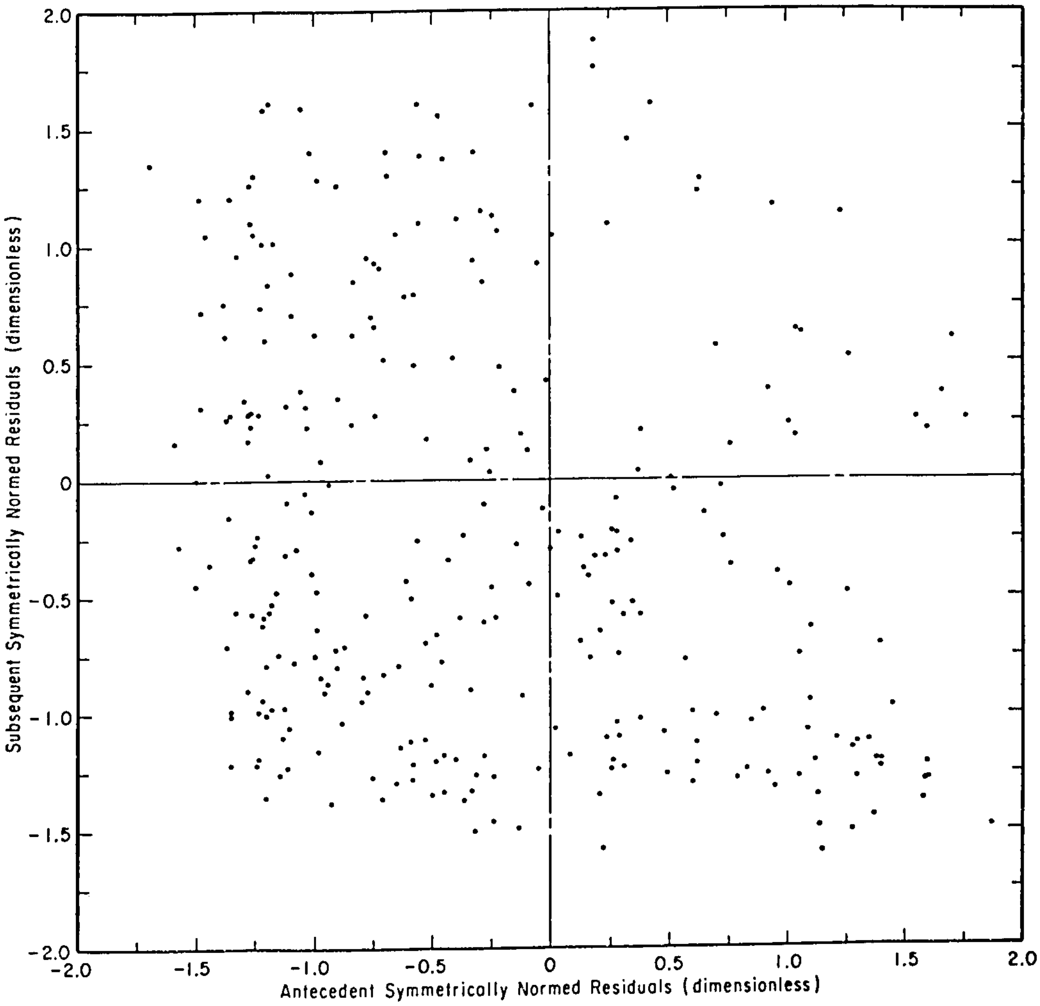

Figure 34. Scatter diagram: Sequential pairs of symmetrically normed residuals, data number 6885.

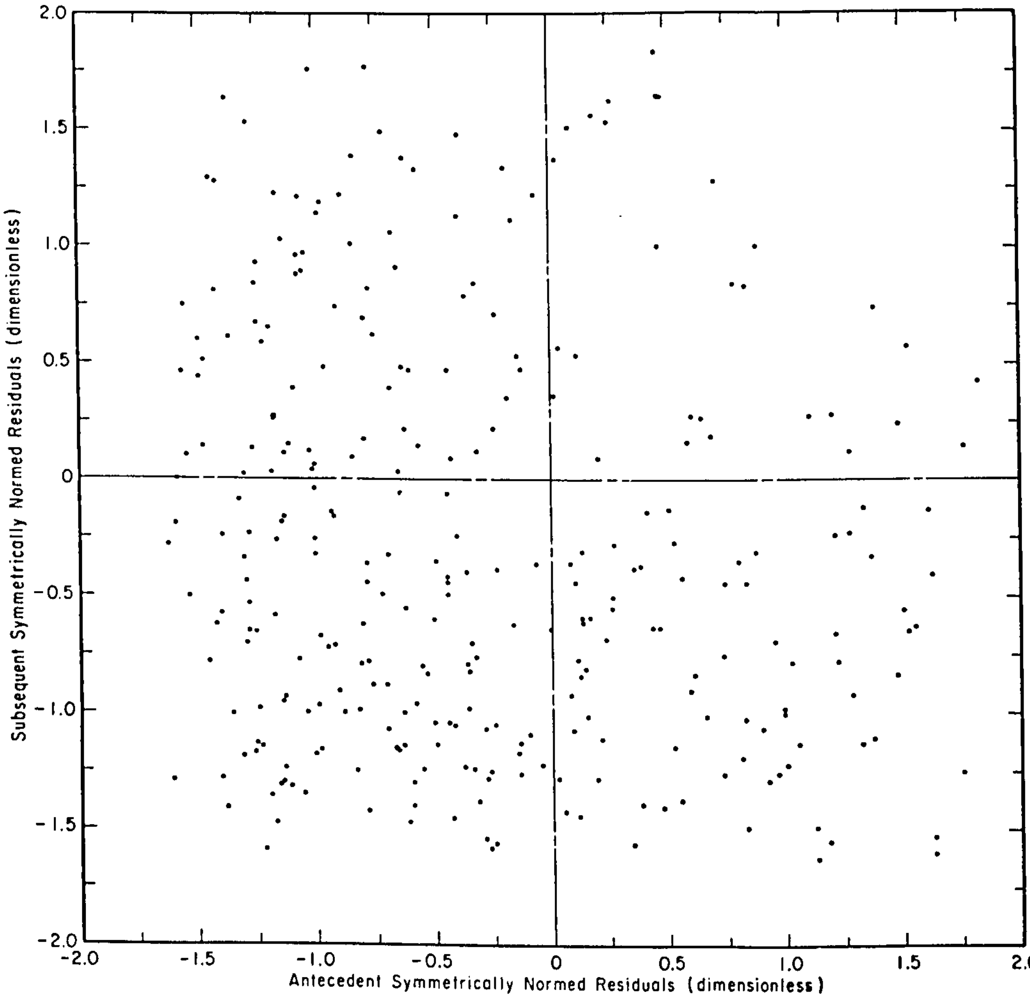

Figure 35. Scatter diagram: Sequential pairs of symmetrically normed residuals, data number 6886-1.

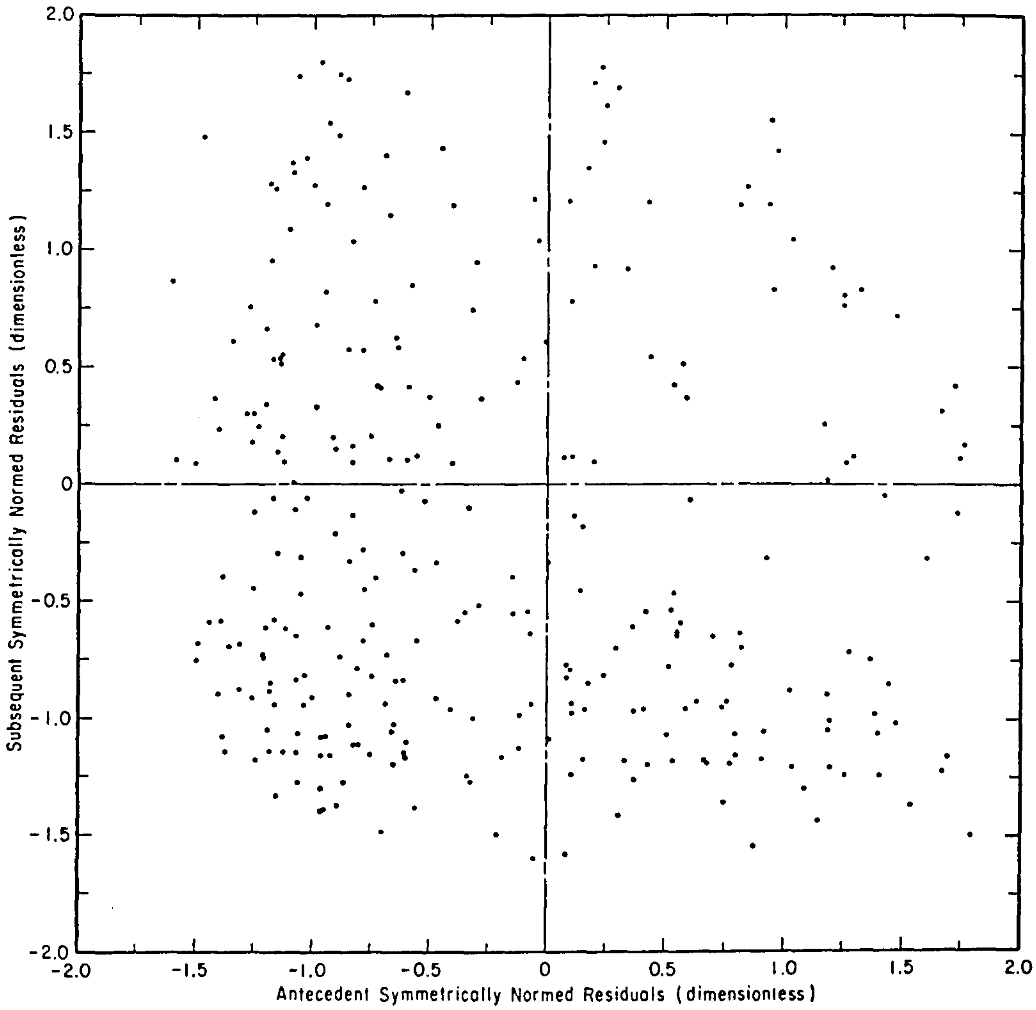

Figure 36.. Scatter diagram: Sequential pairs of symmetrically normed residuals, data number 6886-2.

where

$$c = \begin{cases} \sigma_+ \ , & \text{if SNR} > 0 \\ \\ \sigma_- \ , & \text{if SNR} < 0 \end{cases} \quad , \qquad (40)$$

and SNR denotes the SNR regarded as a random variable.

VIII. THE EMPIRICAL PROBABILITY LAW FOR THE SYMMETRICALLY NORMED RESIDUAL

The cumulative distribution function for the SNR is defined as:

$$F_{SNR}(w) = P\,[\text{SNR} \leq w] \quad , \qquad (41)$$

where $P[\cdot]$ is the probability of the event specified within the brackets. This distribution function can be estimated from the 300 values of the SNR's for each record of Hurricane Carla. Let $(SNR)_k$ be SNR's ranked in order of increasing size:

$$(SNR)_1 \leq (SNR)_2 \leq (SNR)_3 \leq \cdots \leq (SNR)_{300} \ . \qquad (42)$$

A statistically reasonable estimate of $F_{SNR}(w_k)$ for

$$w_k = (SNR)_k \qquad (43)$$

is

$$\hat{F}_{SNR}(w_k) = \frac{k}{301} \qquad (44)$$

(Gumbel, 1954). Thus, a graph of $\hat{F}_{SNR}(w_k)$ versus w_k for $k = 1,2,3,\cdots,300$ gives the distribution function estimate. The graphs are shown in Figures 37 through 48.

The corresponding probability densities may be obtained by differentiating the distribution function numerically. For the present study, this was done by selecting a band on the SNR axis which is 0.5 unit wide and fitting a least square line to all the ranked points lying within the band. The slope of the line is the probability density estimate assigned to the midpoint SNR value for the band. This was repeated for all 300 possible midpoints on the SNR axis. The resulting probability densities are given in Figures 49 through 60.

IX. EMPIRICAL PROBABILITY INTERVALS FOR $\hat{p}(f_m)$ BY SIMULATION

Suppose a new spectral density estimate, $\hat{p}^*(f_m)$, is developed by simulation from equation (39) by the following procedure. A random number, uniformly distributed on the interval, (0,1), is generated in the digital computer. One of the pieces of record is selected for study and

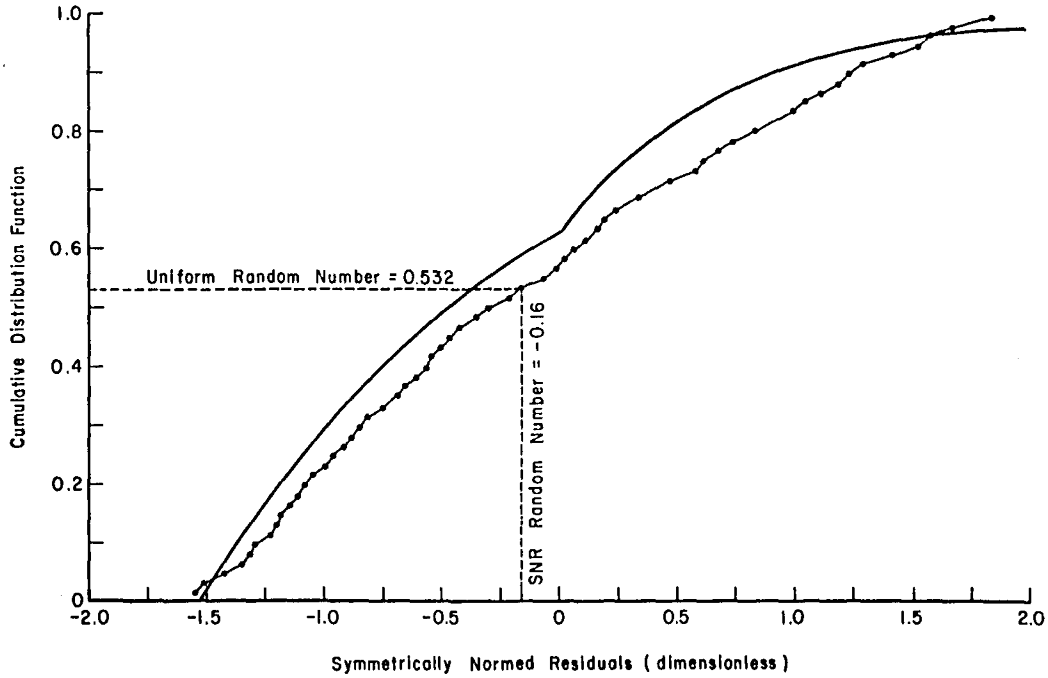

Figure 37. Cumulative distribution function, Hurricane Carla data number 6877, 0600 hours, 8 September 1961.

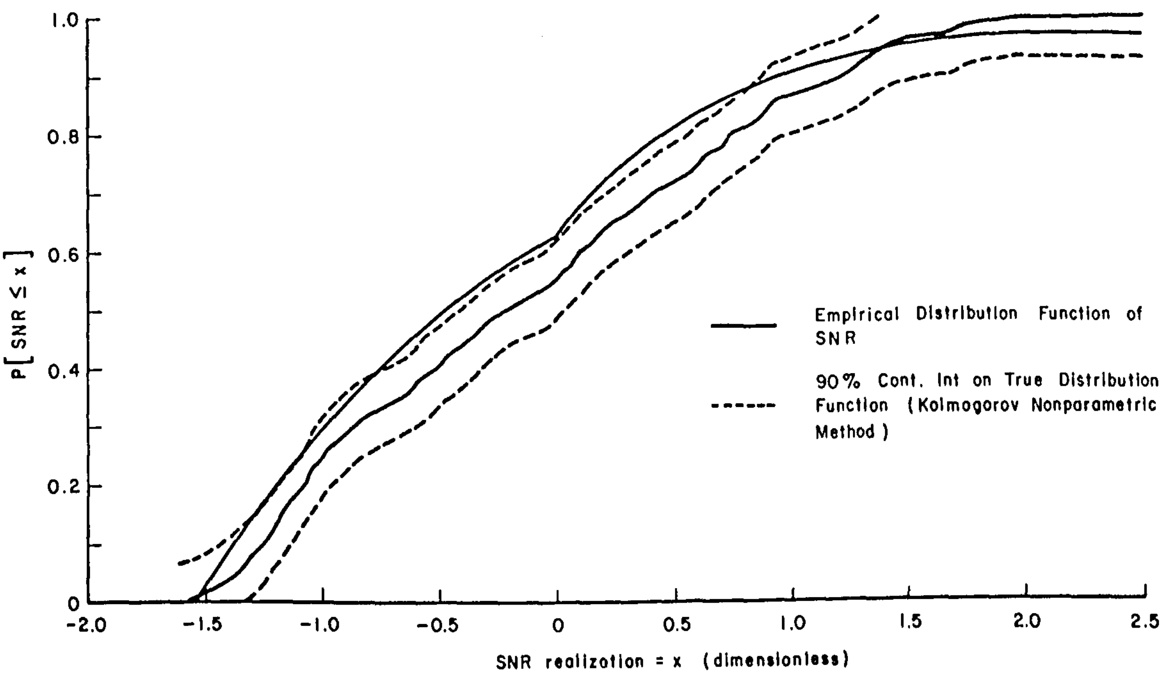

Figure 38. Cumulative distribution function, Hurricane Carla data number 6878.

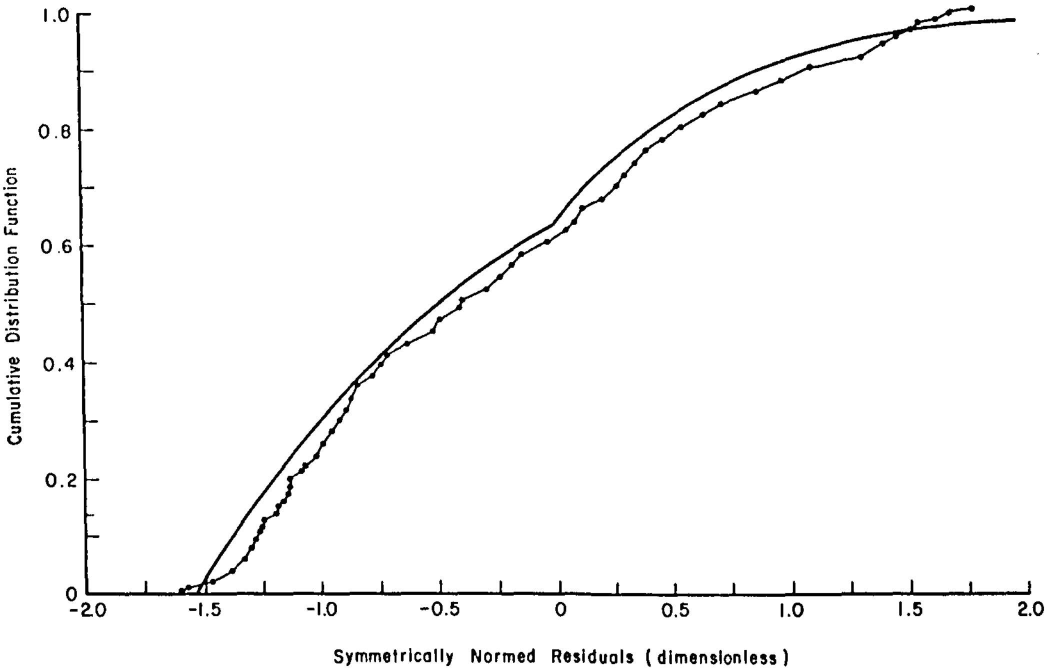

Figure 39. Cumulative distribution function, Hurricane Carla data number 6879, 1800 hours, 8 September 1961.

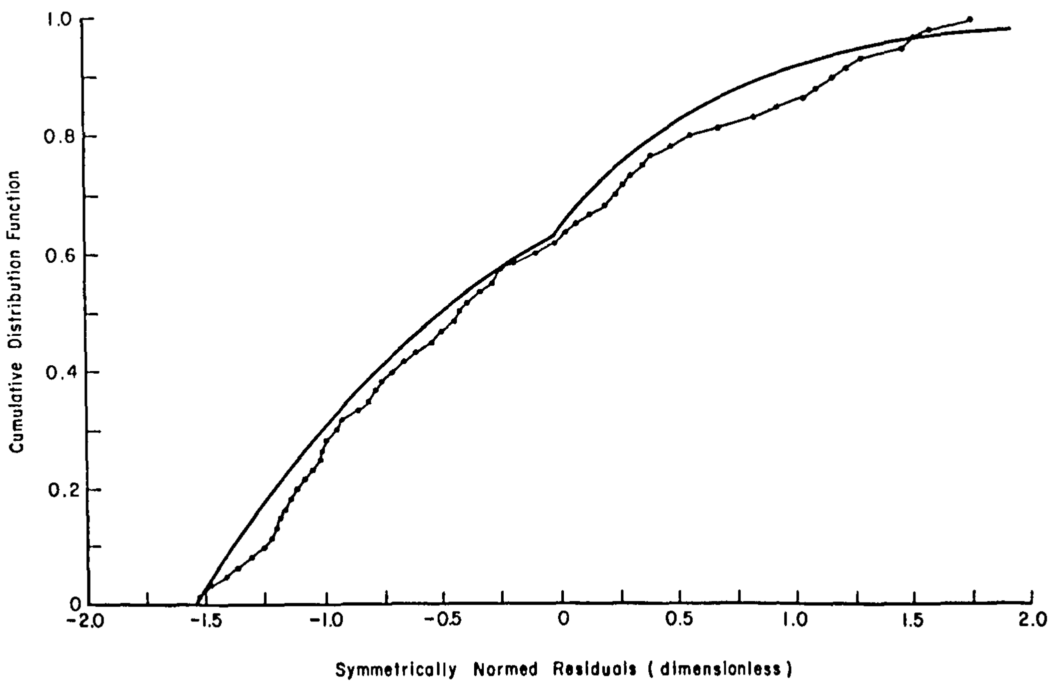

Figure 40. Cumulative distribution function, Hurricane Carla data number 6880, 0000 hours, 9 September 1961.

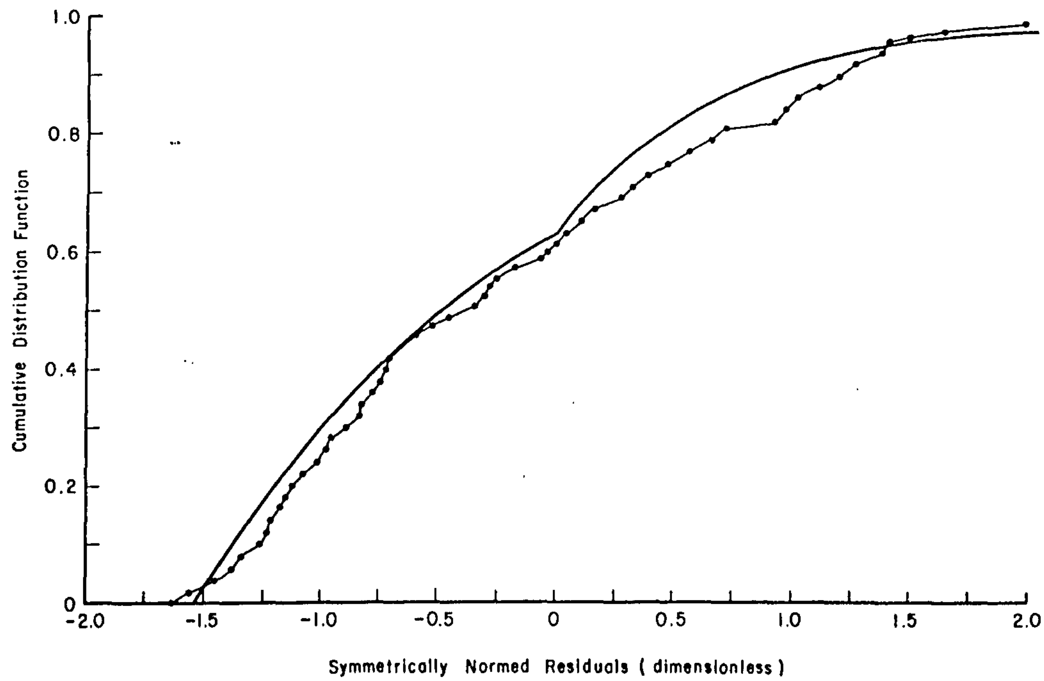

Figure 41. Cumulative distribution function, Hurricane Carla data number 6881-1, 0600 hours, 9 September 1961.

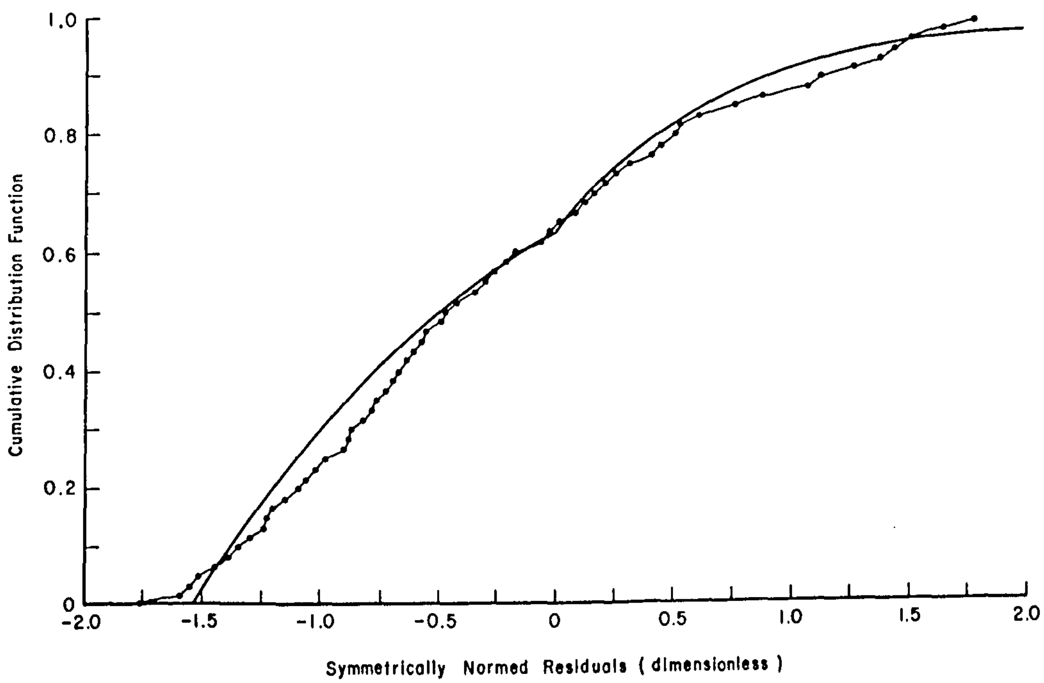

Figure 42. Cumulative distribution function, Hurricane Carla data number 6881-2, 0620 hours, 9 September 1961.

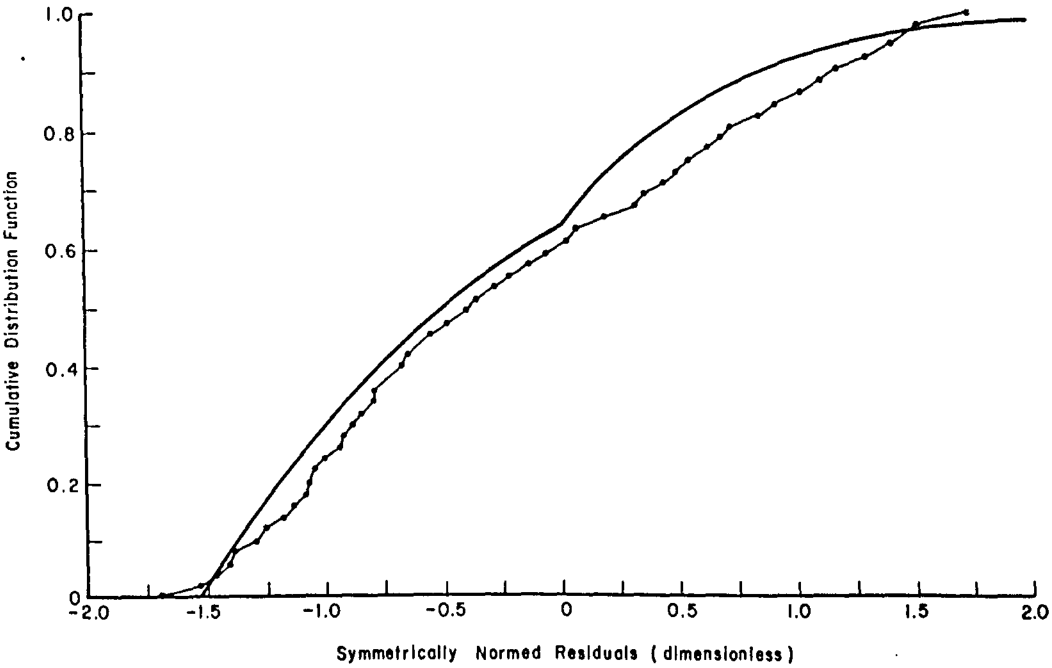

Figure 43. Cumulative distribution function, Hurricane Carla data number 6882, 1200 hours, 9 September 1961.

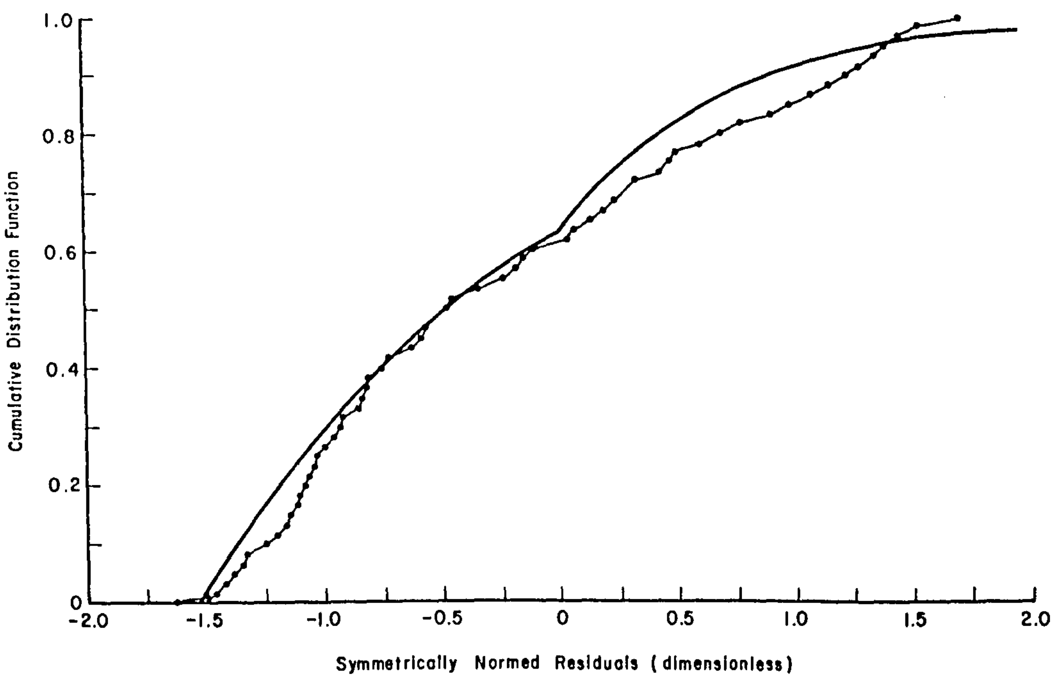

Figure 44. Cumulative distribution function, Hurricane Carla data number 6883, 1500 hours, 9 September 1961.

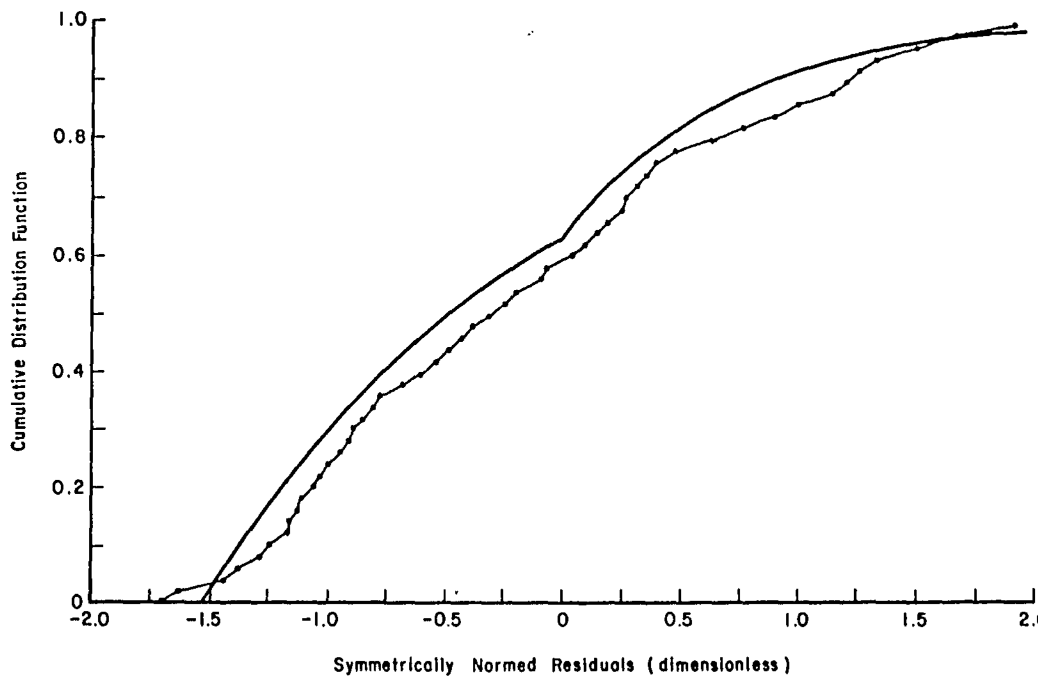

Figure 45. Cumulative distribution function, Hurricane Carla data number 6884, 1800 hours, 9 September 1961.

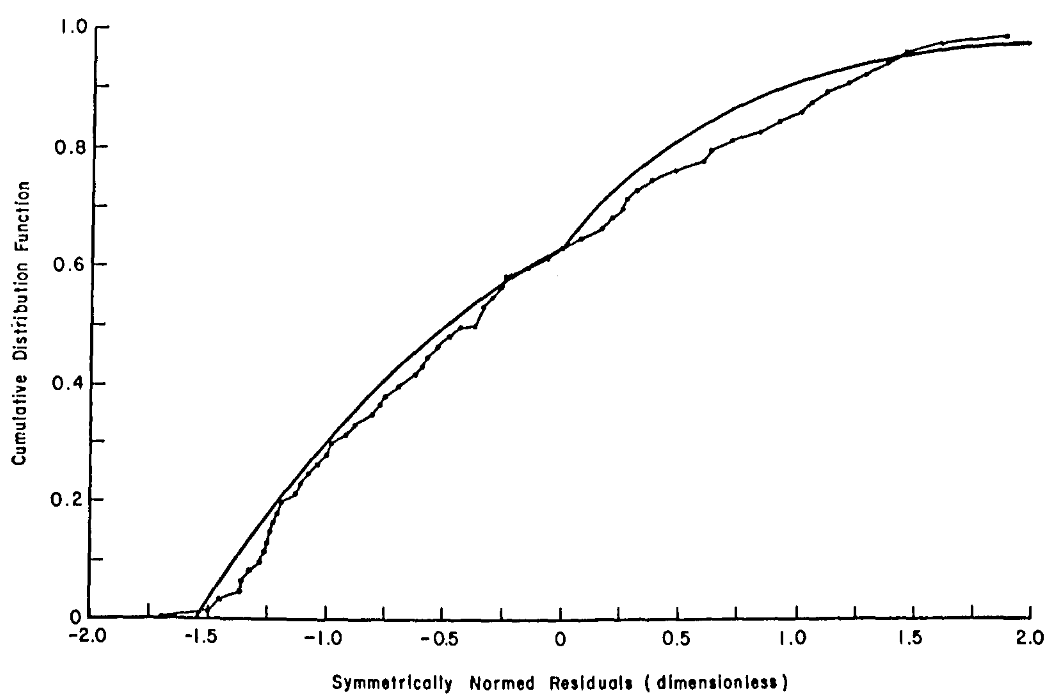

Figure 46. Cumulative distribution function, Hurricane Carla data number 6885, 2100 hours, 9 September 1961.

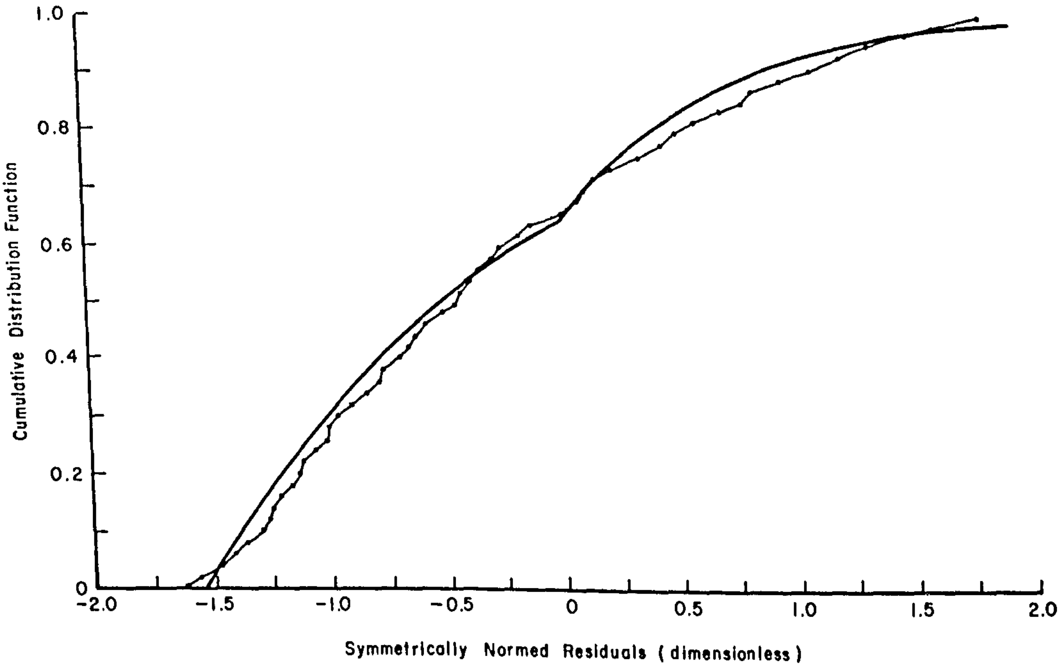

Figure 47. Cumulative distribution function, Hurricane Carla data number 6886-1, 0000 hours, 10 September 1961.

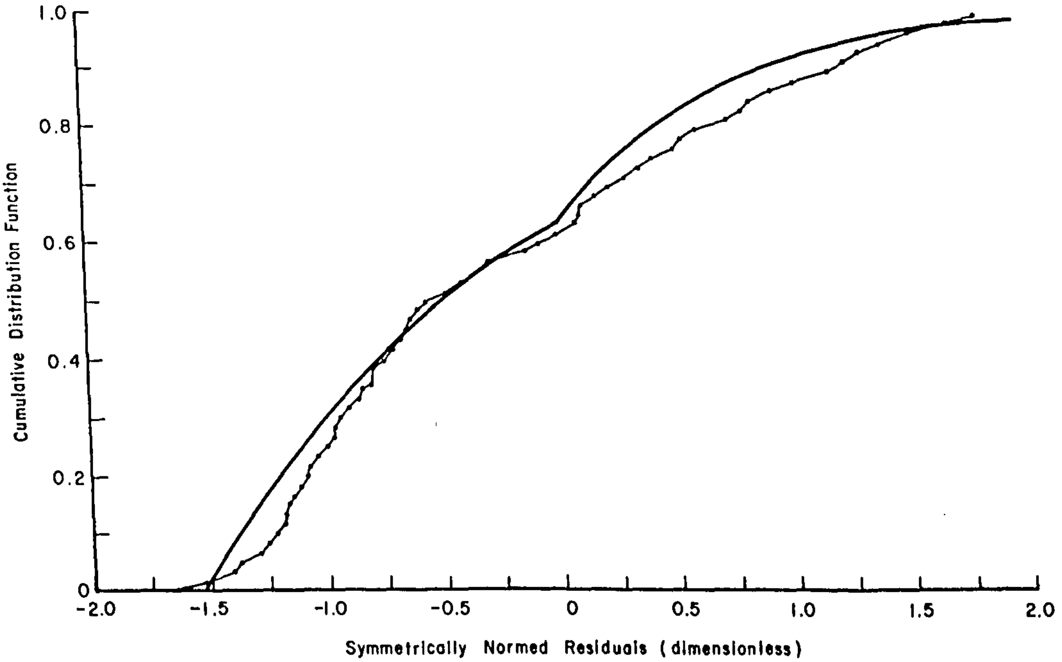

Figure 48. Cumulative distribution function, Hurricane Carla data number 6886-2, 0020 hours, 10 September 1961.

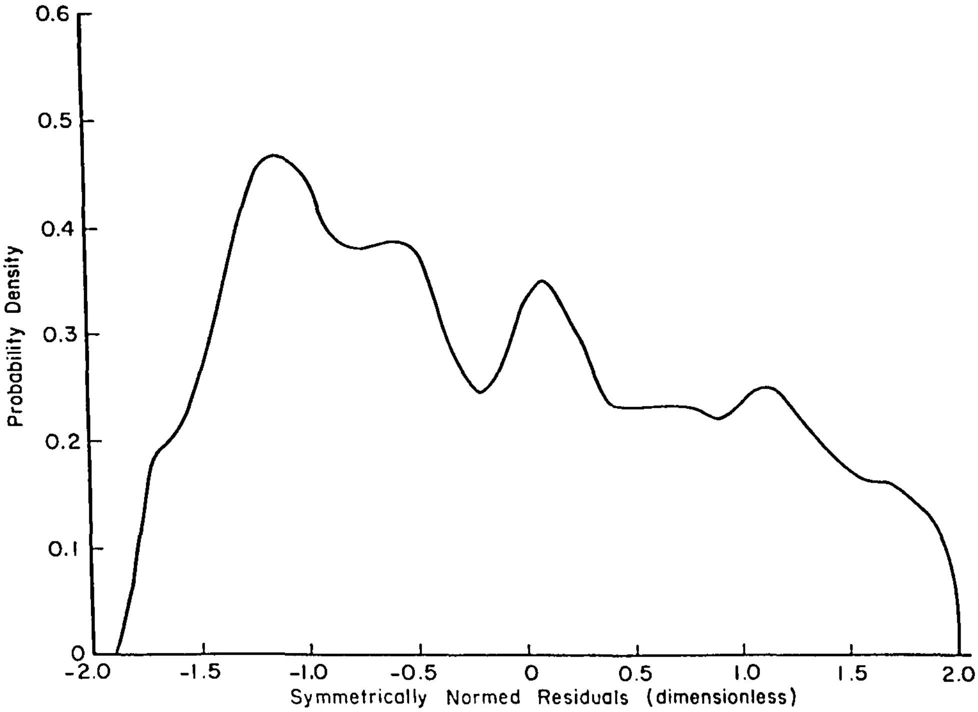

Figure 49. Probability density, Hurricane Carla data number 6877, 0600 hours, 8 September 1961.

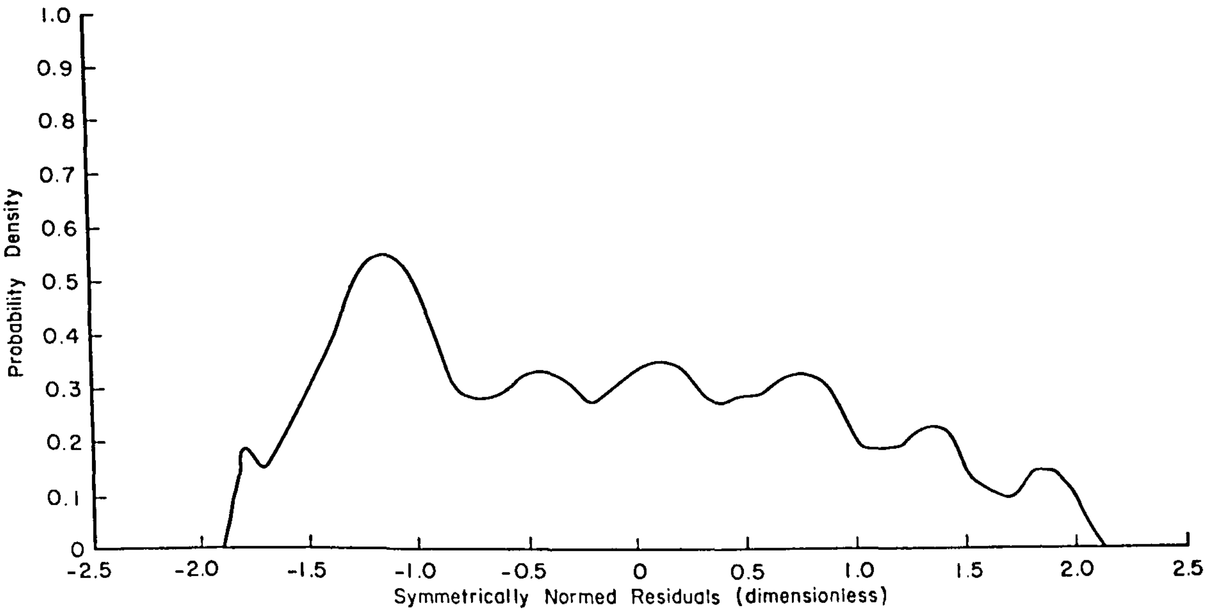

Figure 50. Density function, Hurricane Carla data number 6878.

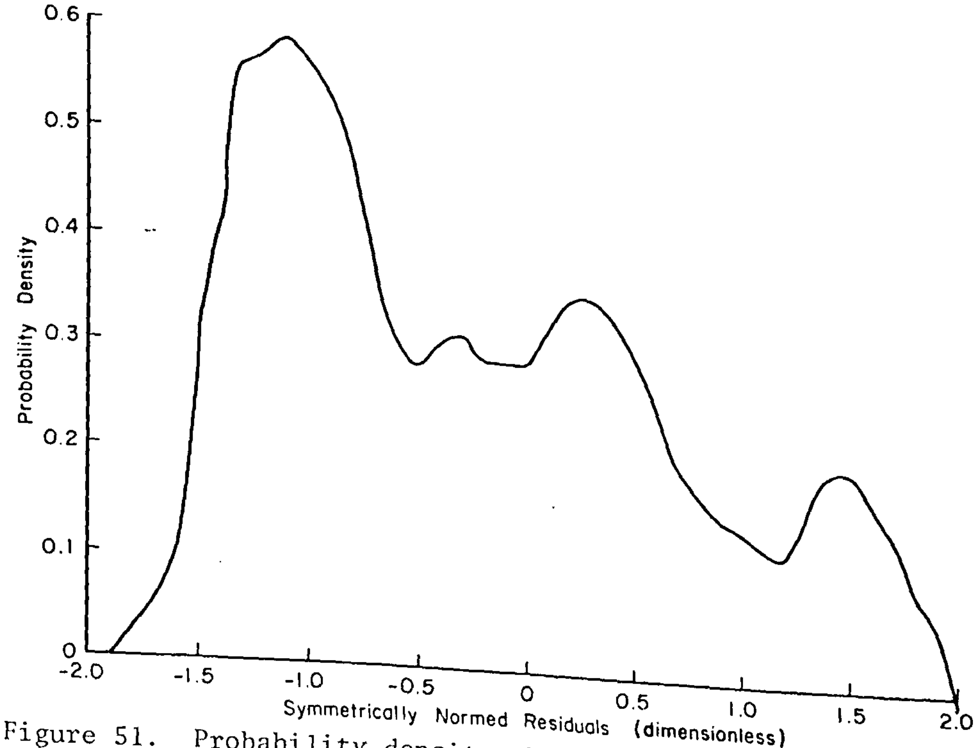

Figure 51. Probability density, Hurricane Carla data number 6879, 1800 hours, 8 September 1961.

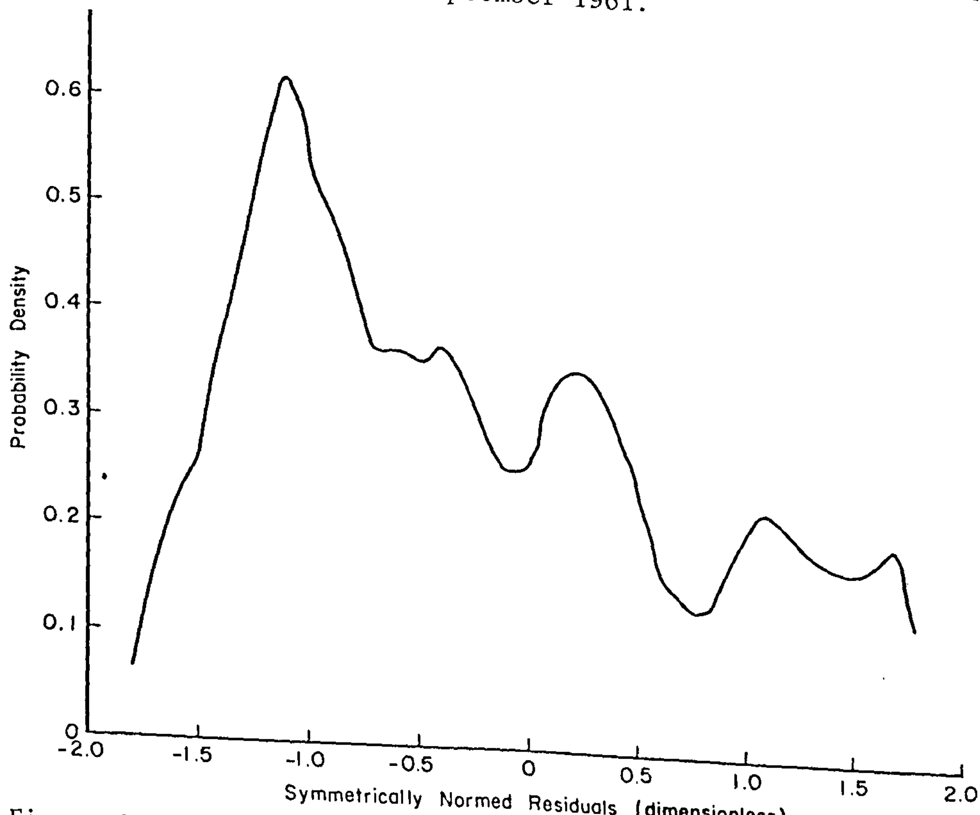

Figure 52. Probability density, Hurricane Carla data number 6880, 0000 hours, 9 September 1961.

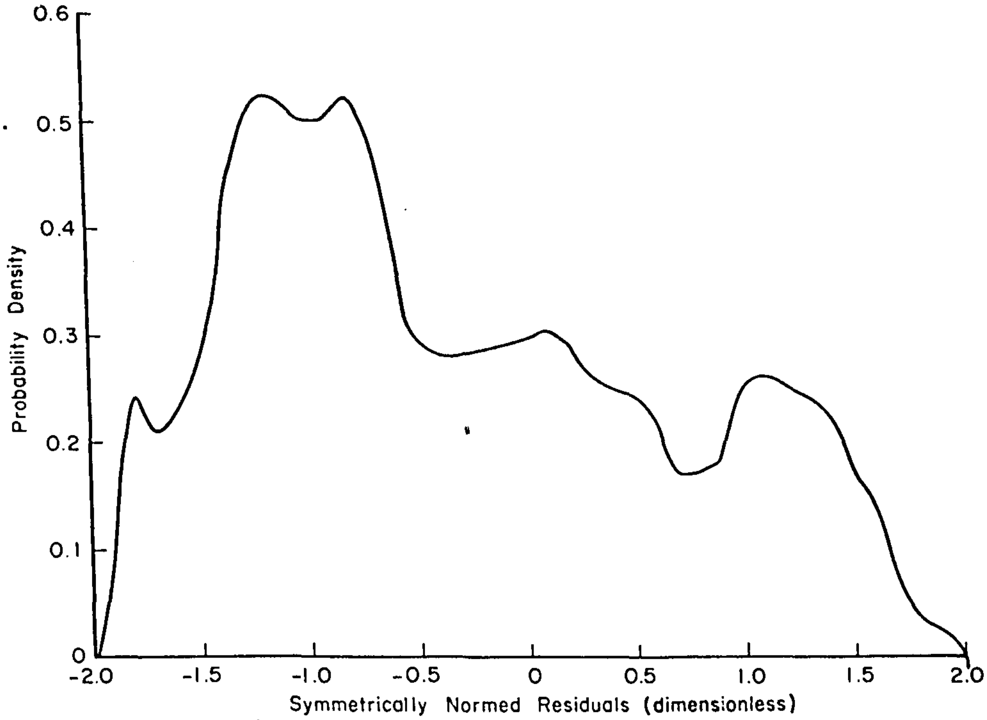

Figure 53. Probability density, Hurricane Carla data number 6881-1, 0600 hours, 9 September 1961.

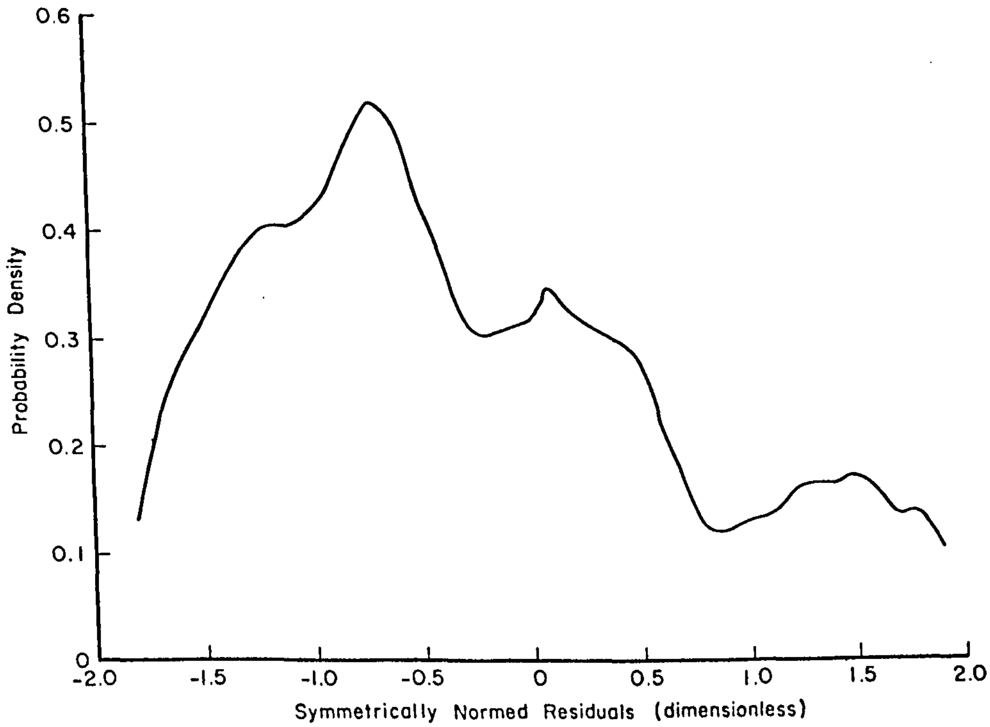

Figure 54. Probability density, Hurricane Carla data number 6881-2, 0620 hours, 9 September 1961.

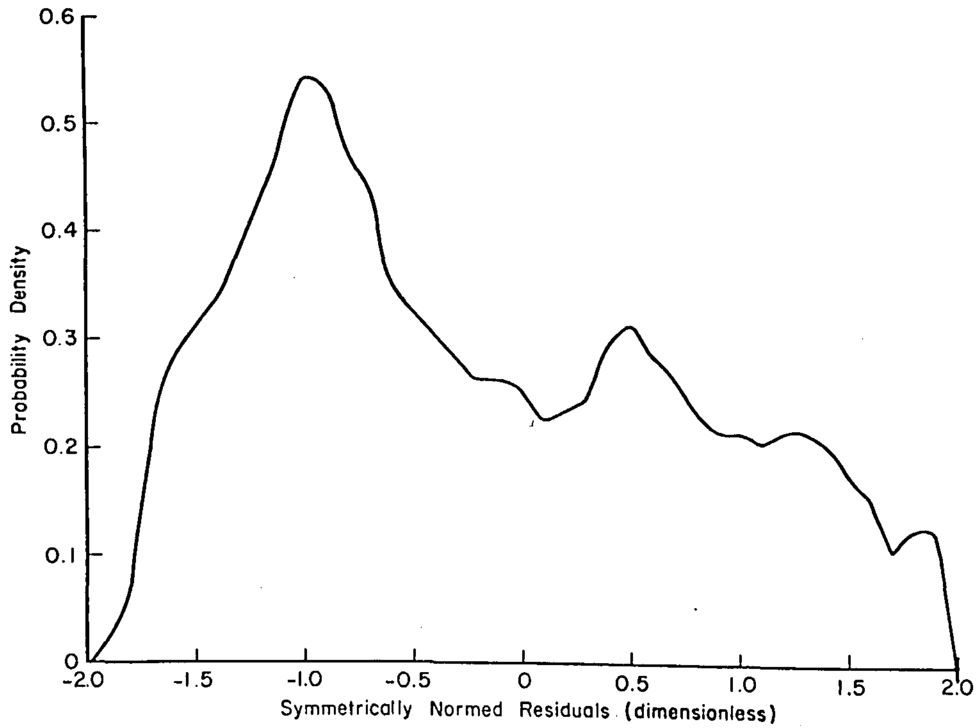

Figure 55. Probability density, Hurricane Carla data number 6882, 1200 hours, 9 September 1961.

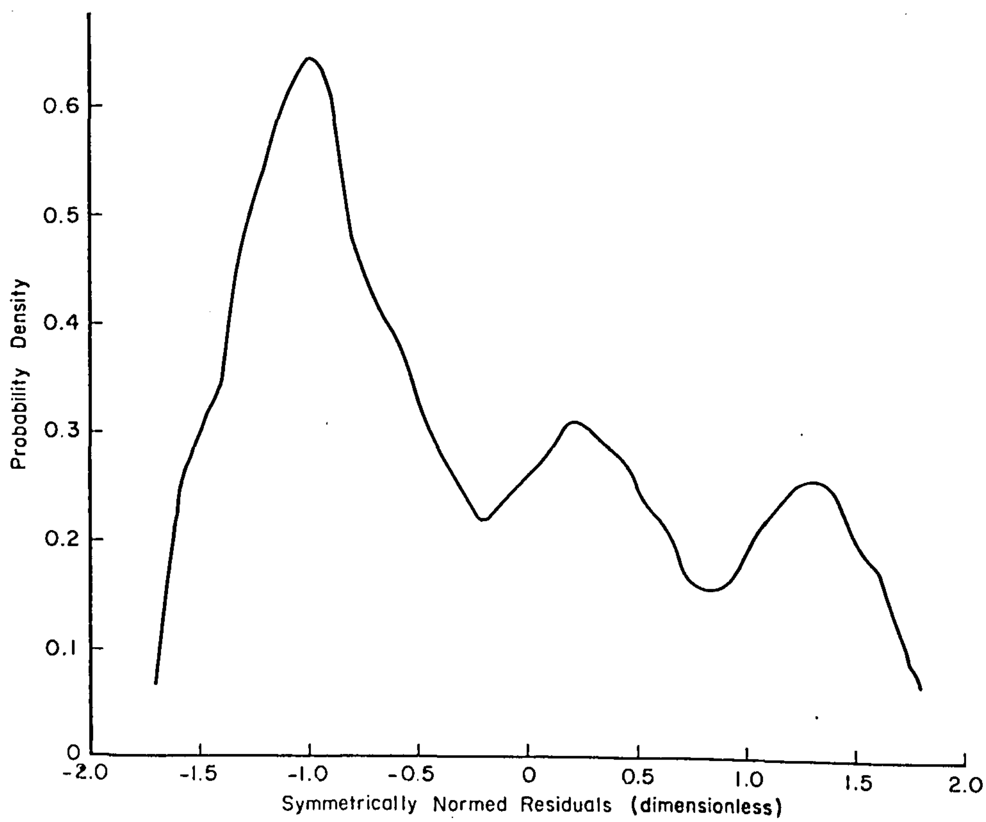

Figure 56. Probability density, Hurricane Carla data number 6883, 1500 hours, 9 September 1961.

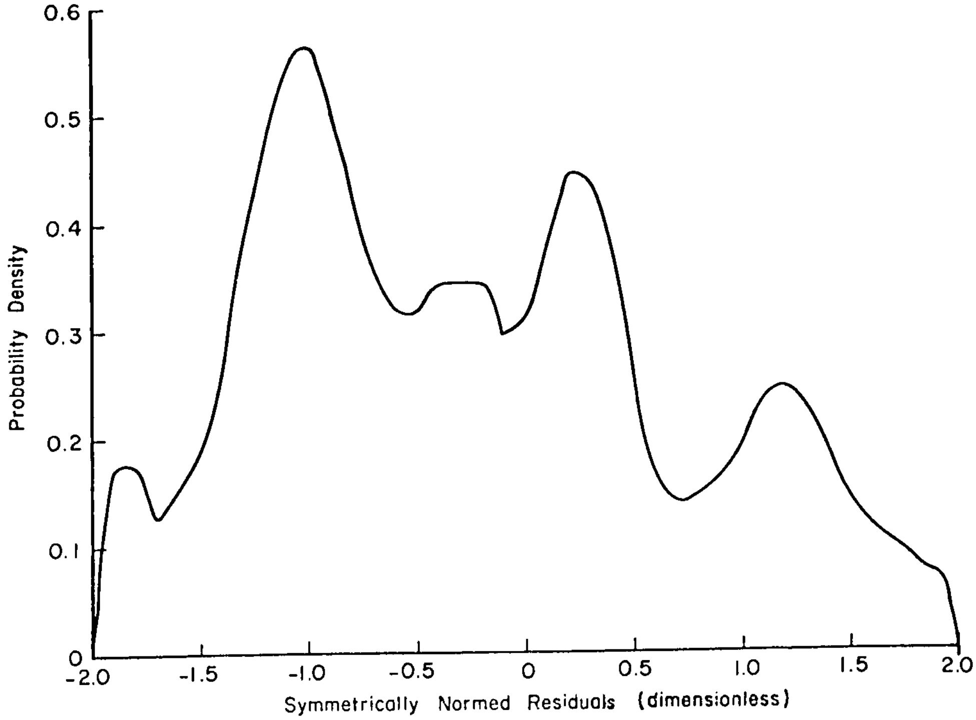

Figure 57. Probability density, Hurricane Carla data number 6884, 1800 hours, 9 September 1961.

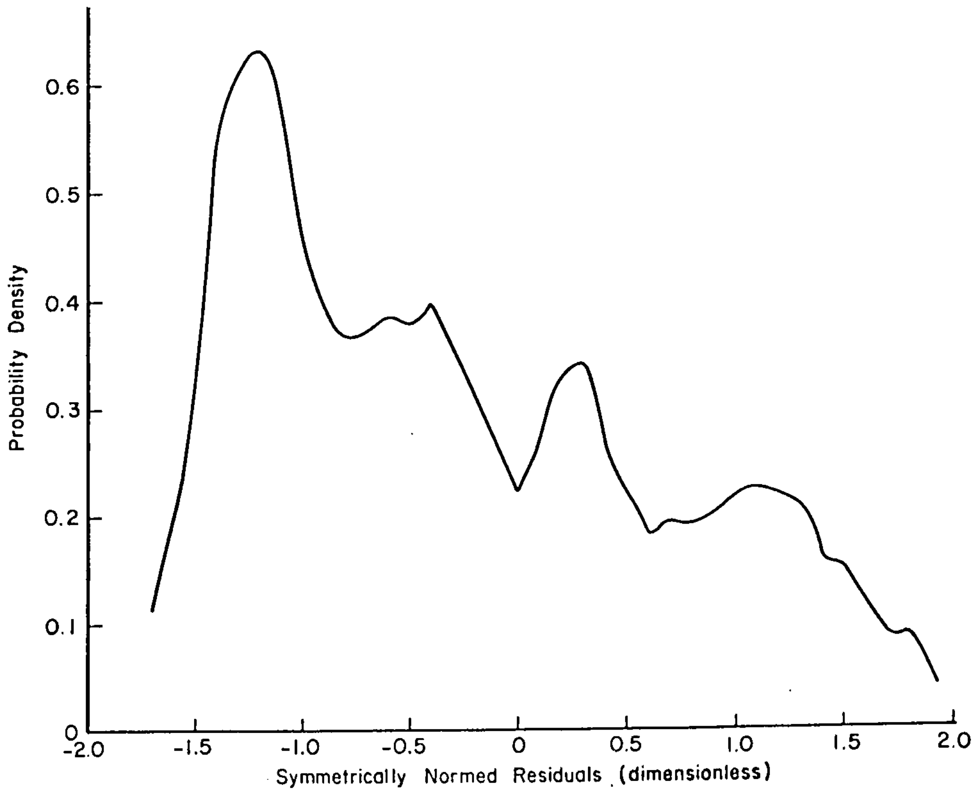

Figure 58. Probability density, Hurricane Carla data number 6885, 2100 hours, 9 September 1961.

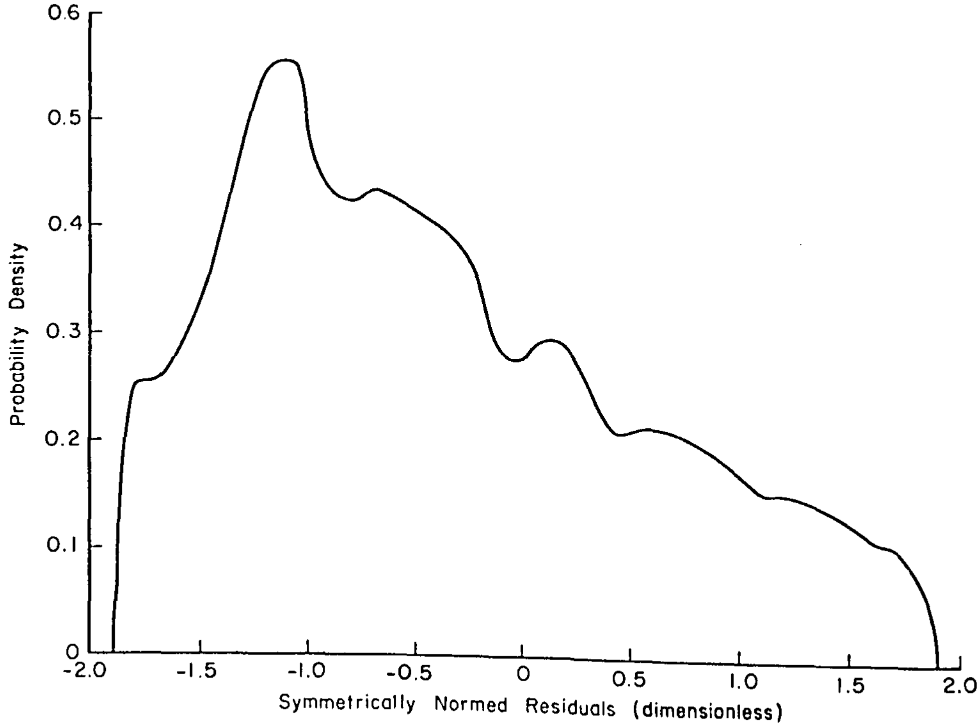

Figure 59. Probability density, Hurricane Carla data number 6886-1, 0000 hours, 10 September 1961.

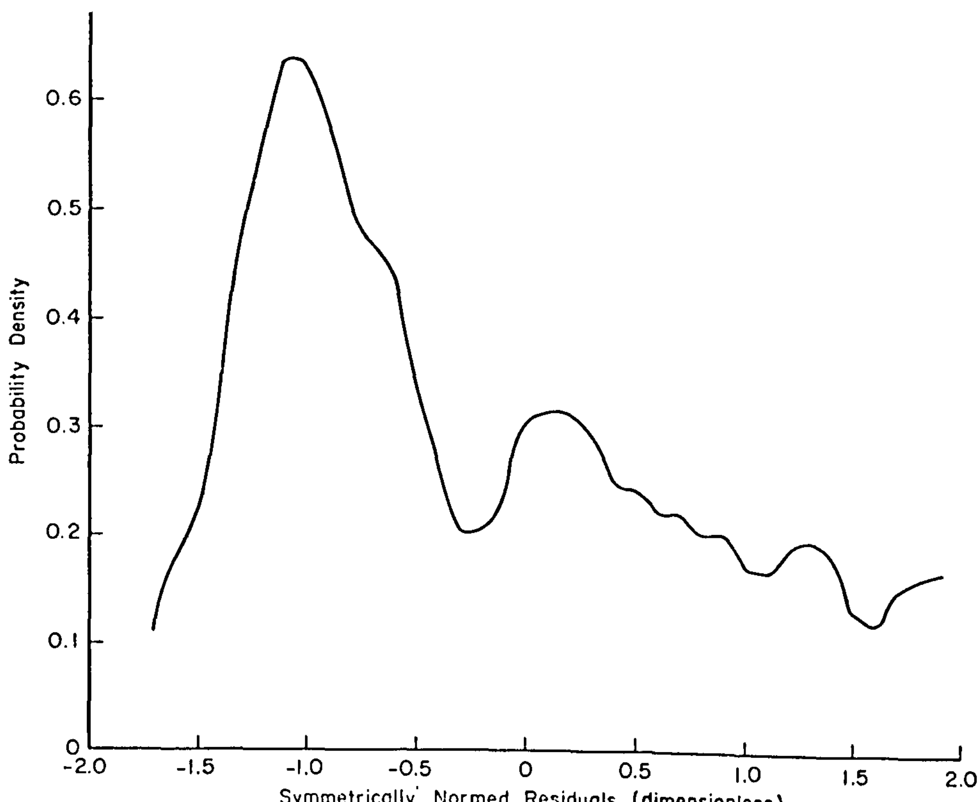

Figure 60. Probability density, Hurricane Carla data number 6886-2, 0020 hours, 10 September 1961.

the corresponding cumulative distribution function figure is picked from Figures 37 through 48. The coordinate value on the vertical axis of the distribution function which equals the uniform random number is located. Reading horizontally from this coordinate value to the empirical distribution curve and then down vertically to the SNR axis yields a random SNR value. This procedure is illustrated in Figure 37 by the dotted line. The uniform random number is 0.532. The corresponding random SNR value is -0.16.

The distribution function for the SNR values obtained by this procedure will be identical to the graphed empirical distribution function $F_{SNR}(w)$. This follows from the following argument. The SNR, so developed are less than or equal to w if, and only if, the uniform random number is less than or equal to $F_{SNR}(w)$. This is true because the two numbers are tied together via the graphed curve. Hence,

$$P\ [\text{random SNR} \leq w] = P\ [U \leq F_{SNR}(w)] \quad , \tag{45}$$

where U denotes the uniform random number. But by definition, the distribution function for a uniform random number is:

$$F_U(u) = P\ [U \leq u] = u \quad . \tag{46}$$

Hence, returning to equation (45),

$$P\ [\text{random SNR} \leq w] = P\ (U \leq F_{SNR}(w)] = F_{SNR}(w) \quad . \tag{47}$$

The above procedure is repeated for 300 independent uniform random numbers to obtain 300 random SNR values. These 300 SNR values are just as likely to have happened as the originally occurring values, provided the decomposition in equation (39) is accepted as valid and provided the independence assumption truly holds.

Hence, equation (39) can be used with the 300 SNR values and the $\hat{p}(f_m)$, $\sigma_{+,m}$, and $\sigma_{-,m}$ frequency functions to create a new set of spectral lines, $\hat{p}^*(f_m)$. These spectral lines might just as well occurred as the original set if the random spectral fluctuations had accidentally gone that way.

Finally, the 300 simulated spectral lines, $\hat{p}^*(f_m)$, are smoothed according to equation (31) to produce new simulated spectral densities, $\hat{\hat{p}}^*(f_m)$.

The above procedure in its entirety was repeated 900 times for each of the 12 pieces of Hurricane Carla data. Thus, 900 statistically equivalent spectral densities were generated by simulation for each hurricane data record.

How much do the $\hat{\hat{p}}^*(f_m)$ as a group differ from the spectral density, $\hat{\hat{p}}(f_m)$, used in the simulation? The answer to this question was developed for the 10 frequencies, 0.070, 0.072, 0.074, 0.077, 0.083, 0.088, 0.101, 0.132, 0.168, and 0.243 sec.$^{-1}$. The 900 values of $\hat{\hat{p}}^*(f_m)$ were ranked for each frequency and the two values with ranks 45 and 855 were selected as estimates of the 5th and 95th percentiles for $\hat{\hat{p}}^*(f_m)$. These percentile estimates are plotted versus frequency as dots in Figures 61 through 72.

X. COMPARISON WITH CHI-SQUARED PROBABILITY INTERVALS FOR $\hat{\hat{p}}(f_m)$

If the sea surface is Gaussian, the spectral density will follow a probability law closely related to a chi-squared random variable with 16 degrees of freedom (for the Hurricane Carla estimates) (Borgman, 1972). Symbolically,

$$\frac{16\ \hat{\hat{p}}(f_m)}{p(f_m)} = \chi^2_{16} \qquad (48)$$

where $p(f_m)$ denotes the true or population spectral density. Thus, if $\chi^2_{16,0.05}$ and $\chi^2_{16,0.95}$ denote the 5th and 95th percentiles for a chi-squared random variable with 16 degrees of freedom, then:

$$P\left[\frac{\chi^2_{16,0.05}\ p(f_m)}{16} < p(f_m) < \frac{\chi^2_{16,0.95}\ p(f_m)}{16}\right] = 0.90 \quad . \qquad (49)$$

The interval $\left(\chi^2_{16,0.05}\ p(f_m) \big/ 16\ ,\ \chi^2_{16,0.95}\ p(f_m) \big/ 16\right)$ thus provides a 90 percent probability interval for $\hat{\hat{p}}(f_m)$. However, $p(f_m)$ is not known. As an approximation, $\hat{\hat{p}}(f_m)$ may be substituted for $p(f_m)$. An analogous approximation was made in the simulations. The resulting upper and lower limits are plotted as asterisks in Figures 61 through 72 versus each of the selected frequencies. The spectral density values $\hat{\hat{p}}(f_m)$ are shown in the figures as pluses.

As was noted in an earlier paper based on an analysis of part of the data (Borgman, 1972), the chi-squared probability intervals do not differ excessively from the simulated probability intervals. They are both about the same, although there are substantial variations from record to record. The upper bounds show appreciably more scatter than do the lower bounds. Another comparison of the two kinds of probability intervals is given in Figure 73. The two ratios,

$$\text{simulation upper bound} \ / \ \hat{\hat{p}}(f_m)$$

and,

$$\text{simulation lower bound} \ / \ \hat{\hat{p}}(f_m) \quad ,$$

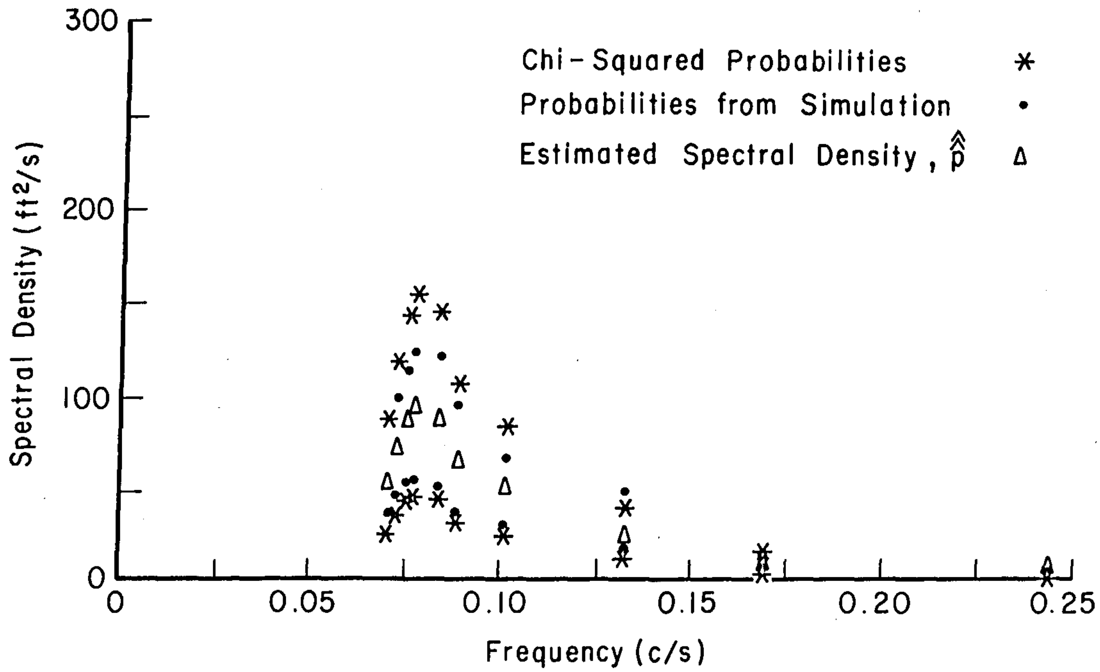

Figure 61. Probability intervals for $\hat{\hat{p}}$, Hurricane Carla data number 6877.

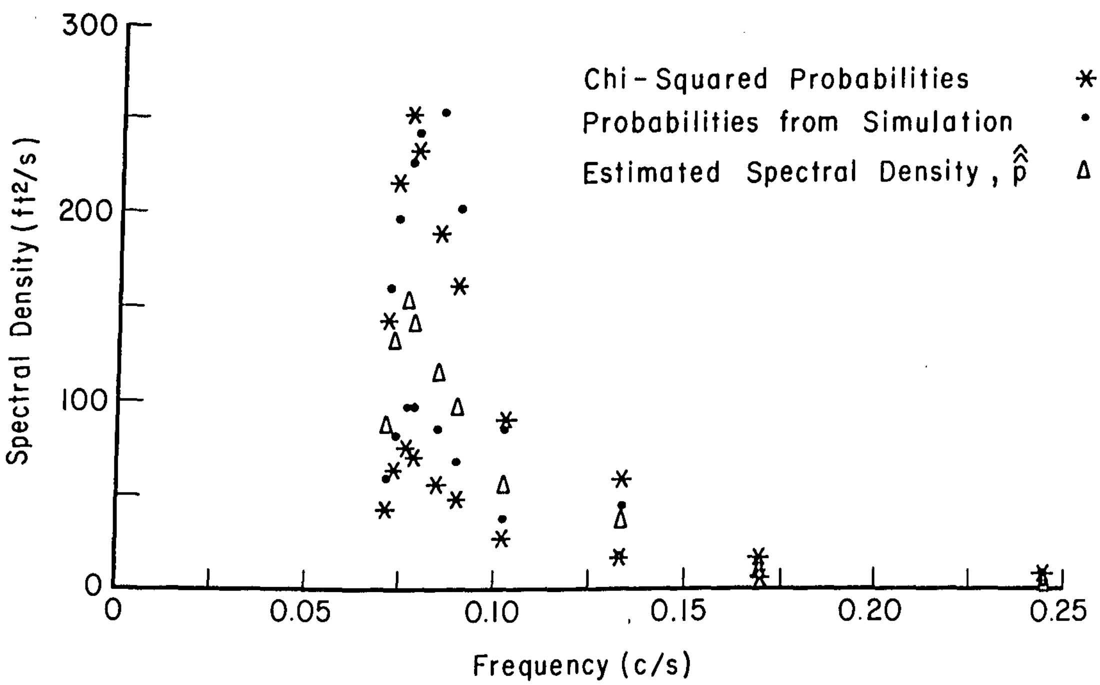

Figure 62. Probability intervals for $\hat{\hat{p}}$, Hurricane Carla data number 6878.

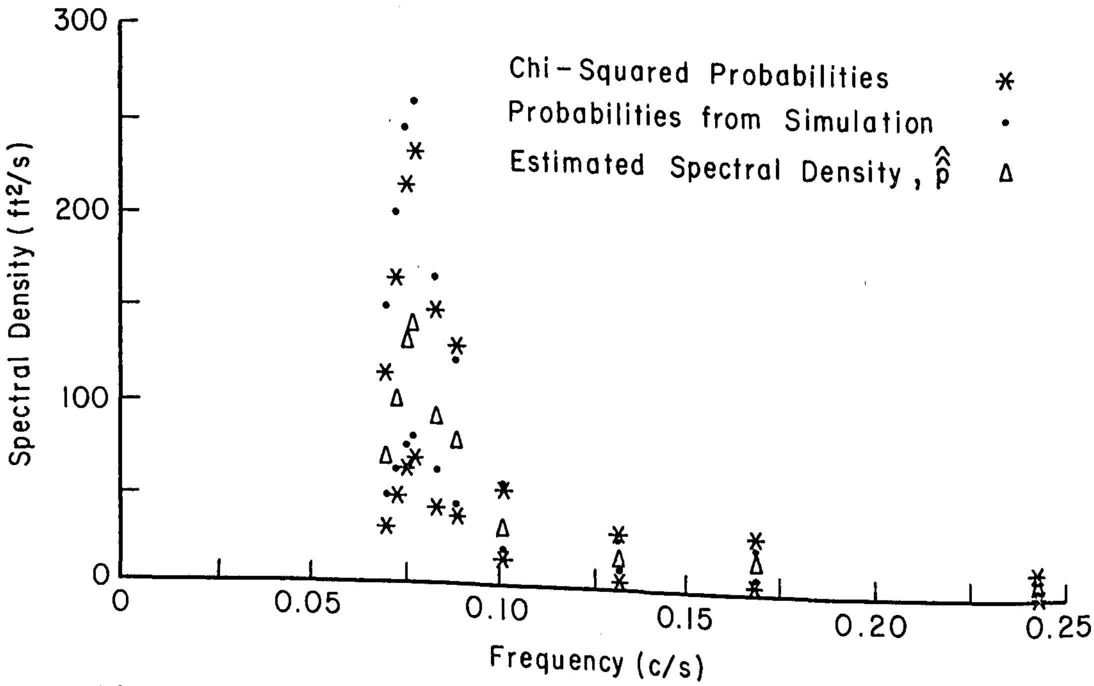

Figure 63. Probability intervals for $\hat{\hat{p}}$, Hurricane Carla data number 6879.

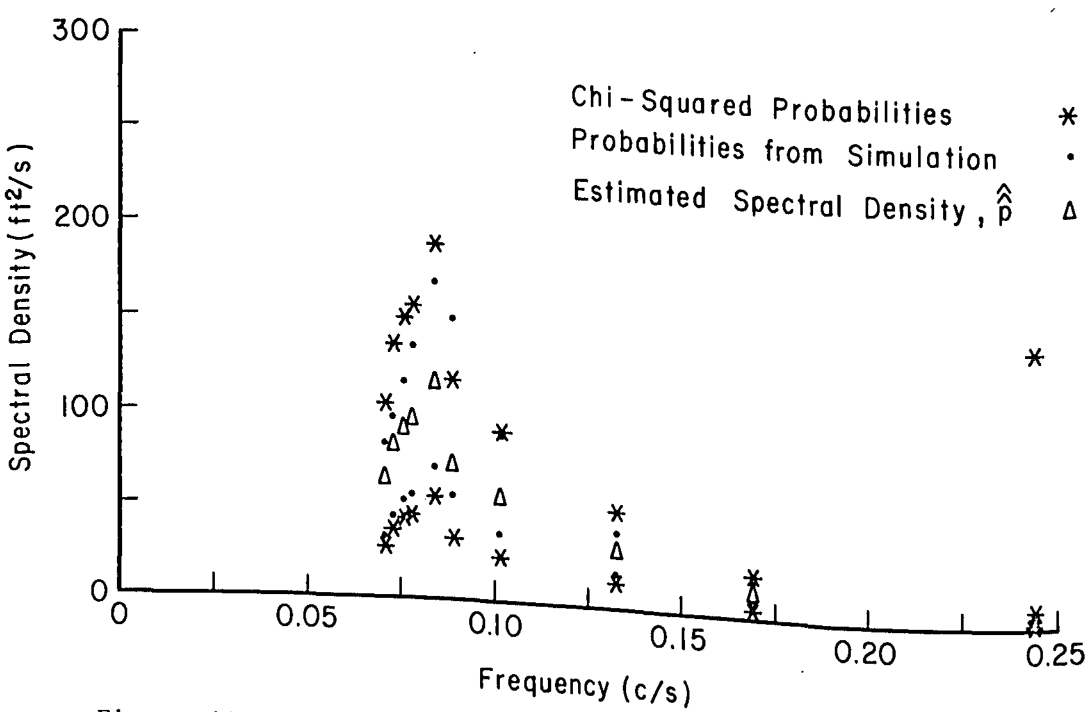

Figure 64. Probability intervals for $\hat{\hat{p}}$, Hurricane Carla data number 6880.

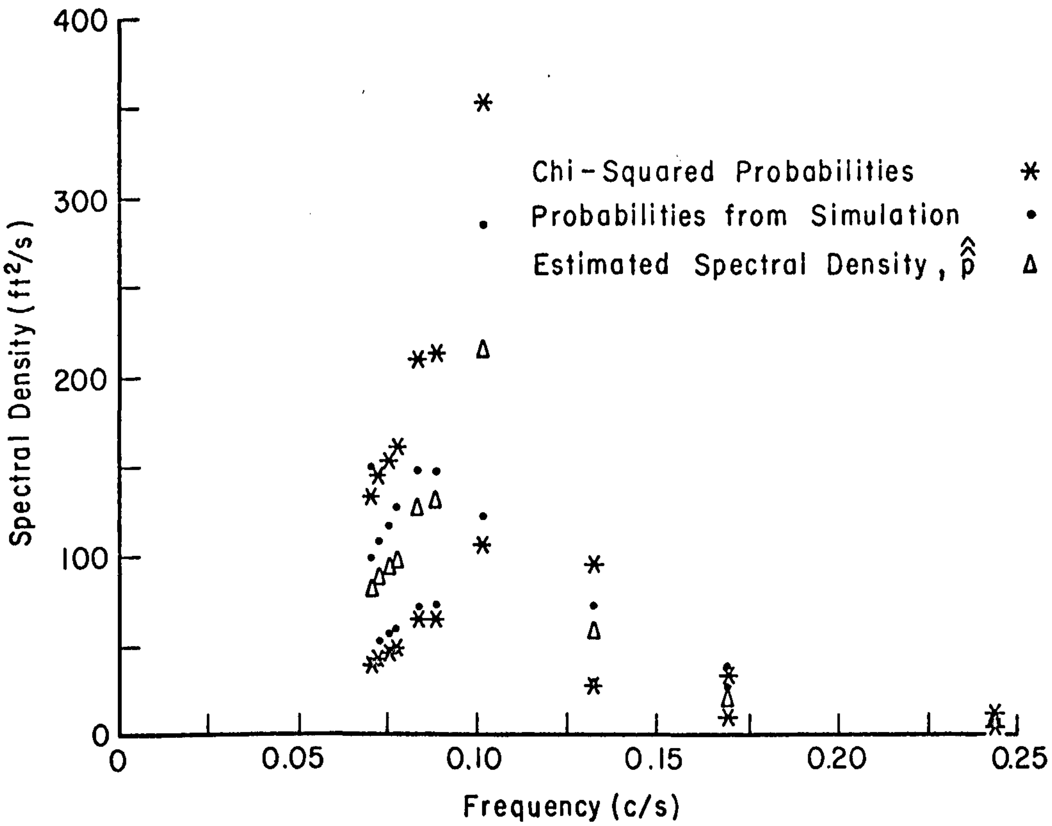

Figure 65. Probability intervals for $\hat{p}$, Hurricane Carla data number 6881-1.

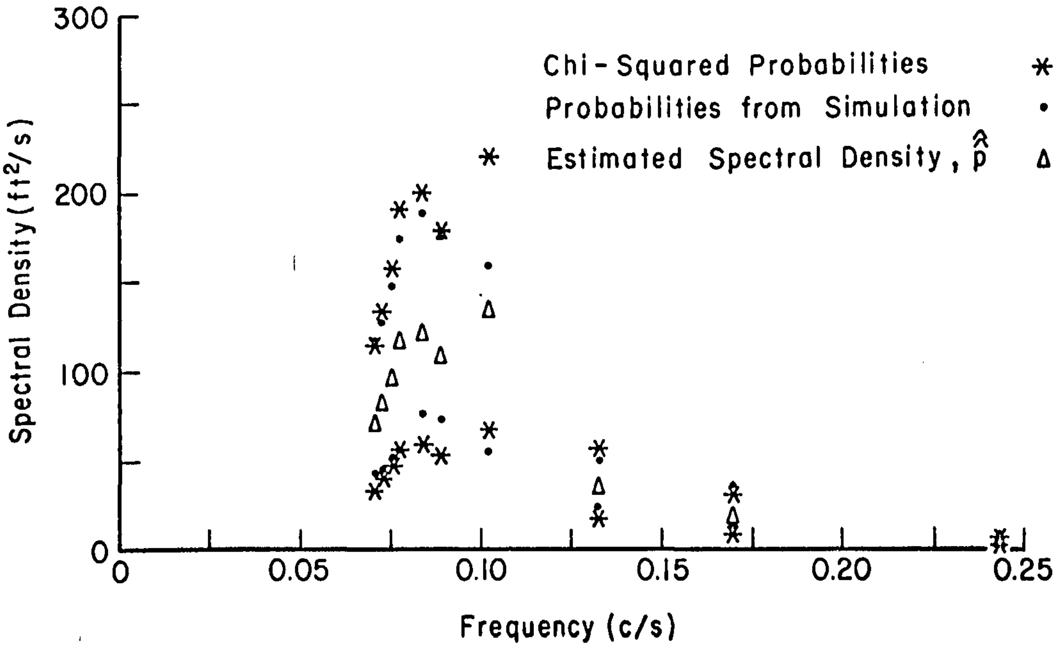

Figure 66. Probability intervals for $\hat{p}$, Hurricane Carla data number 6881-2.

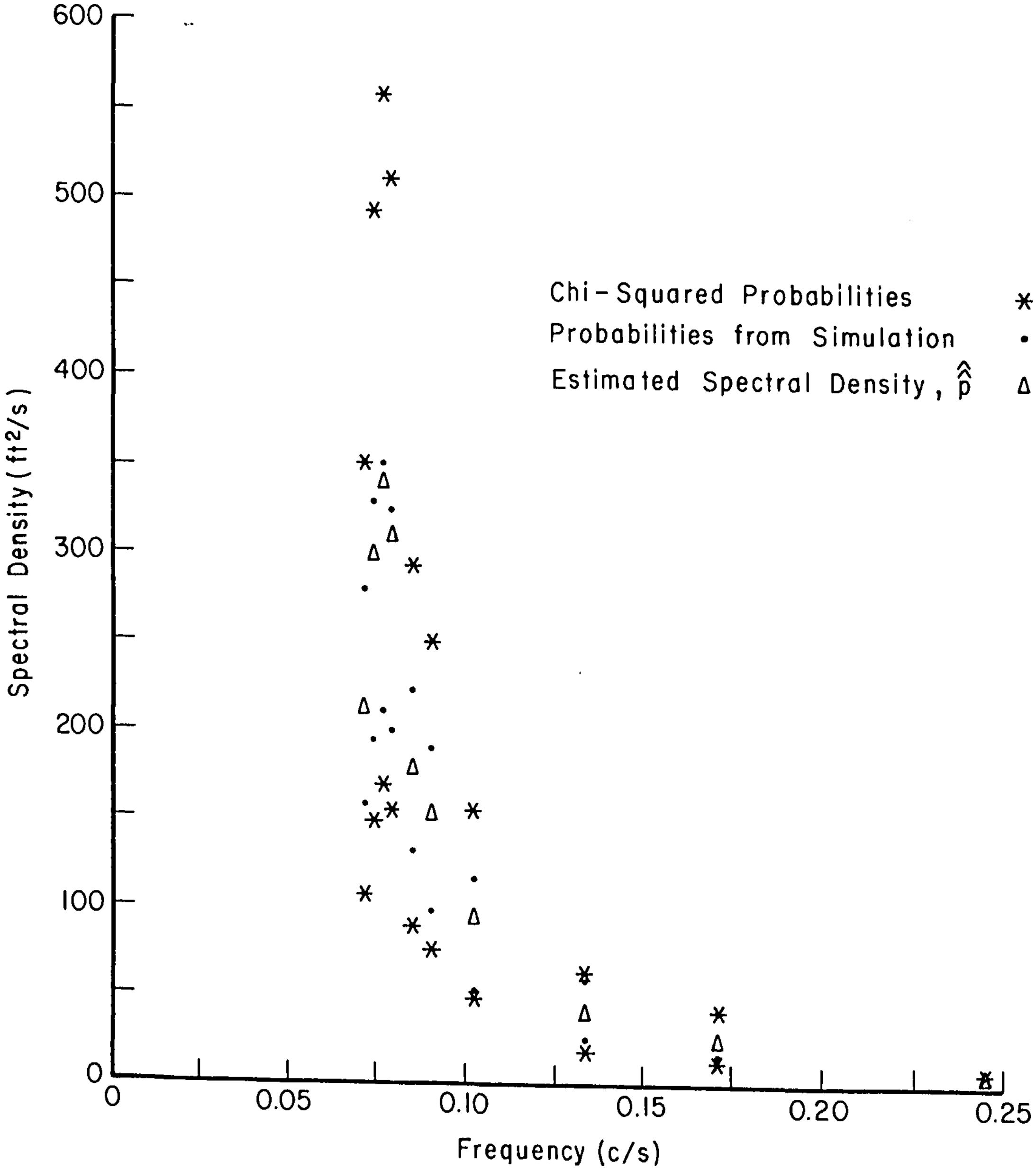

Figure 67. Probability intervals for $\hat{\hat{p}}$, Hurricane Carla data number 6882.

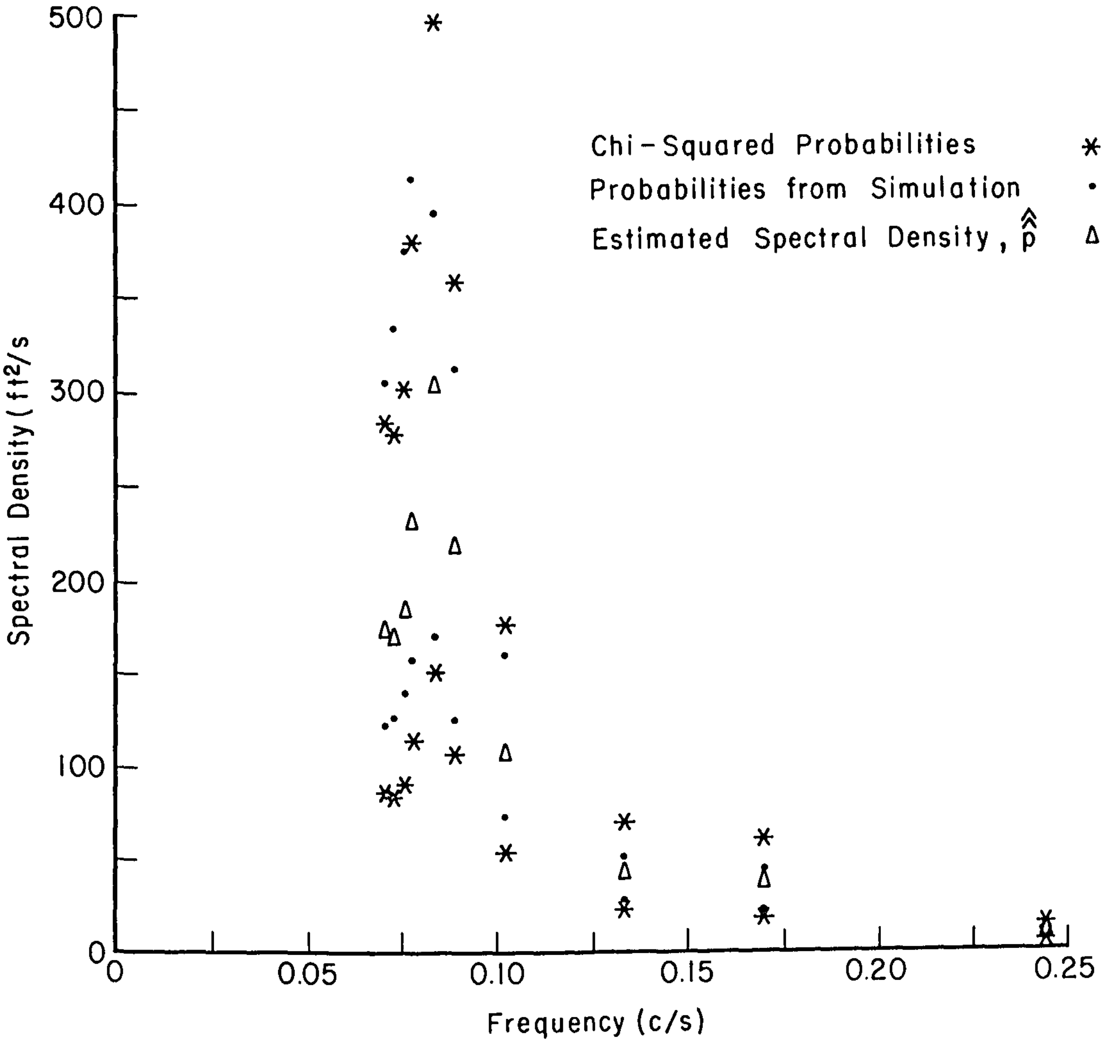

Figure 68. Probability intervals for $\hat{\hat{p}}$, Hurricane Carla data number 6883.

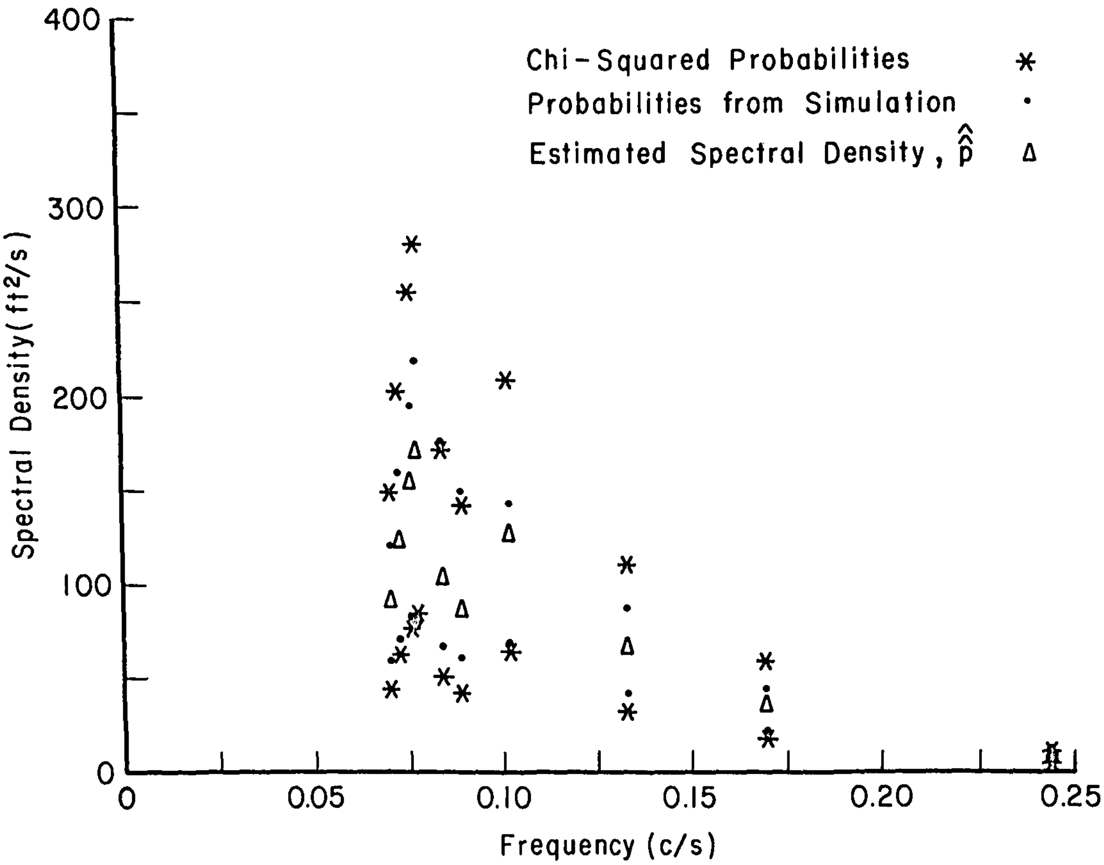

Figure 69. Probability intervals for $\hat{\hat{p}}$, Hurricane Carla data number 6884.

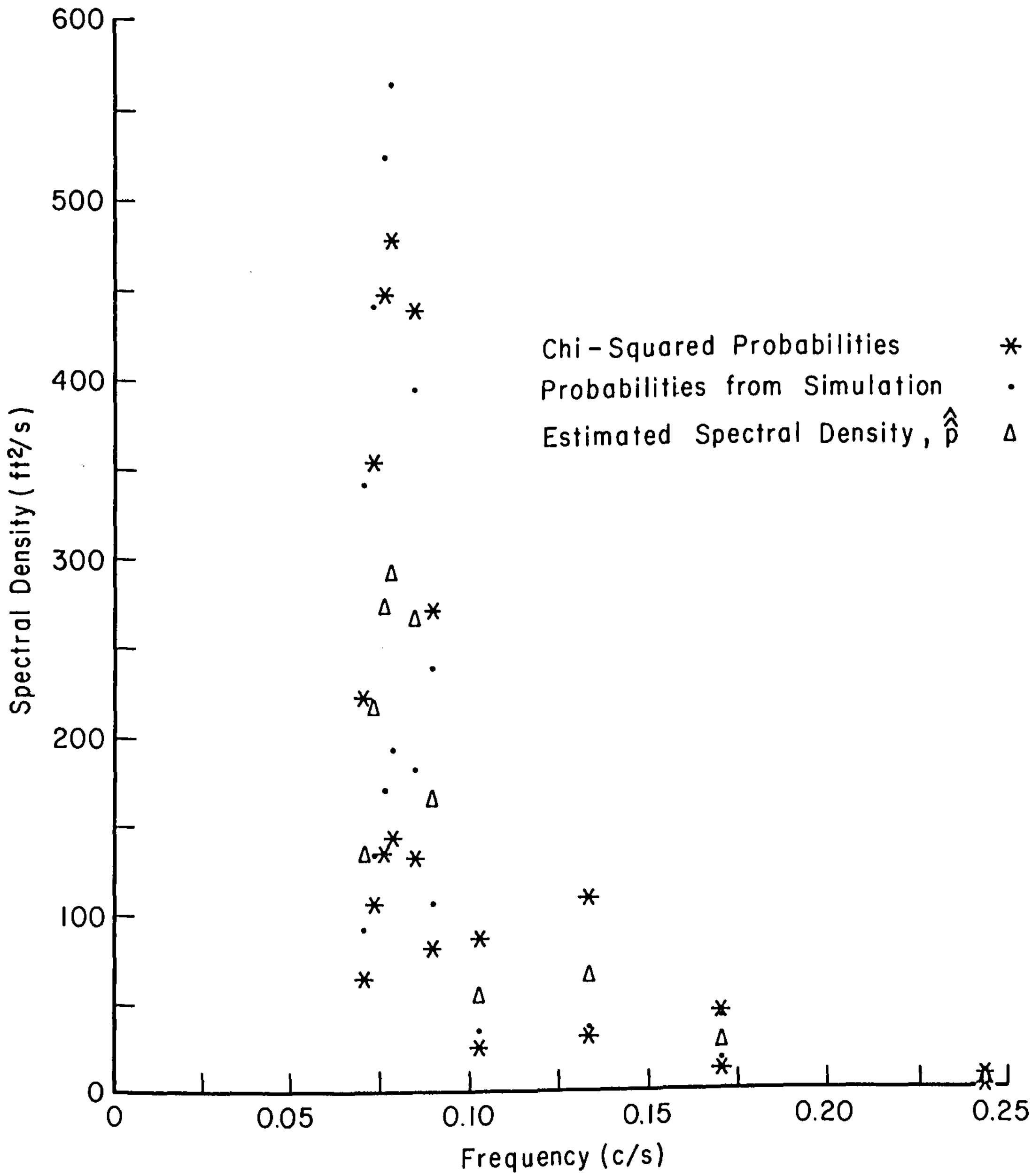

Figure 70. Probability intervals for $\hat{p}$, Hurricane Carla data number 6885.

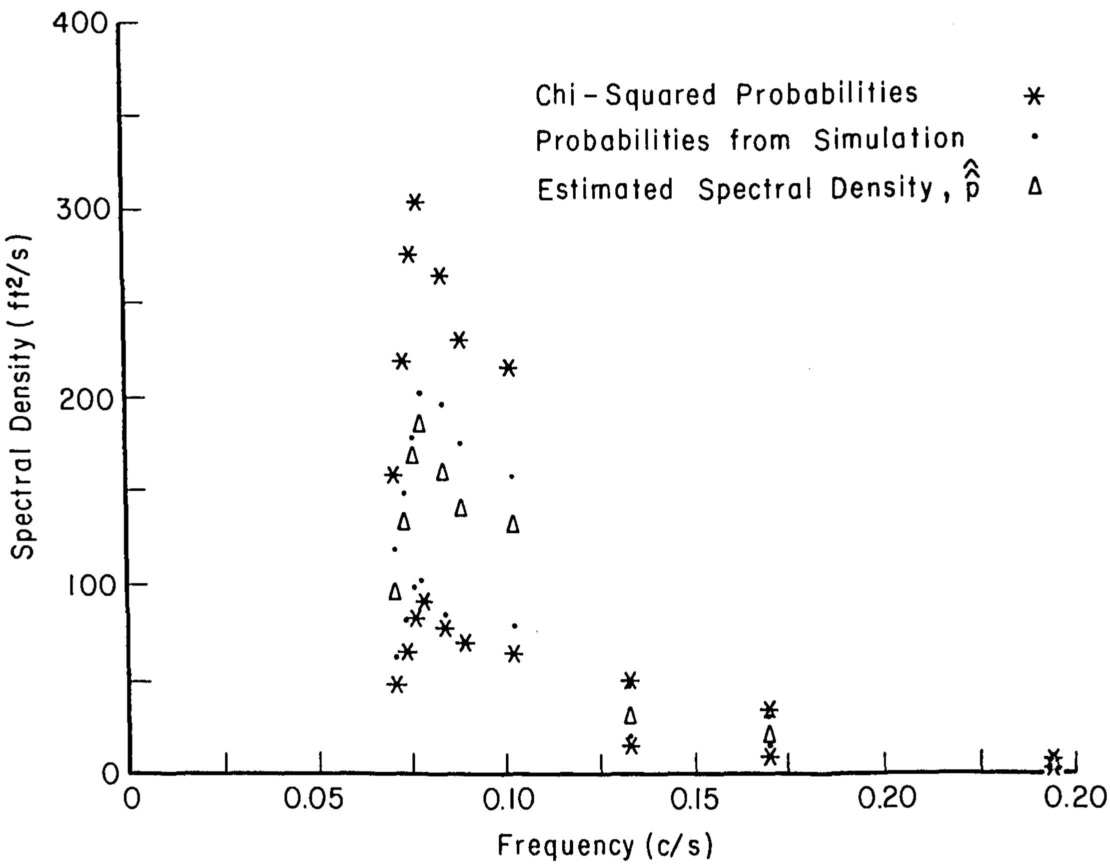

Figure 71. Probability intervals for $\hat{\hat{p}}$, Hurricane Carla data number 6886-1.

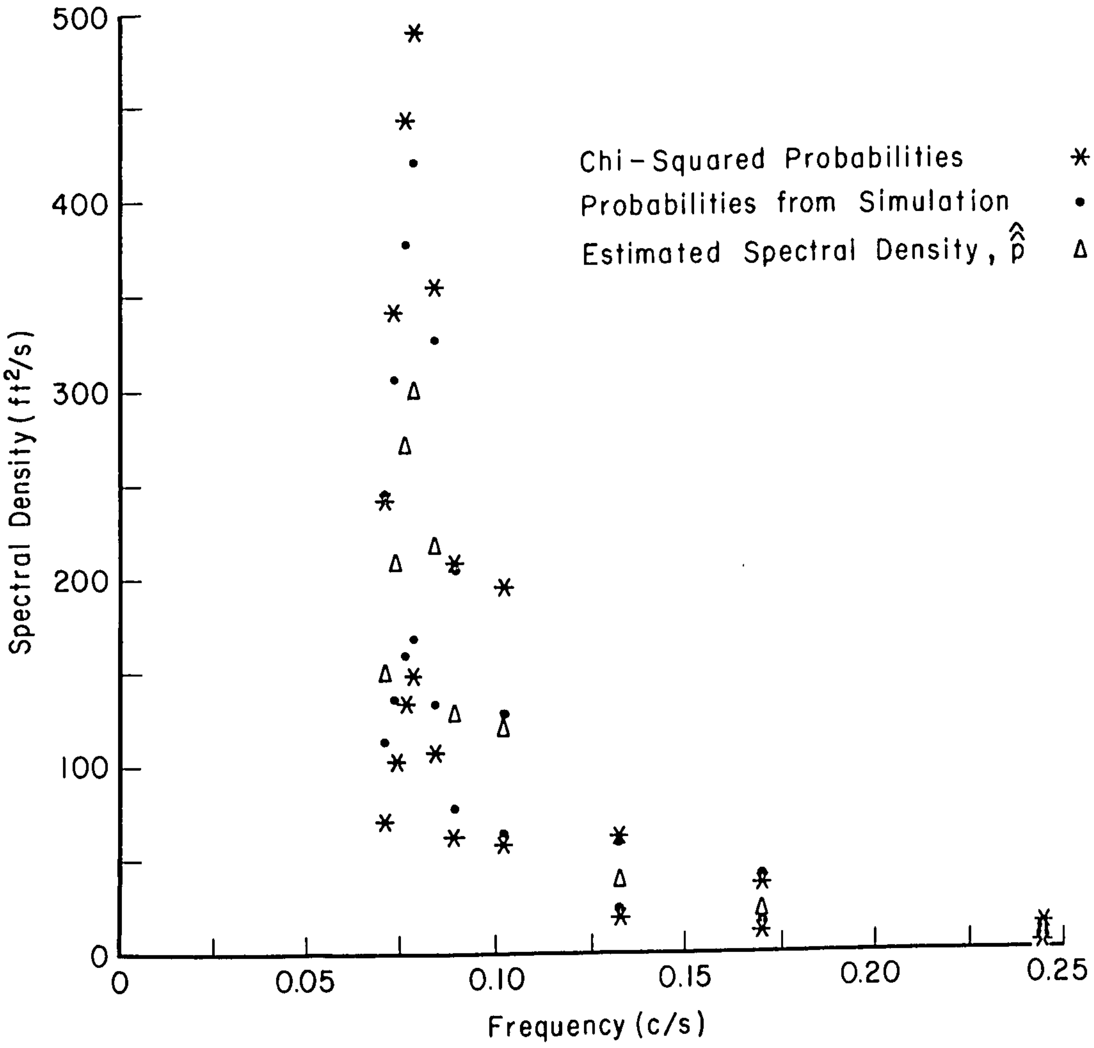

Figure 72. Probability intervals for $\hat{\hat{p}}$, Hurricane Carla data number 6886-2.

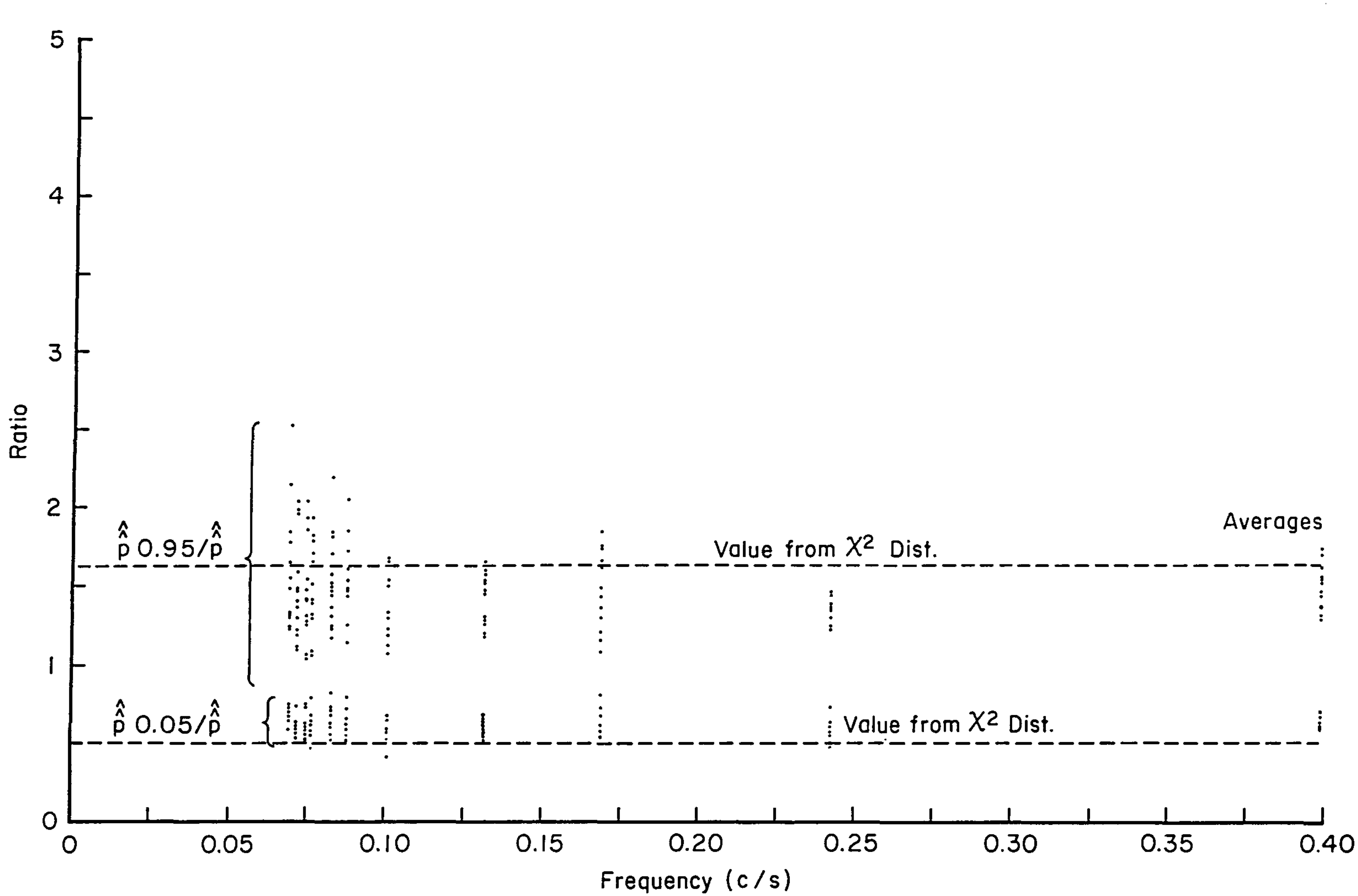

Figure 73. Ratio of probability interval bounds to the spectrum estimate.

are plotted versus frequency for all 12 data records. The average over the 10 frequencies for each record is plotted on the right of the graph above the frequency value, 4.0 sec.$^{-1}$. For the chi-squared distribution the corresponding values are theoretically,

$$\text{95th percentile } \hat{p}(f_m) \;/\; p(f_m) = \chi^2_{16,0.95} \Big/ 16 = 1.64 \qquad (50)$$

$$\text{5th percentile } \hat{p}(f_m) \;/\; p(f_m) = \chi^2_{16,0.05} \Big/ 16 = 0.50 \quad . \qquad (51)$$

These values are shown as dashlines in the figure.

On the average the two types of probability intervals agree fairly well.

XI. COMPARISON OF THE EMPIRICAL DISTRIBUTION FUNCTION OF THE SYMMETRICALLY NORMED RESIDUALS WITH THE CHI-SQUARED VERSION

If the chi-squared distribution is reasonably valid for $\hat{\hat{p}}(f_m)$, it may also hold for the spectral lines, at least approximately. The theoretical relation to be checked for validity is:

$$\hat{p}(f_m) \Big/ p(f_m) = \chi^2_2 \;/\; 2 \quad . \qquad (52)$$

The chi-squared analogy to σ^2_+ in equation (38) is:

$$\text{theoretical } \sigma^2_+ = E\left[\left\{\hat{p}(f_m) - p(f_m)\right\}^2 \,\middle|\, \hat{p}(f_m) > p(f_m)\right]$$

$$= p^2(f_m)\, E\left[\left\{\frac{\hat{p}(f_m)}{p(f_m)} - 1\right\}^2 \,\middle|\, \frac{\hat{p}(f_m)}{p(f_m)} > 1\right]$$

$$= \frac{p^2(f_m)}{4}\, E\left[\left\{\chi^2_2 - 2\right\}^2 \,\middle|\, \chi^2_2 > 2\right] \quad . \qquad (53)$$

By exact analogy:

$$\text{theoretical } \sigma^2_- = \frac{p^2(f_m)}{4}\, E\left[\left\{\chi^2_2 - 2\right\}^2 \,\middle|\, \chi^2_2 < 2\right] \quad . \qquad (54)$$

Since the probability density for χ^2_2 random variable is:

$$f_{\chi^2_2}(w) = \begin{cases} \dfrac{e^{-w/2}}{2} & , \text{ for } w > 0 \\ 0 & , \text{ for } w < 0 \end{cases} \quad , \qquad (55)$$

and,

$$P\left[\chi_2^2 > 2\right] = \int_2^\infty \frac{e^{-w/2}}{2}\,dw = e^{-1} \tag{56}$$

$$P\left[\chi_2^2 < 2\right] = 1 - e^{-1} \quad , \tag{57}$$

it follows that the conditional densities needed to evaluate equations (53) and (54) are:

$$f_{\chi_2^2 \mid \chi_2^2 > 2}(w) = \begin{cases} \dfrac{e^{-w/2}}{2\,e^{-1}} & , \text{ for } w \geq 2 \\ 0 & , \text{ otherwise} \end{cases} \tag{58}$$

$$f_{\chi_2^2 \mid \chi_2^2 < 2}(w) = \begin{cases} \dfrac{e^{-w/2}}{2(1-e^{-1})} & , \text{ for } 0 \leq w \leq 2 \\ 0 & , \text{ otherwise} \end{cases} \quad . \tag{59}$$

Thus, the quantities in equations (53) and (54) are given by:

$$\begin{aligned} \text{theoretical } \sigma_+^2 &= \frac{p^2(f_m)}{4e^{-1}} \int_2^\infty (w-2)^2 \frac{e^{-w/2}}{2}\,dw \\ &= 2\,p^2(f_m) = \left\{1.414\ p(f_m)\right\}^2 \end{aligned} \tag{60}$$

$$\begin{aligned} \text{theoretical } \sigma_-^2 &= \frac{p^2(f_m)}{4(1-e^{-1})} \int_0^2 (w-2)^2 \frac{e^{-w/2}}{2}\,dw \\ &= \left(\frac{1-2e^{-1}}{1-e^{-1}}\right) p^2(f_m) = \left\{0.6465\ p(f_m)\right\}^2 \quad . \end{aligned} \tag{61}$$

Finally, the chi-squared analogy to equation (38) will be:

$$\text{theoretical SNR} = \frac{\hat{p}(f_m) - p(f_m)}{cp(f_m)} \quad , \tag{62}$$

where

$$c = \begin{cases} 1.414 \quad , & \text{if } \hat{p}(f_m) > p(f_m) \\ 0.6465 \quad , & \text{if } \hat{p}(f_m) < p(f_m) \end{cases} \quad . \tag{63}$$

In terms of the χ_2^2 random variable, equation (62) becomes:

$$\text{theoretical SNR} = c^{-1}\left\{ \frac{\hat{p}(f_m)}{p(f_m)} - 1 \right\}$$

$$= c^{-1}\left\{ \frac{\chi_2^2}{2} - 1 \right\}$$

$$= \frac{1}{2c}\left\{ \chi_2^2 - 2 \right\} \quad . \tag{64}$$

Hence, the theoretical distribution function for the SNR variables (consistent with the chi-squared assumption) is:

$$\text{theoretical } F_{SNR}(w) = P\left[\frac{1}{2c}\left\{ \chi_2^2 - 2 \right\} \leq w \right]$$

$$= P\left[\chi_2^2 \leq 2cw + 2 \right]$$

$$= F_{\chi_2^2}(2cw + 2) = 1 - \exp(-cw - 1)$$

$$= \begin{cases} 1 - \exp(-1.414\, w - 1) \quad , & \text{if } w > 0 \\ 1 - \exp(-0.6465\, w - 1) \quad , & \text{if } w < 0 \end{cases} \quad . \tag{65}$$

The theoretical $F_{SNR}(w)$ is graphed in Figures 37 through 48 as a solid line.

By inspection, it can be seen that distribution function derived from the chi-squared probability law is reasonably close to the empirical distribution functions although there are systematic differences. In general, the empirical curves tend to lie below the theoretical curve for most argument values. The Kolmogorov confidence interval for the difference between the true distribution function and the empirical one is drawn in on record 6878. The chi-squared curve exceeds the upper boundary in the midranges but the two distribution curves are in fair agreement in the vicinity of the 5th and 95th percentiles. This is probably why the probability intervals agree fairly well. It should be noted that record 6878 is one of the more extreme cases and most of the other records attain closer agreement between the two curves.

A numerical error was made in the earlier report (Borgman, 1972, Figs. 7 and 8) relative to the chi-squared related distribution function and probability densities. The theoretical curves in those figures should be ignored.

XII. THE OUTLIER SPECTRAL LINES

In 7 of the 12 records, one or more spectral lines loom high above the others. These are ordinarily associated with the largest spectral density values and determine where the peak of the spectral density will occur in most cases. The spectral density decreases appreciably if these extreme or outlier spectral lines are deleted from the averaging process in the density determination.

A list of all the outliers is given in Table 3. Spectral lines which exceeded 500 are shown and one value which went to 477 is included. The spectral density value at that same frequency is tabled as well as the spectral density which results if the outlier spectral lines for that record were all deleted from the averaging. The spectral density without the lines is usually about 60 percent of what the density is with the lines included in the averaging.

Two other measures of the "extremeness" of the lines are listed in Table 3. The first is the ratio of the spectral line value to the density computed with the outliers deleted. If chi-squared theory holds, this ratio should behave like a $\chi_2^2 / 2$ random variable. The 99.5 percentile for a $\chi_2^2 / 2$ random variable is 5.3. Six of the 14 outliers listed exceed 5.3 in value. However, it is difficult to interpret this. One is examining the larger members of 300 lines. Hence, extremal statistical theory needs to be introduced. Straightforward application of the theory of extremes would say that the probability that the largest such ratio in a record would be less than 5.3 is:

$$(0.955)^{300} = 0.22 \quad , \qquad (66)$$

providing the chi-squared interrelation and the independence assumptions

Table 3. Characteristics of outlier spectral lines.

Record No.	Freq.	Outlier line (a)	Spectral w/line	Density w/o line (b)	Ratio (a/b)[1]	SNR[2]
6878	0.0732	477	148	96	5.0	4.4
	0.0842	525	117	54	9.8	8.0
6879	0.0757	620	141	67	9.3	7.2
6881-1	0.1025	652	231	166	3.9	3.3
6882	0.0720	557	299	203	2.7	2.9
	0.0745	660	338	251	2.6	3.3
6883	0.0696	586	172	102	5.8	4.6
	0.0781	741	248	132	5.6	4.3
	0.0830	733	302	141	5.2	3.5
	0.0854	606	266	126	4.8	3.2
6885	0.0745	1,123	273	128	8.8	6.9
	0.0818	868	281	171	5.1	9.7
6886-2	0.0769	1,026	298	171	6.0	6.7
	0.0830	582	215	124	4.7	4.3

[1]Ratio a/b refers to the ratio of the numbers indicated by a and b.

[2]The SNR is computed from σ_+ and σ_- based on averages with the outliers deleted.

are both accepted. Two of the seven records have maximum outlier ratios less than 5.3. This is 28 percent which is remarkably close to the 22 percent derived above.

The second measure of extremeness is the value of the SNR as based on σ_+ and σ_- computed without the outliers present. Other than noting that a three-sigma bound is often used in reliability to indicate unusual extremeness, no attempt will be made to interpret these results at this point in the research.

One nonstatistical observation may be more significant than all the statistical computations. This is the twofold fact that (a) the outliers always seem to fall in the maximum energy frequency range, and (b) the outlier lines are exceptionally separated from their neighbors, i.e., there is not a smooth transition with lots of small lines, some moderately large lines, and a few very large lines. It is more like two separate populations with no moderate range values between the two. This situation occurs in statistics in "gross error" or outlier questions. However, there is really insufficient statistical data to draw any firm conclusions.

From an oceanographic viewpoint, the one or several outlier spectral lines might well dominate the waves present so that an aerial photo would show waves of that frequency proceeding in their particular direction. This is, of course, just conjecture since aerial photos for Hurricane Carla at that space-time location are not available. The other spectral lines present might be contributing noise and making the waves highly short-crested.

The spectral line outliers may be some sort of resonant phenomena within the storm waves whereby energy tends to be concentrated on certain frequencies. Again, this is beyond the present research and is only noted in passing.

In the situations where several outlier lines are present in the record, an investigation was made as to whether there could really be only one wave train present with the other lines showing up as leakage due to purely mathematical manipulations. Appendix B gives a derivation of the FFT leakage for a single cosine wave. It is shown that, at least in a gross sense, the leakage is delineated by the following formulas. Let the wave profile be given by:

$$\eta_n = a \cos\left(\frac{2\pi m_0 n}{N} - \phi\right), \qquad (67)$$

where m_0 is not necessarily an integer. The approximate FFT spectral lines, if $20 \leq m_0 + m << N$, are given by the formula:

$$\hat{p}(f_m) \approx \frac{a^2 N \Delta t}{4} \left\{\frac{\sin\pi(m_0 - m)}{\pi(m_0 - m)}\right\}^2 . \qquad (68)$$

From this, leakage would always be to the immediate neighboring lines. The outlier lines in Table 3 are always separated by one or more small lines in each case. Hence, one has to conclude that the cases with two or more outlier spectral lines cannot be explained by a single wave train with FFT leakage.

XIII. WHY DOES CHI-SQUARED WORK FOR HURRICANE WAVES?

One of the mysteries arising from the data is the surprisingly good probabilities arising from the chi-squared derivations. If linear wave theory was holding and the seas were Gaussian, this would be expected (Borgman, 1972, 1973). However, the hurricane waves were decidedly non-linear. The waves in many of the records have been plotted by computer and examined visually. The nonlinearities are really there. Why does the the chi-squared work so well?

Investigation of this question led to a central limit theorem for dependent random variables which showed that the chi-squared relations hold exactly as N tends to infinity even for a non-Gaussian sea surface. The primary limitation is that water level elevations at the recorder separated by more than a certain constant time interval should be statistically independent of each other. The amount of the separation required to achieve independence is unimportant in the validity of the theorem although it will affect the speed of convergence to the asympototic result. Time sequences with above dependency properties are said to be "m-dependent," in statistical terminology.

A sufficient condition, then, for the central limit theorem to hold is that the probability density of the water level elevation measured from mean water level satisfies at least one of two "tail" conditions. The density, $f(\eta)$, should be such that there exists positive constants a, b, and c, and a positive integer n, such that:

$$f(\eta) \leq a|y|^n e^{-b|y|} \quad , \quad |y| > c \quad , \tag{69}$$

or alternately, there exists a positive constant A such that:

$$f(\eta) = 0 \quad , \quad \text{if} \quad |y| > A \quad . \tag{70}$$

The second condition is a special case of the first since if the second condition holds then $c = A$ and any a, b, and n values will permit the first condition to be satisfied.

Equation (69) is not an unreasonable restriction. For low seas, the sea surface has been found to be normally distributed. As the wave heights increase, a gamma density might be a reasonable guess as to the proper probability law. Both of these densities satisfy equation (69). In fact, from a practical viewpoint, no one seriously suggests that water level elevations can be infinite as required by the normal or the gamma densities. In fact, there will be a large value of A (e.g., A = water depth) such that equation (70) will hold.

The full details of the derivation for the m-dependent central limit theorem and the asymptotic chi-squared properties of the spectral estimates are given in Appendic C. One useful secondary result, summarized in item (C-8) of the appendix, is that the normed FFT coefficients,

$$\left(\frac{U_m}{\sqrt{Np_m \Delta t/2}} , \frac{V_m}{\sqrt{Np_m \Delta t/2}} \right), \ m_0 + 1 \leq m \leq m_0 + r \ , \tag{71}$$

asymptotically follow a multivariate probability law with zero mean and covariance matrix equal to an identity matrix.

As an illustration of the asymptotic normality, 100 water level elevations were selected from the Hurricane Carla data number 6883. The elevations were taken 6 seconds apart from the beginning of the data until 100 elevations were obtained. Also, the 50 pairs of Fourier coefficients centered around the frequency associated with the largest spectral density value (Fig. 8) were tabulated from the computer listings. The water level elevations and the FFT coefficients were plotted on normal probability paper (after norming them) as shown in Figure 74. An examination of the figure shows that the FFT coefficients follow a reasonably straight line while the water level elevations exhibit a concave upward curve. The skewness of the water level elevations was computed to be 0.55 while the FFT coefficients only showed a skewness of 0.03. Thus, the FFT coefficients were reasonably close to normality even though the water level elevations were decidedly nonnormal.

It would be interesting to explore the normalizing influence of the Fourier transform relative to the other wave records in Hurricane Carla. However, time did not permit that to be included in this investigation.

XIV. IMPLICATIONS FOR DIRECTIONAL SPECTRUM RELIABILITY

The asymptotic normality of the finite Fourier transform coefficients are extremely important relative to the estimation of the reliability of the directional spectrum and of other quantities such as energy diffraction computed from the FFT coefficients. The FFT coefficients, at least for large data sets, can be taken as normally distributed and independent. These properties can be carried through the various formulas used in computing the particular quantity to obtain reliability measures for the quantity.

XV. SUMMARY AND CONCLUSIONS

1. The statistical properties of the spectral lines for 12 pieces of data measured during Hurricane Carla (8 to 10 September 1961) were examined in detail. The spectral lines were found to show negligible serial correlation. The spectral lines could be reduced to what appears to be random noise by subtracting from the lines the spectral density obtained by smoothing the lines with a moving average and then

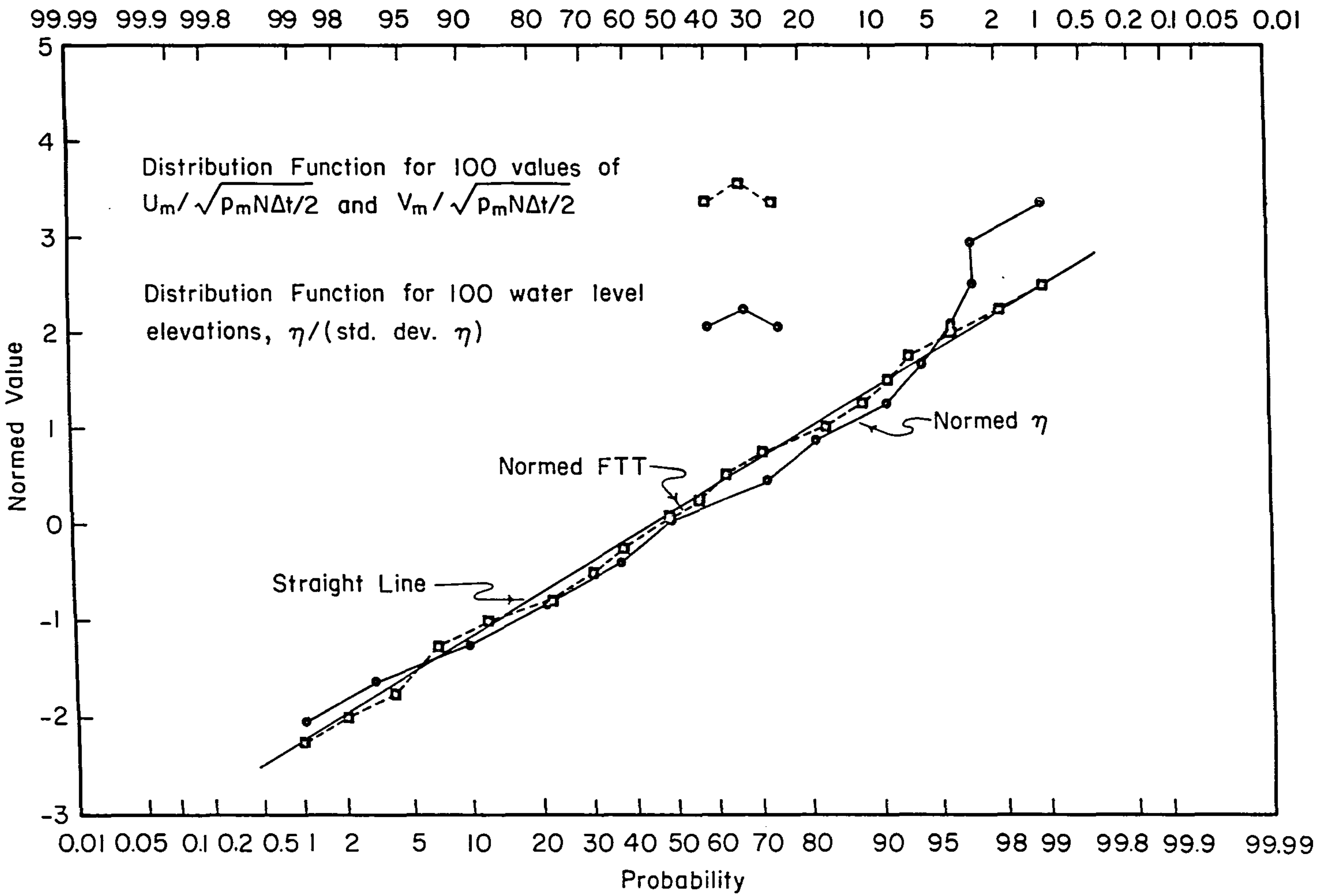

Figure 74. Comparison of the distribution function of normed water level elevations and FFT coefficients, Hurricane Carla data 6883.

dividing the positive and negative deviations by the local root-mean-square positive and negative deviations respectively.

2. A simulation procedure based on the probability behavior of the random noise of the spectral line deviation was used to generate probability intervals for the spectral density estimates.

3. The simulation probability intervals were found to agree reasonably well with that predicted from the chi-squared probability law. Although the chi-squared probabilities are expected to be valid for "low wave" spectral densities, it was somewhat surprising to have them work for the nonlinear hurricane waves.

4. An investigation of the above item led to the discovery that the finite Fourier transform coefficients will be approximately independent and normally distributed for large data sets even though the water level elevations are not normally distributed. This face was derived from probability theory after assuming (a) m-dependence of the water level elevations about mean water level, and (b) a water level probability density which is bounded for large y by the function $a|y|^n e^{-b|y|}$ (a, b, and n are arbitrary constants). A central limit theorem was derived from these assumptions which led to the finite Fourier transform coefficients being asymptotically normally distributed and independent as the data length tended to infinity.

5. Under the conditions of the item above, the smoothed spectral estimates were found to be asymptotically chi-squared distributed providing the true spectrum is constant over the smoothing interval. If the true spectrum is not constant, the spectral density estimates would still be reasonably close to having chi-squared behavior although there would be some deviations as evidenced by the deviations of the simulation results from the chi-squared results.

6. The wave spectral lines exhibit members which appear unusually large as compared with the rest of the spectrum. The "outlier" lines always appear associated with the "peak energy" part of the spectral density. These unusual lines of energy might predominate the wave record so that a satellite picture would show waves of those frequencies riding on top of the rest of "noisy" wave combinations. However, this is just conjecture.

7. The outlier spectral lines mentioned above do not persist for long periods of time. In the two cases where Hurricane Carla wave data were available 20 minutes apart, the outliers were found in one set of the data pair but not in the other.

8. The conclusion of the study relative to reliability of directional spectrum estimation is that the finite transform coefficients may be taken as being serially uncorrelated and approximately normally distributed with zero mean, variance $p_m N \Delta t/2$, and the appropriate

cross-variances. This asymptotic normality can be carried forward to provide reliability measures for quantities, such as the directional spectrum, which are computed from the Fourier coefficients.

LITERATURE CITED

BLACKMAN, R.B., and TUKEY, J.W., *The Measurement of Power Spectra*, Dover Publications, New York, 1958.

BORGMAN, L.E., "Confidence Intervals for Ocean Wave Spectra," *Proceedings of the 13th International Conference on Coastal Engineering*, Vancouver, B.C., 1972.

BORGMAN, L.E., "Statistical Properties of Fast Fourier Transform Coefficients Computed From Real-Valued, Covariance-Stationary Periodic Random Sequences," Research Paper No. 23, College of Commerce and Industry, University of Wyoming, Laramie, Wyo., 1973.

COOLEY, J.W., and TUKEY, J.W., "An Algorithm for the Machine Calculation of Complex Fourier Series," *Mathematics of Computations*, Vol. 19, Apr. 1965, pp. 297-301.

FREUND, J.E., *Mathematical Statistics*, 2d ed., Prentice-Hall, Englewood Cliffs, N.J., 1971.

GOODMAN, N.R., "On the Joint Estimation of the Spectra, Cospectrum and Quadrature Spectrum of a Two-Dimensional Stationary Gaussian Process," Scientific Paper No. 10, Engineering Statistics Laboratory, College of Engineering, New York University, New York, 1957.

GUMBEL, E.J., "Statistical Theory of Extreme Values and Some Practical Applications," Series 33, National Bureau of Standards Applied Mathematics, U.S. Government Printing Office, Washington, D.C., 1954.

LOEVE, M., *Probability Theory*, Van Nostrand, Princeton, N.J., 1960.

PIERSON, W.J., Jr., "Wind-Generated Gravity Waves," *Advances in Geophysics*, Vol. 2, 1955, pp. 93-178.

RAO, C.R., *Linear Statistical Inference and Its Applications*, 2d ed., Wiley and Sons, New York, 1973.

ROBINSON, E.A., *Multichannel Time Series Analysis with Digital Computer Programs*, Holden-Day, San Francisco, Calif., 1967, pp. 62-64.

ROSEN, B., "On the Central Limit Theorem for Sums of Dependent Random Variables," Z. *Wahrscheinlichkeitstheorie und Verw. Gebiete*, Vol. 1, 1967, pp. 48-82.

APPENDIX A

EFFECTIVE WIDTH

The effective width of a moving average smoothing function is defined to be the width of square pulse required to have the same area and same middle height. For example, consider the pulse:

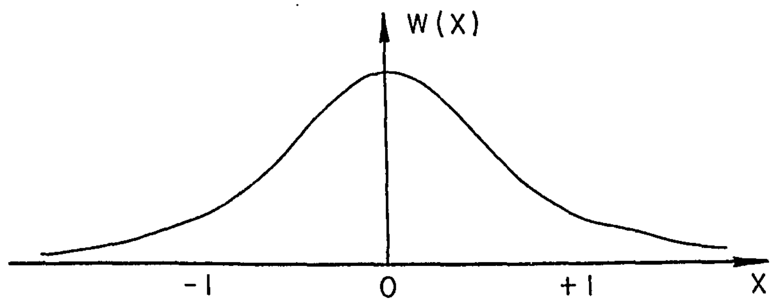

This pulse has area

$$A = \int_{-\infty}^{\infty} w(x)\ dx$$

and middle height $w(0)$. The effective width would be the value of e.w. such that

$$(e.w.) \times w(0) = A$$

or

$$(e.w.) = A/w(0) \quad .$$

APPENDIX B

EFFECT OF A DETERMINISTIC LINE ON THE SPECTRUM

Suppose that η_n for $0 \leq n \leq N-1$ is a cosine curve,

$$\eta_n = a \cos\left[2\pi m_0 \frac{n}{N} - \phi\right] \quad , \tag{B-1}$$

where m_0 is not necessarily an integer. What will be the effect on the spectral density? The fast Fourier transform of η_n gives:

$$A_m = \Delta t \sum_{n=0}^{N-1} a \cos\left[2\pi m_0 \frac{n}{N} - \phi\right] e^{-i2\pi mn/N}$$

$$= \frac{a}{2} \Delta t \sum_{n=0}^{N-1} \left[e^{i(2\pi m_0 \frac{n}{N} - \phi)} + e^{-i(2\pi m_0 \frac{n}{N} - \phi)}\right] e^{-i2\pi mn/N}$$

$$= \frac{a\Delta t}{2} \left[e^{-i\phi} \sum_{n=0}^{N-1} \left\{e^{i2\pi(m_0-m)/N}\right\}^n\right.$$

$$\left. + e^{+i\phi} \sum_{n=0}^{N-1} \left\{e^{-i2\pi(m_0-m)/N}\right\}^n\right] \quad . \tag{B-2}$$

Since, by the geometric series,

$$1 + r + r^2 + r^3 + \ldots + r^{N-1} = (1 - r^N)/(1 - r) \quad ,$$

it follows that:

$$A_m = \frac{a\Delta t}{2} \left[e^{-i\phi} \frac{1 - e^{i2\pi(m_0-m)}}{1 - e^{i2\pi(m_0-m)/N}} + e^{i\phi} \frac{1 - e^{-i2\pi(m_0+m)}}{1 - e^{-i2\pi(m_0+m)/N}}\right] \tag{B-3}$$

$$A_m = \frac{a\Delta t}{2}\left[e^{-i\phi}\, \frac{e^{i\pi(m_0-m)}}{e^{i\pi(m_0-m)/N}} \cdot \frac{e^{-i\pi(m_0-m)} - e^{i\pi(m_0-m)}}{e^{-i\pi(m_0-m)/N} - e^{i\pi(m_0-m)/N}}\right.$$

$$\left. + e^{i\phi}\, \frac{e^{-i\pi(m_0+m)}}{e^{-i\pi(m_0+m)/N}} \cdot \frac{e^{i\pi(m_0+m)} - e^{i\pi(m_0+m)}}{e^{i\pi(m_0+m)/N} - e^{-i\pi(m_0+m)/N}}\right]$$

$$= \frac{a\Delta t}{2}\left[e^{i\{\pi\, m_0(1-\frac{1}{N}) - \phi\} - i\{\pi\, m(1-\frac{1}{N})\}}\, \frac{\sin\,\pi(m_0-m)}{\sin\,\pi(m_0-m)/N}\right.$$

$$\left. + e^{-i\{\pi\, m_0(1-\frac{1}{N}) - \phi\} - i\{\pi\, m(1-\frac{1}{N})\}}\, \frac{\sin\,\pi(m_0+m)}{\sin\,\pi(m_0+m)/N}\right]$$

$$= \frac{a\Delta t}{2}\left[e^{i(\alpha-\beta)}\, \frac{\sin\,\pi(m_0-m)}{\sin\,\pi(m_0-m)/N} + e^{-i(\alpha-\beta)}\, \frac{\sin\,\pi(m_0+m)}{\sin\,\pi(m_0+m)/N}\right], \qquad \text{(B-4)}$$

with

$$\alpha = \pi m_0(1-\frac{1}{N}) - \phi$$

$$\beta = \pi m(1-\frac{1}{N}) \quad . \qquad \text{(B-5)}$$

Hence, A_m can be written in terms of real and imaginary parts as:

$$A_m = \frac{a\Delta t}{2}\left[\frac{\sin\,\pi(m_0-m)}{\sin\,\pi(m_0-m)/N}\cos(\alpha-\beta) + \frac{\sin\,\pi(m_0+m)}{\sin\,\pi(m_0+m)/N}\cos(\alpha+\beta)\right]$$

$$+ i\,\frac{a\Delta t}{2}\left[\frac{\sin\,\pi(m_0-m)}{\sin\,\pi(m_0-m)/N}\sin(\alpha-\beta) - \frac{\sin\,\pi(m_0+m)}{\sin\,\pi(m_0+m)/N}\sin(\alpha+\beta)\right] . \qquad \text{(B-6)}$$

It follows that:

$$\left|A_m\right|^2 = \left(\frac{a\Delta t}{2}\right)^2 \left[\frac{\sin^2\,\pi(m_0-m)}{\sin^2\,\pi(m_0-m)/N} + \frac{\sin^2\,\pi(m_0+m)}{\sin^2\,\pi(m_0+m)/N}\right.$$

$$+ 2 \frac{\sin\left[\pi(m_0-m)\right] \sin\left[\pi(m_0+m)\right]}{\sin\left[\pi(m_0-m)/N\right] \sin\left[\pi(m_0+m)/N\right]} \{\cos(\alpha-\beta) \cos(\alpha+\beta)$$

$$- \sin(\alpha-\beta) \sin(\alpha+\beta)\}\Bigg]$$

$$= \frac{a\Delta t}{2}^{2} \left[\frac{\sin^2 \pi(m_0-m)}{\sin^2 \pi(m_0-m)/N} + \frac{\sin^2 \pi(m_0+m)}{\sin^2 \pi(m_0+m)/N}\right.$$

$$\left. + \frac{2 \sin\left[\pi(m_0-m)\right] \sin\left[\pi(m_0+m)\right]}{\sin\left[\pi(m_0-m)/N\right] \sin\left[\pi(m_0+m)/N\right]} \cos 2\alpha \right] \tag{B-7}$$

$$\hat{p}(f_m) = \left|A_m\right|^2/N\Delta t = \frac{a^2 N\Delta t}{4} \left[\frac{\sin^2 \pi(m_0-m)}{N^2 \sin^2 \pi(m_0-m)/N} + \frac{\sin^2 \pi(m_0+m)}{N^2 \sin^2 \pi(m_0+m)/N}\right.$$

$$\left. + \frac{2 \sin\left[\pi(m_0-m)\right] \sin\left[\pi(m_0+m)\right]}{N^2 \sin\left[\pi(m_0-m)/N\right] \sin\left[\pi(m_0+m)/N\right]} \cos \{2\pi m_0 (1-\frac{1}{N}) - 2\phi\}\right] . \tag{B-8}$$

If m_0 is an integer with $0<m_0<N/2$,

$$\hat{p}(f_m) = \begin{cases} a^2 N\Delta t/4 & , \text{ if } m = \pm m_0 \\ 0 & , \text{ otherwise.} \end{cases} \tag{B-9}$$

If N is much larger than either m_0-m and m_0+m, which is usually the case in applications, then approximately,

$$\begin{aligned} N \sin \pi(m_0-m)/N &\approx \pi(m_0-m) \\ N \sin \pi(m_0+m)/N &\approx \pi(m_0+m) \\ 1/N &\approx 0 \quad . \end{aligned} \tag{B-10}$$

Hence, equation (B-8) can be written approximately as:

$$\hat{p}(f_m) \approx \frac{a^2 N\Delta t}{4} \left[\left\{ \frac{\sin \pi(m_0-m)}{\pi(m_0-m)} \right\}^2 + \left\{ \frac{\sin \pi(m_0-m)}{(m_0+m)} \right\}^2 \right.$$

$$\left. + 2 \left\{ \frac{\sin \pi(m_0-m)}{\pi(m_0-m)} \right\} \left\{ \frac{\sin \pi(m_0+m)}{\pi(m_0+m)} \right\} \cos\,(2\,\pi m_0 - 2\phi) \right] . \qquad \text{(B-11)}$$

If $20 \leq m_0+m \ll N$, a reasonable assumption in many applications, then the first term inside the square brackets will dominate the other two. This fact is illustrated in the following computations, where

$$T_1 \doteq \left\{ \frac{\sin \pi(m_0-m)}{\pi(m_0-m)} \right\}^2 \qquad \text{(B-12)}$$

$$T_2 = \left\{ \frac{\sin \pi(m_0+m)}{\pi(m_0+m)} \right\}^2 \leq \frac{1}{400\,\pi^2} < 0.0003 \qquad \text{(B-13)}$$

$$|T_3| = \left| 2 \left\{ \frac{\sin \pi(m_0-m)}{\pi(m_0-m)} \right\} \left\{ \frac{\sin \pi(m_0+m)}{\pi(m_0+m)} \right\} \cos\,(2\,\pi m_0 - 2\phi) \right.$$

$$< \frac{1}{10\,\pi} \left| \frac{\sin \pi(m_0-m)}{\pi(m_0-m)} \right| \qquad \text{(B-14)}$$

$m_0-m_1 = 0.5$		Upper bound	
m	T_1	T_2	T_3
m_1	0.405	0.0003	0.020
m_1-1	0.045	0.0003	0.0068
m_1-2	0.016	0.0003	0.0041
m_1-3	0.0083	0.0003	0.0029

$m_0 - m_1 = 0.25$		Upper bound	
m	T_1	T_2	T_3
m_1+3	0.0067	0.0003	0.0026
m_1+2	0.016	0.0003	0.0041
m_1+1	0.090	0.0003	0.0096
m_1	0.811	0.0003	0.029
m_1-1	0.032	0.0003	0.0057
m_1-2	0.010	0.0003	0.0032
m_1-3	0.0048	0.0003	0.0022

The main characteristics of equation (B-11) are determined by the first term and in a gross sense,

$$\hat{p}(f_m) \approx \frac{a^2 N\Delta t}{4} \left\{ \frac{\sin \pi(m_0-m)}{\pi(m_0-m)} \right\}^2 \tag{B-15}$$

if $20 \leq m_0+m \ll N$ and $|m_0-m| \ll N$.

APPENDIX C

ASYMPTOTIC CHI-SQUARED PROPERTIES OF THE FFT SPECTRAL LINES FOR NON-GAUSSIAN, M-DEPENDENT WAVE TRAINS

1. Basic Definitions and Assumptions.

Let η_j, $j = 0,\pm1,\pm2,\pm3,\ldots$ be water level elevations about mean water level. It will be assumed that $\{\eta_j\}$ is a stationary second-order stochastic process which is not necessarily Gaussian and that the random sequence $\{\eta_j\}$ has the properties that, uniformly in n,

$$E\,[\eta_n] = 0 \tag{C-1}$$

$$E\,[\eta_n^2] \leq M < \infty \quad . \tag{C-2}$$

Let $Y_n = \eta_{a+n}$ for $n = 0,1,2,3,\ldots,N-1$. That is $\{Y_n\}$ is a finite sequence of the water level elevations starting at η_a and terminating with η_{a+N-1}. The time interval between water level elevation values is denoted by Δt. The finite Fourier transform coefficients are defined as:

$$A_m^{(N)} = \Delta t \sum_{n=0}^{N-1} Y_n \, e^{-i2\pi mn/N}$$

$$= U_m^{(N)} - i\, V_m^{(N)} \quad , \tag{C-3}$$

where $i = \sqrt{-1}$. The superscript N is attached to A_m to indicate that the FFT coefficients are computed on the basis of a sequence of length N.

It will be assumed that the sequence η_j is m-dependent. That is, $\{\eta_b, \eta_{b+1},\ldots, \eta_{b+s}\}$ and $\{\eta_{c-r}, \eta_{c-r+1},\ldots, \eta_c\}$ are statistically independent sets of random variables if $b - c > m$ (Rosen, 1967).

The probability density for η_j will be assumed to satisfy either conditions (a) or (b) under item 5 given in the following. The FFT coefficients will be said to be degenerate if $p_m = 0$ and hence $U_m = V_m \equiv 0$.

2. Motivation.

Consider the set of nondegenerate coefficients:

$$S = \left\{ U^{(N)}_{m_0+1},\ V^{(N)}_{m_0+1},\ U^{(N)}_{m_0+2},\ V^{(N)}_{m_0+2},\ \ldots,\ U^{(N)}_{m_0+r},\ V^{(N)}_{m_0+r} \right\} ,$$

where $m_0 = \langle \alpha^N \rangle$ and $\langle x \rangle$ denotes the largest integer less than or equal to x. In the above, the constant α satisfies the inequality $0<\alpha<0.5$ and r is an integer constant with $r \geq 1$. It will be shown that under the assumptions of item 1, the set S asymptotically is multivariate normal as $N \to \infty$. If the true spectrum is constant over this set of r Fourier coefficients, then $\hat{p}(f_m)/p(f_m)$ for the spectral lines for the frequencies spanned by the band will be asymptotically distributed as $\chi^2_2/2$ and the spectral density based on the average over the whole band will be asymptotically distributed as $\chi^2_{2r}/2r$.

The first step, then, is to prove that the set S is asymptotically multivariate normal as $N \to \infty$. This requires the next two listed items.

3. A Central Limit Theorem for m-Dependent Sums (Rosen, 1967).

Consider the double sequence of random variables:

$$\begin{matrix} X_1^{(1)}, & X_2^{(1)}, & \ldots, & X_{k_1}^{(1)} \\ X_1^{(2)}, & X_2^{(2)}, & \ldots, & X_{k_2}^{(2)} \\ \vdots & \vdots & & \vdots \\ X_1^{(N)}, & X_2^{(N)}, & \ldots, & X_{k_N}^{(N)} \\ \vdots & \vdots & & \vdots \end{matrix} .$$

That is, the nth line of the array consists of a sequence of k_N random variables. Let $S^{(N)}$ be defined as:

$$S^{(N)} = \sum_{k=1}^{k_N} X_k^{(N)} \qquad \text{(C-4)}$$

(i.e., the sum of the nth row). The central limit theorem is concerned with the conditions under which the probability law of $S^{(N)}$ converges to the normal probability law as $N \to \infty$. Other quantities which will be used in the theorem are:

$$\sigma^2\left(S^{(N)}\right) = \text{Variance of } S^{(N)} \tag{C-5}$$

$$\sigma^2_{kN} = \text{Variance of } X_k^{(N)} \tag{C-6}$$

$$f_{kN}(x) = \text{probability density for } X_k^{(N)} \quad . \tag{C-7}$$

Theorem: If the random variables in the same row of the array are m-dependent and if:

(a) $E\left(X_k^{(N)}\right) = 0$ for all k and N,

(b) $\sigma^2\left(S^{(N)}\right) = 1 \quad , \quad N = 1,2,3,4,\ldots \quad ,$

(c) $\lim_{N \to \infty} \sum_{k=1}^{k_N} \int_{|\chi|>\varepsilon} x^2 f_{kN}(x)\, dx = 0 \quad ,$ for every $\varepsilon > 0$,

and

(d) $\lim_{N \to \infty} \sum_{k=1}^{k_N} \sigma^2_{kN} < \infty \quad ,$

then the probability law for $S^{(N)}$ converges to a normal probability law having zero mean and unit variance k tends to infinity.

Comments: Rosen gives the theorem in a more general form by stating condition (c) in terms of the distribution.function and a Stieltjes integral. However, the above form of condition (c) in terms of the probability density is sufficient for the present use.

Proof: Given by Rosen (1967).

4. Multivariate Central Limit Theorem (Rao, 1973).

Let F_n denote the joint distribution function of the k-dimensional random variable $\left(Z_n^{(1)}, Z_n^{(2)}, \ldots, Z_n^{(k)}\right)$ $n = 1,2,\ldots$ and $F_{\lambda n}$ the distribution function of the linear function $\lambda_1 Z_n^{(1)} + \lambda_2 Z_n^{(2)} + \ldots + \lambda_k Z_n^{(k)}$. Also let F be the joint distribution function of a k-dimensional random variable $Z^{(1)}, Z^{(2)}, \ldots, Z^{(k)}$. If for each vector λ, $F_{\lambda n} \to F_\lambda$, the distribution function of $\lambda_1 Z^{(1)} + \lambda_2 Z^{(2)} + \ldots + \lambda_k Z^{(k)}$, then $F_n \to F$.

Proof: See Rosen (1967).

5. Some Conditions for which (c) in the Theorem of Item 3 Holds.

Suppose that c_{nk} are constants uniformly bounded in n and k,

$$X_{nk} = c_{nk} Y_{nk}/\sqrt{n} \quad ,$$

and the probability density of Y_{nk} is denoted by $g_{nk}(y)$. If:

(a) there exists positive constants a, b, and c such that

$$g_{nk}(y) \leq ae^{-b|y|}, \quad \text{if} \quad |y|>c$$

uniformly in n and k, or

(b) there exists a positive constant A such that

$$g_{nk}(y) = 0 \quad , \quad \text{if} \quad |y|>A$$

uniformly in n and k.

Then for any $\varepsilon>0$,

$$L = \lim_{n \to \infty} \sum_{k=1}^{n} \int_{|x|>\varepsilon} x^2 f_{nk}(x)\, dx = 0 \quad .$$

Proof: The probability density for Y_{nk} expressed in terms of $f_{nk}(x)$ is:

$$g_{nk}(y) = \left(|c_{nk}|/ \sqrt{n} \right) f_{nk}\left(c_{nk} y \,/\, \sqrt{n} \right) \quad .$$

Hence, L may be written in terms of y integration as:

$$L = \lim_{n \to \infty} \sum_{k=1}^{n} \int_{\left|\frac{c_{nk}y}{\sqrt{n}}\right| > \varepsilon} \frac{c_{nk}^2 y^2}{n} \frac{|c_{nk}|}{\sqrt{n}} f_{nk}\left(\frac{c_{nk}y}{\sqrt{n}}\right) dy$$

$$= \lim_{n \to \infty} \frac{1}{n} \sum_{k=1}^{n} c_{nk}^2 \int_{|y| > \varepsilon\sqrt{n}/|c_{nk}|} y^2 g_{nk}(y)\, dy \quad .$$

Let B be the uniform bound on $\{c_{nk}\}$.

(a) Proof of the conclusion under hypothesis (a) above: for $\alpha>0$, and fixed $n, a,$ and b, define $G(\alpha)$ as:

$$G(\alpha) = \int_{\alpha}^{\infty} y^2 a y^n e^{-by} dy = \frac{a}{b^{n+1}} \int_{b\alpha}^{\infty} e^{-x} x^{n+2} dx \quad .$$

Clearly $G(\alpha)$ is a monotone decreasing function of α and $G(\alpha) \to 0$ as $\alpha \to \infty$.

Hence, including both tails of $g_{nk}(y)$,

$$\frac{1}{n} \sum_{k=1}^{n} c_{nk}^2 \int_{|y| > \frac{\varepsilon\sqrt{n}}{|c_{nk}|}} y^2 g_{nk}(y)\, dy \le \frac{2}{n} \sum_{k=1}^{n} c_{nk}^2 \int_{y > \frac{\varepsilon\sqrt{n}}{|c_{nk}|}} y^{n+2} a e^{-by} dy$$

$$\le \frac{2}{n} \sum_{k=1}^{n} B^2\, G\left(\frac{\varepsilon\sqrt{n}}{|c_{nk}|}\right) = 2B^2\, G\left(\frac{\varepsilon\sqrt{n}}{|c_{nk}|}\right) \to 0$$

as n tends to infinity.

(b) Proof of the conclusion under hypothesis (b) above: $g_{nk}(y)$ satisfies hypothesis (a) with $C = A$, $n = 0$, $a = 1$, and $b = 1$.

6. A Useful Lemma.

Let $c_1, c_2, c_3, \ldots$ be a sequence of constants and $W_1, W_2, W_3, \ldots$ be a sequence of random variables. Suppose that

$$\lim_{n \to \infty} c_n = c < \infty \quad ,$$

and that there exists a random variable Z with finite variance such that the probability law for $c_n W_n$ converges to the probability law for Z as $n \to \infty$. Then the probability law for cW_n also converges to that for Z as $n \to \infty$.

Proof: The proof is a straightforward application of a relation given by Rao (1973). In his terminology, the above lemma may be stated as:

$$c_n W_n \xrightarrow{L} Z \quad \text{implies} \quad cW_n \xrightarrow{L} Z$$

His relation states that this holds provided, for any $\varepsilon > 0$,

$$\lim_{n \to \infty} P\left[|c_n W_n - cW_n| > \varepsilon\right] = 0 \quad .$$

(In Rao's notation this would be stated as $|c_n W_n - cW_n| \xrightarrow{P} 0$). Now

$$P\left[|c_n W_n - cW_n| > \varepsilon\right] = P\left[|W_n| > \frac{\varepsilon}{|c_n - c|}\right] < \frac{(c_n - c)^2 \operatorname{Var}(W_n)}{\varepsilon^2}$$

by the Tchebichev inequality (Loeve, 1960). Since $\operatorname{Var}(W_n) \to \operatorname{Var}(Z)$ and $(c_n - c)^2 \to 0$ as $n \to \infty$, it follows that:

$$\lim_{n \to \infty} P\left[|c_n W_n - cW_n| > \varepsilon\right] = 0$$

as required. Hence, the lemma is proven.

7. Asymptotic Normality of Linear Combinations of Nondegenerate FFT Coefficients.

Let λ_{ms} for $s = 1,2$ and $m_0 + 1 \leq m \leq m_0 + r$ be any sequence of bounded constants and define:

$$T^{(N)} = \sum_{m=m_0+1}^{m_0+r} \lambda_{m1} \frac{U_m^{(N)}}{\sqrt{N \Delta t p_m/2}} + \sum_{m=m_0+1}^{m_0+r} \lambda_{m2} \frac{V_m^{(N)}}{\sqrt{N \Delta t p_m/2}} \quad ,$$

where the various terms are defined in item 1, and the assumptions listed there hold. Let $\sigma^2(T^{(N)})$ be the variance of $T^{(N)}$. Then,

$$\lim_{n \to \infty} \sigma^2\left(T^{(N)}\right) = \sum_{m=m_0+1}^{m_0+r} \left(\lambda_{m1}^2 + \lambda_{m2}^2\right) .$$

The probability law of

$$T^{(N)} \Big/ \sqrt{\sum_{m=m_0+1}^{m_0+r} \left(\lambda_{m1}^2 + \lambda_{m2}^2\right)}$$

converges to a normal probability law with zero mean and unit variance as N tends to infinity.

Proof: The terms $U_m^{(N)}$ and $V_m^{(N)}$ are asymptotically uncorrelated with each other and with other pairs $\left(U_m^{(N)}, V_m^{(N)}\right)$ provided $0 < m < N/2$ and $0 < m' < N/2$ (Borgman, 1973). The asymptotic variance of both $U_m^{(N)}$ and $V_m^{(N)}$ is $p_m N \Delta t/2$ (Borgman, 1973). Hence, $U_m/\sqrt{N \Delta t p_m/2}$ and $V_m^{(N)}/\sqrt{N \Delta t p_m/2}$ have unit variance. It follows that:

$$\sigma^2\left(T^{(N)}\right) \to \sum_{m=m_0+1}^{m_0+r} \left(\lambda_{m1}^2 + \lambda_{m2}^2\right)$$

as $N \to \infty$ (Freund, 1971).

After substitution for U_m and V_m in terms of Y_n, $T^{(N)}$ can be expressed as:

$$\frac{T^{(N)}}{\sigma\left(T^{(N)}\right)} = \sum_{k=1}^{N} \frac{Y_n^{(N)}}{\sqrt{N}\,\sigma\left(T^{(N)}\right)} \left\{ \sum_{m=m_0+1}^{m_0+r} \frac{\left(\lambda_{m1} \cos 2\pi\frac{m(k-1)}{N} + \lambda_{m2} \sin \frac{2\pi m(k-1)}{N}\right)}{\sqrt{p_m \Delta t/2}} \right\}.$$

Let

$$c_{Nk} = \sum_{m=m_0+1}^{m_0+r} \frac{\left(\lambda_{m1} \cos \frac{2\pi m(k-1)}{N} + \lambda_{m2} \sin \frac{2\pi m(k-1)}{N}\right)}{\sigma\left(T^{(N)}\right)\sqrt{p_m \ \Delta t/2}}$$

$$X_k^{(N)} = \frac{cnk \ Y_n^{(N)}}{\sqrt{N}}$$

and

$$k_N = N \quad .$$

Then,

$$\frac{T^{(N)}}{\sigma\left(T^{(N)}\right)} = \sum_{k=1}^{N} X_k^{(N)}$$

is in the form required for the application of the theorem in item 3.

Since $E[Y_k^{(N)}] = E[\eta_{a+k}] = 0$, condition (a) is satisfied. The division by $\sigma(T^{(N)})$ satisfied condition (b). The variance of $X_k^{(N)}$ is given by:

$$\sigma_{kN}^2 = \frac{c_{Nk}^2}{N} \ \mathrm{Var}\left(Y_k^{(N)}\right) \quad .$$

But,

$$\left|c_{Nk}\right| \le \sum_{m=m_0+1}^{m_0+r} \frac{\left|\lambda_{m1}\right| + \left|\lambda_{m2}\right|}{\sigma\left(T^{(N)}\right)\sqrt{p_m \ \Delta t/2}} = B_N$$

so,

$$\sum_{k=1}^{N} \sigma_{kN}^2 = \frac{\mathrm{Var}\left(Y_k^{(N)}\right)}{N} \sum_{k=1}^{N} c_{Nk}^2 = \mathrm{Var}\left(Y_k^{(N)}\right) B_N^2$$

which is bounded as $N \to \infty$. This verifies condition (d).

Finally condition (c) will be satisfied if the probability density for the water level elevations obey the bounding conditions (a) and (b) in item 5. This was assumed in item 1. (Note: $B = \lim_{n \to \infty} B_N + 1$ will provide the uniform bound for c_{nk} needed in item 5.)

Thus, all conditions are satisfied and $T^{(N)}/\sigma(T^{(N)})$ converges in law to a zero mean, unit-variance normal probability law. Since

$$\sigma^2\ (T_n) \to \sum_{m=m_0+1}^{m_0+r} \left(\lambda_{m1}^2 + \lambda_{m2}^2 \right) = \sigma^2$$

as $N \to \infty$, it follows from item 6 that the probability law of $T^{(N)}/\sigma$ converges to zero mean, unit-variance normal probability law. This completes the proof.

8. Asymptotic Normality of the FFT Coefficients.

Let $\left(U_m^{(N)}\ ,\ V_m^{(N)} \right)$ for $m = m_0+1,\ m_0+2,\ \ldots,\ m_0+r$ be a set of nondegenerate FFT coefficients. Then the multivariate probability law for

$$\left(\frac{U_m^{(N)}}{\sqrt{Np_m\ \Delta t/2}}\ ,\ \frac{V_m^{(N)}}{\sqrt{Np_m\ \Delta t/2}} \right),\ m_0+1 \le m \le m_0+r$$

will be a multivariate normal with covariance matrix equal to an identity matrix and mean vector having all components equal to zero.

Proof: In items 4 and 7.

9. Asymptotic Chi-Squared Distribution for Spectral Estimates.

For the range of m-values, $m_0+1 \le m \le m_0+r$, suppose that $p_m = p$ is a nonzero constant. Let:

$$\hat{p} = \frac{1}{r} \sum_{m=m_0+1}^{m_0+r} \left(U_m^2 + V_m^2 \right) \Big/ N\ \Delta t\ .$$

Then, $2r\hat{p}/p$ is asymptotically a chi-squared random variable with $2r$ degrees of freedom.

Proof:

$$r\hat{p} = \sum_{m=m_0+1}^{m_0+r} \left[\left(\frac{U_m}{\sqrt{N \Delta t}} \right)^2 + \left(\frac{V_m}{\sqrt{N \Delta t}} \right)^2 \right]$$

or

$$\frac{2r\hat{p}}{p} = \sum_{m=m_0+1}^{m_0+r} \left[\left(\frac{U_m}{\sqrt{Np \ \Delta t/2}} \right)^2 + \left(\frac{V_m}{\sqrt{Np \ \Delta t/2}} \right)^2 \right] .$$

By item 8, the terms squared in the sum are asymptotically independent, zero mean, unit-variance normal random variables. Hence, the right-hand side is asymptotically chi-squared with $2r$ degrees of freedom (Freund, 1971).

Borgman, Leon E.
The statistical anatomy of ocean wave spectra / by Leon E. Borgman. — Fort Belvoir, Va. : U.S. Coastal Engineering Research Center, 1976.
102 p. : ill. (Technical paper – Coastal Engineering Research Center ; no. 76-10) Also (Research report – University of Wyoming, Geology Department ; no. 73-1) Also (Contract – Coastal Engineering Research Center ; DACW72-72-C-0001)
Bibliography : p. 86.
The statistical variations in wave energy spectral estimates for hurricane waves are examined empirically for 12 separate intervals of wave records measured during Hurricane Carla in September 1961. This report gives the analysis for Hurricane Carla and develops certain implications and consequences of the empirical results.
1. Wave spectra. 2. Hurricane waves. 3. Hurricane Carla. 4. Spectrum analysis. I. Title. II. Series : U.S. Coastal Engineering Research Center. Technical paper no. 76-10. III. Series : Wyoming. University. Geology Department. Research Report 73-1. IV. Series : U.S. Coastal Engineering Research Center. Contract DACW72-72-C-0001.
TC203 .U581tp no. 76-10 627 .U581tp

Borgman, Leon E.
The statistical anatomy of ocean wave spectra / by Leon E. Borgman. — Fort Belvoir, Va. : U.S. Coastal Engineering Research Center, 1976.
102 p. : ill. (Technical paper – Coastal Engineering Research Center ; no. 76-10) Also (Research report – University of Wyoming, Geology Department ; no. 73-1) Also (Contract – Coastal Engineering Research Center ; DACW72-72-C-0001)
Bibliography : p. 86.
The statistical variations in wave energy spectral estimates for hurricane waves are examined empirically for 12 separate intervals of wave records measured during Hurricane Carla in September 1961. This report gives the analysis for Hurricane Carla and develops certain implications and consequences of the empirical results.
1. Wave spectra. 2. Hurricane waves. 3. Hurricane Carla. 4. Spectrum analysis. I. Title. II. Series : U.S. Coastal Engineering Research Center. Technical paper no. 76-10. III. Series : Wyoming. University. Geology Department. Research Report 73-1. IV. Series : U.S. Coastal Engineering Research Center. Contract DACW72-72-C-0001.
TC203 .U581tp no. 76-10 627 .U581tp

Borgman, Leon E.
The statistical anatomy of ocean wave spectra / by Leon E. Borgman. — Fort Belvoir, Va. : U.S. Coastal Engineering Research Center, 1976.
102 p. : ill. (Technical paper – Coastal Engineering Research Center ; no. 76-10) Also (Research report – University of Wyoming, Geology Department ; no. 73-1) Also (Contract – Coastal Engineering Research Center ; DACW72-72-C-0001)
Bibliography : p. 86.
The statistical variations in wave energy spectral estimates for hurricane waves are examined empirically for 12 separate intervals of wave records measured during Hurricane Carla in September 1961. This report gives the analysis for Hurricane Carla and develops certain implications and consequences of the empirical results.
1. Wave spectra. 2. Hurricane waves. 3. Hurricane Carla. 4. Spectrum analysis. I. Title. II. Series : U.S. Coastal Engineering Research Center. Technical paper no. 76-10. III. Series : Wyoming. University. Geology Department. Research Report 73-1. IV. Series : U.S. Coastal Engineering Research Center. Contract DACW72-72-C-0001.
TC203 .U581tp no. 76-10 627 .U581tp

Borgman, Leon E.
The statistical anatomy of ocean wave spectra / by Leon E. Borgman. — Fort Belvoir, Va. : U.S. Coastal Engineering Research Center, 1976.
102 p. : ill. (Technical paper – Coastal Engineering Research Center ; no. 76-10) Also (Research report – University of Wyoming, Geology Department ; no. 73-1) Also (Contract – Coastal Engineering Research Center ; DACW72-72-C-0001)
Bibliography : p. 86.
The statistical variations in wave energy spectral estimates for hurricane waves are examined empirically for 12 separate intervals of wave records measured during Hurricane Carla in September 1961. This report gives the analysis for Hurricane Carla and develops certain implications and consequences of the empirical results.
1. Wave spectra. 2. Hurricane waves. 3. Hurricane Carla. 4. Spectrum analysis. I. Title. II. Series : U.S. Coastal Engineering Research Center. Technical paper no. 76-10. III. Series : Wyoming. University. Geology Department. Research Report 73-1. IV. Series : U.S. Coastal Engineering Research Center. Contract DACW72-72-C-0001.
TC203 .U581tp no. 76-10 627 .U581tp

Borgman, Leon E.
The statistical anatomy of ocean wave spectra / by Leon E. Borgman. – Fort Belvoir, Va. : U.S. Coastal Engineering Research Center, 1976.
102 p. : ill. (Technical paper – Coastal Engineering Research Center ; no. 76-10) Also (Research report – University of Wyoming, Geology Department ; no. 73-1) Also (Contract – Coastal Engineering Research Center ; DACW72-72-C-0001)
Bibliography : p. 86.
The statistical variations in wave energy spectral estimates for hurricane waves are examined empirically for 12 separate intervals of wave records measured during Hurricane Carla in September 1961. This report gives the analysis for Hurricane Carla and develops certain implications and consequences of the empirical results.
1. Wave spectra. 2. Hurricane waves. 3. Hurricane Carla. 4. Spectrum analysis. I. Title. II. Series : U.S. Coastal Engineering Research Center. Technical paper no. 76-10. III. Series : Wyoming. University. Geology Department. Research Report 73-1. IV. Series : U.S. Coastal Engineering Research Center. Contract DACW72-72-C-0001.
TC203 .U581tp no. 76-10 627 .U581tp

Borgman, Leon E.
The statistical anatomy of ocean wave spectra / by Leon E. Borgman. – Fort Belvoir, Va. : U.S. Coastal Engineering Research Center, 1976.
102 p. : ill. (Technical paper – Coastal Engineering Research Center ; no. 76-10) Also (Research report – University of Wyoming, Geology Department ; no. 73-1) Also (Contract – Coastal Engineering Research Center ; DACW72-72-C-0001)
Bibliography : p. 86.
The statistical variations in wave energy spectral estimates for hurricane waves are examined empirically for 12 separate intervals of wave records measured during Hurricane Carla in September 1961. This report gives the analysis for Hurricane Carla and develops certain implications and consequences of the empirical results.
1. Wave spectra. 2. Hurricane waves. 3. Hurricane Carla. 4. Spectrum analysis. I. Title. II. Series : U.S. Coastal Engineering Research Center. Technical paper no. 76-10. III. Series : Wyoming. University. Geology Department. Research Report 73-1. IV. Series : U.S. Coastal Engineering Research Center. Contract DACW72-72-C-0001.
TC203 .U581tp no. 76-10 627 .U581tp

Borgman, Leon E.
The statistical anatomy of ocean wave spectra / by Leon E. Borgman. – Fort Belvoir, Va. : U.S. Coastal Engineering Research Center, 1976.
102 p. : ill. (Technical paper – Coastal Engineering Research Center ; no. 76-10) Also (Research report – University of Wyoming, Geology Department ; no. 73-1) Also (Contract – Coastal Engineering Research Center ; DACW72-72-C-0001)
Bibliography : p. 86.
The statistical variations in wave energy spectral estimates for hurricane waves are examined empirically for 12 separate intervals of wave records measured during Hurricane Carla in September 1961. This report gives the analysis for Hurricane Carla and develops certain implications and consequences of the empirical results.
1. Wave spectra. 2. Hurricane waves. 3. Hurricane Carla. 4. Spectrum analysis. I. Title. II. Series : U.S. Coastal Engineering Research Center. Technical paper no. 76-10. III. Series : Wyoming. University. Geology Department. Research Report 73-1. IV. Series : U.S. Coastal Engineering Research Center. Contract DACW72-72-C-0001.
TC203 .U581tp no. 76-10 627 .U581tp

Borgman, Leon E.
The statistical anatomy of ocean wave spectra / by Leon E. Borgman. – Fort Belvoir, Va. : U.S. Coastal Engineering Research Center, 1976.
102 p. : ill. (Technical paper – Coastal Engineering Research Center ; no. 76-10) Also (Research report – University of Wyoming, Geology Department ; no. 73-1) Also (Contract – Coastal Engineering Research Center ; DACW72-72-C-0001)
Bibliography : p. 86.
The statistical variations in wave energy spectral estimates for hurricane waves are examined empirically for 12 separate intervals of wave records measured during Hurricane Carla in September 1961. This report gives the analysis for Hurricane Carla and develops certain implications and consequences of the empirical results.
1. Wave spectra. 2. Hurricane waves. 3. Hurricane Carla. 4. Spectrum analysis. I. Title. II. Series : U.S. Coastal Engineering Research Center. Technical paper no. 76-10. III. Series : Wyoming. University. Geology Department. Research Report 73-1. IV. Series : U.S. Coastal Engineering Research Center. Contract DACW72-72-C-0001.
TC203 .U581tp no. 76-10 627 .U581tp